



## **MASTER'S THESIS IN PETROLEUM GEOLOGY**

Structural interpretation and structural modelling of  
carbonate and clastic reservoir analogue, Løvehovden,  
northern Billefjord, Svalbard



mpi

Gerard Bonet

Centre for Integrated Petroleum Research  
University of Bergen, June 2009



## *Abstract*

The Master's Thesis is centred in the topics of structural geology and structural modelling. I present a reinterpretation of the Løvehovden reverse Tertiary faults from Dallmann et al. (2004) as syn-depositional Carboniferous extensional faults based on sedimentological and structural evidence.

The structural models are intended to quantify basin thickness variations, compaction, flexural isostatic rebound and Tertiary shortening. Trishear models are tested in order to assess the Løvehovden Master Fault propagation, trishear apex and trishear angle of the fault-propagation fold observed in the Løvehovden study area.

The stratigraphic sequence deposited in the study area forms a petroleum system, where the effects of compaction on fluid migration and analogy with the Barents Shelf are here evaluated.

Petroleum potential of the study area is particularly discussed in the Appendix.



## *Preface*

I have centred this Master's Thesis on the topics of structural geology and structural modelling. The structural reinterpretation of the study area is based on field observations and interpretations. Structural models are intended to quantify basin parameters. The petroleum potential evaluation of the Løvehovden area is assessed in Appendix II.

This Master's Thesis has also been aimed to transmit the results in an applied and understandable way. The contents have been guided in order to create a useful work that can be used for many others for further research endeavours in the field of structural modelling connected to petroleum geology.

It has been a process of construction dedicated to build consistency, truthfulness and to provide accurate results. However, the readers will judge these maximas and I hope that the ideas here presented will generate a constructive critique.

I am grateful to have been provided with this unique opportunity to present and to develop my work in one of the most brilliant research centres, the Centre for Integrated Petroleum Research (CIPR), in collaboration with the University of Bergen.

I sincerely hope this work to be of your interest and to keep up with the level of your expectations.



## *Acknowledgments*

The development of this Master's Thesis has been a positive and challenging task. It has opened my mind with regard to the many variables that interact in structural geology and sedimentology applied to petroleum geology.

First of all, I would like to dedicate some words to my three supervisors. To Dr Jan Tveranger, who first introduced me to the nature of the projects managed and developed at CIPR, transmitting me great enthusiasm, which guided my first steps as master student at the University of Bergen. I am most grateful to Dr Alvar Braathen, who advised me during my fieldwork on Svalbard and for having transmitted me clear ideas and constructive critique.

I would like to thank the constant advice of my main supervisor Dr Walter Wheeler, and the opportunity he had given me with having been involved in a project of such relevance for my future professional career.

To my field assistant, Geir Kjeldaas, for his technical and personal support during fieldwork. Some words as well for Simon Buckley who assisted me on the use and handling of his Lidar data interpretation program Lime. To Dr Nestor Cardozo for his advice on the management of the structural modelling program 2D Move.

And to Irene Husa, for her assistance in all the troubles I have encountered regarding program installations, formats, licences and computer crashes.





## Table of content

<i>Abstract</i> .....	<i>i</i>
<i>Preface</i> .....	<i>ii</i>
<i>Acknowledgments</i> .....	<i>iii</i>
<b>1. INTRODUCTION</b> .....	<b>1</b>
1.1 General geology of Svalbard.....	1
1.1.1 Geographicallocation .....	1
1.1.2 Geological provinces and brief tectonic history.....	3
1.1.2.1 Introduction to Svalbard.....	3
1.1.2.2 Geological provinces.....	6
1.1.3 Regional tectonics .....	9
1.1.4 Regional stratigraphy .....	13
1.2 Focus on the Billefjorden Trough, Central Basin.....	16
1.2.1 Structural framework.....	16
1.2.2 Local stratigraphy .....	17
1.2.2.1 Hekla Hoek Pre-Cambrian to Silurian rocks .....	18
1.2.2.2 Devonian rocks.....	19
1.2.2.3 Permo-Carboniferous rocks .....	20
1.2.2.4 Quaternary sediments .....	25
1.3 The Løvehovden area .....	26
1.3.1 History of investigation .....	26
1.3.2 Depositional sequence in the study area .....	28
1.3.2.1 Description of the strata in current terminology .....	30
1.3.2.1.1 Basement rocks .....	31
1.3.2.1.2 Paleozoic .....	31
1.3.2.1.3 Mesozoic-Tertiary .....	38
1.3.2.2 Carboniferous sequence stratigraphic framework .....	40
1.3.3 Structural features .....	41
1.3.3.1 The Billefjorden Fault Zone .....	42
1.3.3.2 The Ebbabreen and Løvehovden faults .....	45
<b>2. FIELDWORK DESCRIPTION AND DATA COMPILATION</b> .....	<b>47</b>
2.1 Methodology .....	47
2.2 Outcrop data compilation .....	48
2.2.1 Domain A .....	48
2.2.2 Domain B <sub>1</sub> .....	49
2.2.3 Domain B <sub>2</sub> .....	56
2.2.4 Domain C .....	57
2.2.5 Structural data analysis .....	58
2.2.5.1 Total structural data plot .....	61
2.2.5.2 Layering.....	62
2.2.5.3 Faults.....	63
2.2.5.4 Joints .....	63

2.2.5.5 Lidar-based bedding data .....	65
2.2.5.6 Lidar-based fault throw data .....	67
2.2.6 Logging .....	67
2.3.6.1 Hangingwall log .....	68
2.3.6.2 Footwall log .....	70
2.3.6.3 Comparison and discussion .....	71
2.2.7 Scanline across the fault zone .....	74
2.2.8 Encountered breccia types, origins and implications.....	76
2.2.8.1 Breccia pipes .....	76
2.2.8.2 Lidar interpretation of breccia pipes on Løvehovden .....	77
2.2.8.3 Fault breccias .....	78
2.2.8.4 Collapse breccias .....	79
.	
<b>3. STRUCTURAL MODELLING .....</b>	<b>81</b>
3.1 Introduction .....	81
3.2. Cross-section construction .....	82
3.2.1 Data preparation .....	82
3.2.2 Orientation of the cross-section .....	83
3.2.3 Projecting data and building the section .....	85
3.3 Testing the BFZ using syn-rift geometry.....	88
3.4 Comparison with a previous model (2004) .....	89
3.5 Reconstruction and thickness variations .....	91
3.5.1 Flexural slip(1): Removing Tertiary shortening on the BFZ .....	91
3.5.2 Flexural slip (2): Removing Tertiary shortening on the BFZ .....	93
3.5.3 Move: Removing Tertiary shortening on the Ebbadalen Fault .....	95
3.5.4 Trishear: Removing the Carboniferous LMF-related deformation .....	96
3.5.4.1 Final model .....	98
3.5.4.2 Tests on the fault position .....	102
3.5.4.3 Tests on the trishear angle .....	104
3.5.4.4 Tests on the trishear apex .....	105
3.5.5 Restore: restoring the central block .....	107
3.5.6 Rotate: removing Permo-Carboniferous-related deformation .....	107
3.5.7 Structural reconstruction summary .....	108
3.5.8 Thickness variations discussion.....	111
3.6 Decompaction .....	113
3.6.1 Discussion.....	121
<b>4. DISCUSSION.....</b>	<b>123</b>
4.1 Reinterpretation of the Løvehovden Fault Zone .....	123
4.2 Results from the structural models .....	128
4.3 Structural and sedimentary interpretation of the outcrop .....	130
4.4 Analogy to the Barents Shelf.....	131
4.5 Error factor and uncertainties.....	132

<b>5. CONCLUSIONS .....</b>	<b>135</b>
<b>References .....</b>	<b>137</b>
<b>Appendix I Stratigraphic columns in Section 1.3.2.1.2 .....</b>	<b>143</b>
<b>Appendix II Petroleum Prospectivity of the Løvehovden area .....</b>	<b>149</b>
1 Burial history & basin evolution .....	149
2 Hydrocarbon potential .....	153
2.1 Elements: source, trap and seal rocks .....	154
2.2 Processes: generation, migration, accumulation .....	157
2.3 Interpreted oil migration paths .....	159
3 Summary of the petroleum system evolution and prospect evaluation .....	162



## **1. INTRODUCTION**

The introductory chapter is intended to describe the stratigraphic and tectonic processes that in general terms summarize the geology of Svalbard. The review will first describe the general geological history of Svalbard, then focus on the study area, Svalbard's Løvehovden area, between Ebbadalen and Ragnardalen at the northern end of Billefjorden geological structures.

### **1.1 General geology of Svalbard**

The geological record starts in Pre-Cambrian until the most recent Quaternary deposits. The tectonic control exerted on the distribution and thickness of the sedimentary units is emphasized. The lithostratigraphical units, beginning with strata from Pre-Caledonian times, are here reviewed along with tectonic events and climate change. A more detailed review of Svalbard, with special emphasis on the Løvehovden area (Nord Billefjorden Trough) is presented at the end of the chapter.

#### **1.1.1 Geographical location**

The Svalbard archipelago is an arctic region consisting of numerous islands. The largest of the islands is Spitsbergen, followed by Nordauslandet (NE land) and Edgeøya (Figure 1.1). The smaller islands include Barentsøya, Kvitøya, Prince Karls Land, Kong Karls Land, Kongsøya, Bjornøya, Svenskøya and Wilhelmøya as well as other smaller groups of islands.

Svalbard lies North of the Arctic Circle, between 74° and 81° N latitude and 10° to 35° E longitude.

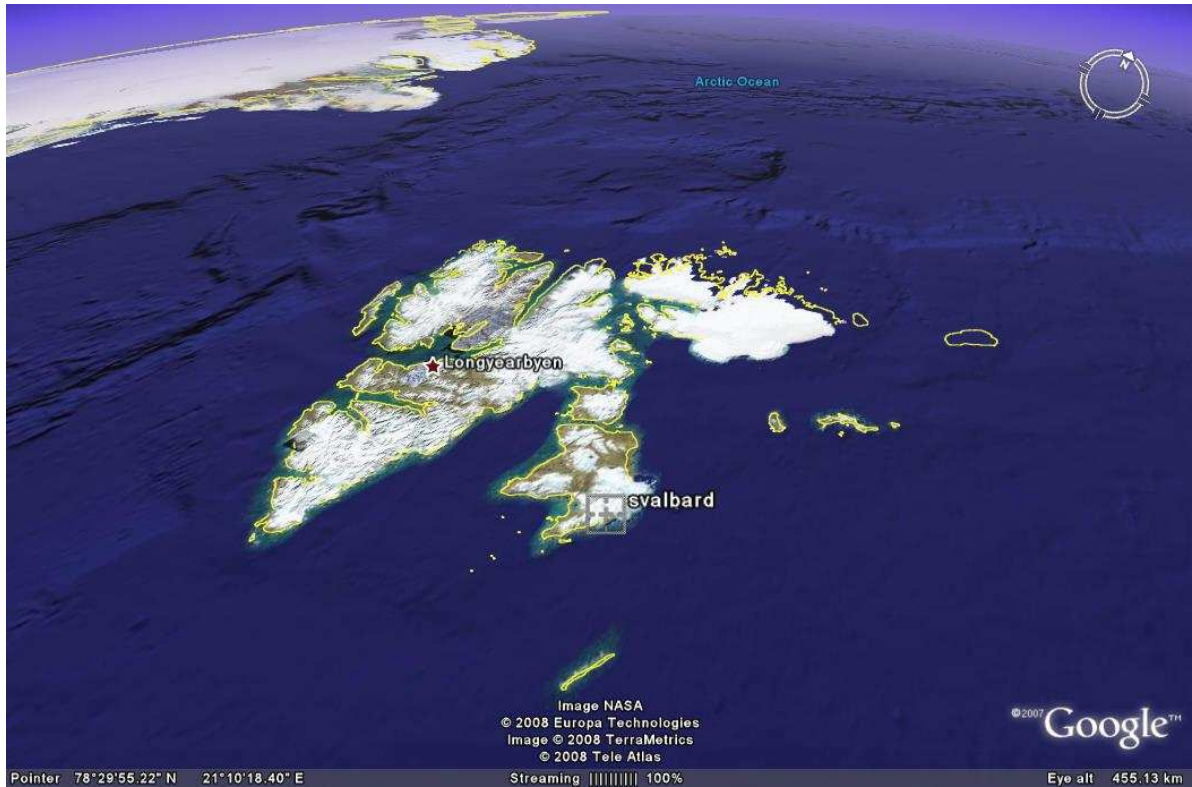


**Figure 1.1** Geographic map of the Svalbard archipelago. It shows the main regions, settlements and islands (not included Bjørnøya, located further south).

(From Norsk Polarinstitutt  
<http://npweb.npolar.no>)

Svalbard's northern boundary is defined by the Arctic Sea. The Barents Sea, instead, limits the southern border. Greenland is located to the west side of Svalbard, separated by the Greenland Sea, although originally Greenland and Svalbard formed part of the same tectonic plate. The Svalbard's eastern limit corresponds to the Scandinavian craton and to the Barents Sea (Figure 1.2).

Svalbard is one of the few places in the world where sections representing most of the Earth's history are easily accessible for study (Elvevold 2007). The continuous bedrock sections extend kilometres, enabling local and regional studies.



**Figure 1.2** *Oblique view of the Svalbard archipelago, looking NE, captured from Google Earth. The location lies in northern Europe and it is a boundary region in between four seas and oceans: the Arctic Ocean (N), Barents Sea (S-SE), Greenland Sea (W) and Norwegian Sea (further South not visible on the view). (Modified from NASA, [www.nasa.com](http://www.nasa.com), served by Google Earth).*

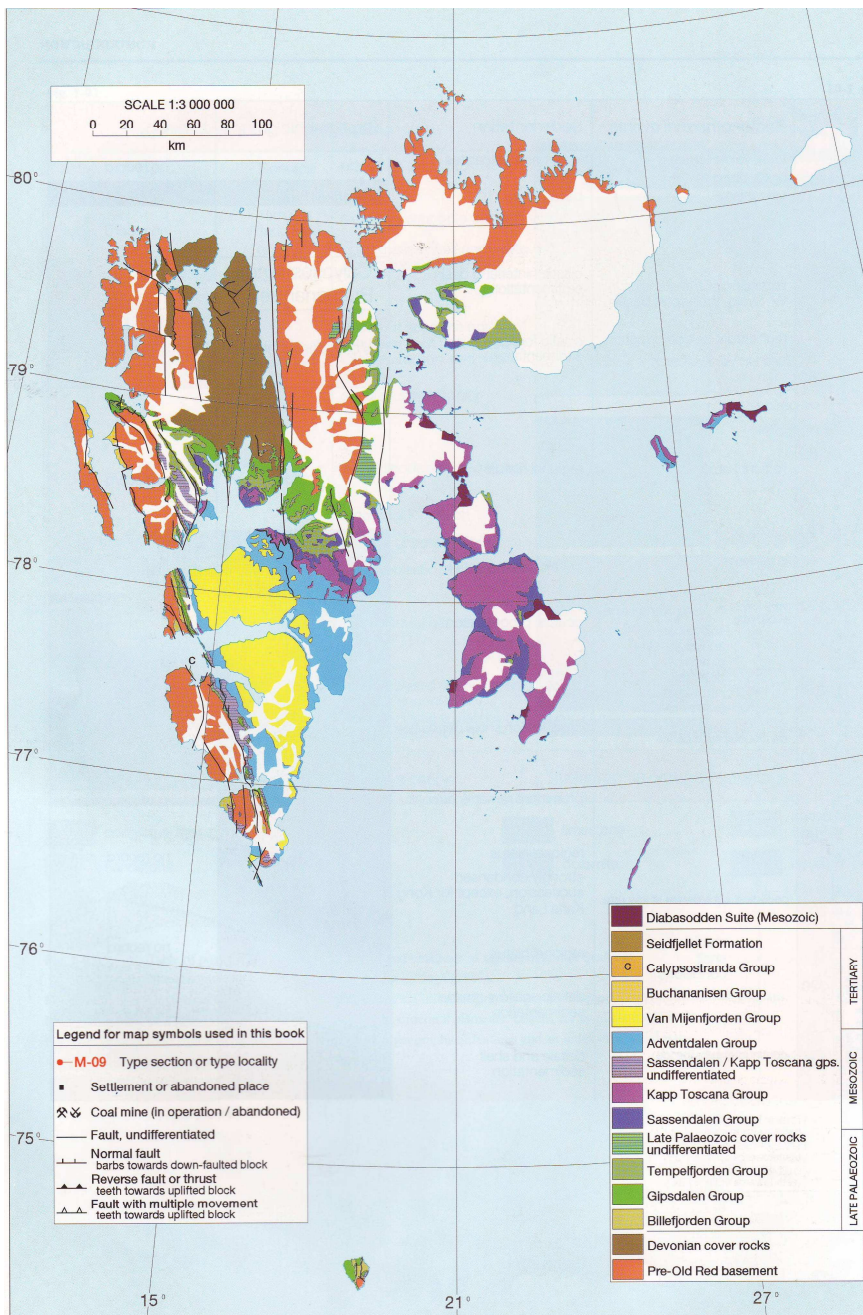
### 1.1.2 Geological provinces and brief tectonic history

The sections of this chapter provide a first approach to the geology and tectonic setting of Svalbard. A basic overview of the distribution of the main geological units is offered together with the chronology of the tectonic events, which emplaced Svalbard at its actual location.

#### 1.1.2.1 Introduction to Svalbard

The Svalbard archipelago represents the emergent part of the Barents continental shelf, on the north-western corner. Even though the emergent lands hardly constitute 5% of the total

submerged area (Worsley 2006), the Quaternary glacial dynamics have enhanced the exposure. The exposure has facilitated geological studies, beginning with exploration for economic minerals and more recently including geological surveys aimed to establish plausible analogies with the inaccessible Barents basins. The regional geology of Svalbard is shown in Figure 1.3.



In general terms, the geological record may be split into the rocks of Pre-Caledonian and Post-Caledonian times. The Pre-Caledonian rocks date from Pre-Cambrian Age and are composed by granite, schist and gneiss. These igneous and metamorphic rocks are Svalbard's basement. The Post-Caledonian rocks (from Cambrian to Tertiary) are mainly of sedimentary origin.

**Figure 1.3** *Regional Geology of Svalbard (Modified from Dallmann et al. 1999)*



The Post-Caledonian rocks form the Upper Paleozoic, Mesozoic and Cainozoic sedimentary cover. Important climate changes and tectonic controls have been recorded on the Mesozoic-Cainozoic rocks by the northward drift movement from equatorial to arctic latitudes from the Late Devonian/Early Carboniferous to the present day geographic location (Stemmerik & Worsley 2005). Recent Quaternary volcanic activity has been recorded in a narrow zone in Breibogen, Bock-fjorden (Sushchevskaya 2004).

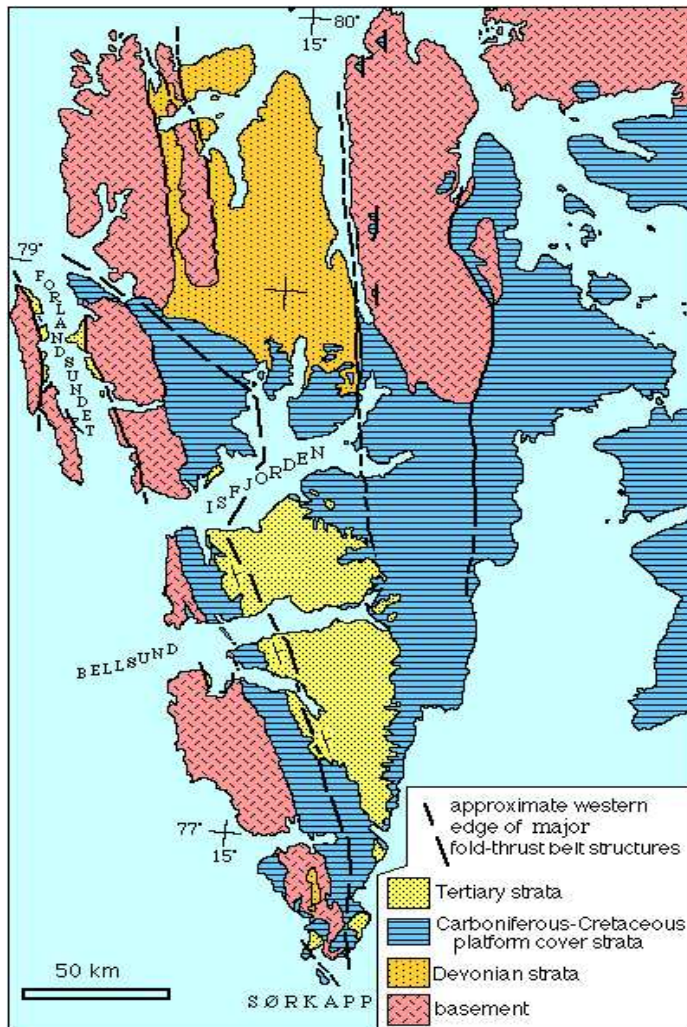
According to Elvevold (2007) and the Norwegian Polar Institute (<http://npweb.npolar.no/english/subjects/geologi>), the geological record of Svalbard can be divided into three main geological units by following a criteria based on age and texture.

I. The Basement rocks, whose genesis took place from Pre-Cambrian to Silurian times. From igneous and metamorphic nature, they are the oldest rocks preserved in Svalbard. They are typically deformed by the Caledonian orogeny.

II. The sedimentary cover, partly formed by the detrital sediments from the Caledonian orogen denudation. Those sediments are preserved in the Devonian successions. Further sedimentological processes, derived from denudation and relative sea level changes, deposited new sediments. The post-Devonian deposits are of carbonatic and evaporitic marine origin, sandstones and mudstones from continental origin and marine clastic rocks. Some of the sediments were deposited on the Central Basin. A major Mesozoic-Tertiary orogenic event is recorded in a thrust belt along the coast of Spitsbergen. In the Tertiary, clastic sediments were deposited to the east, nowadays preserved in the Tertiary Basin (Figure 1.3).

III. The most recent distinct package of strata is recent deposits formed by Quaternary glacial erosion, shaping the landscape as we see it nowadays.

### 1.1.2.2 Geological provinces



The geological provinces of Svalbard comprise well differentiated geological units, which are classified on Figure 1.4 based on age and geographical location.

**Figure 1.4** Map showing the main geological provinces of Svalbard. The Western Fold and Thrust Belt (black dashed-lines), the Hekla Hoek basement, the Devonian basin, the Tertiary basin, the Carboniferous strata from the Central Basin and the eastern Platform Areas. (From [www.hi.is](http://www.hi.is), modified from Hjelle (1993))

1. Basement → The Hekla Hoek basement consists of metamorphic complex of Pre-Cambrian to Early Silurian age. These rocks crop out mainly along the north east and western coasts of Spitsbergen (Figure 1.4). The degree of metamorphism decreases towards the east. Four principal zones of Caledonian metamorphic rocks have been found in Svalbard, each representing two sets of paired metamorphic provinces (Ohta 1978). These two sets result

from different degrees of migmatization. The four lithological zones are rather homogeneous though some lithologic contrast is found between the lower and upper successions. According to the observations from Ohta (1978), it is plausible to think that the geosyncline formed by the Hekla Hoek strata forms a large unit in the geological history of Svalbard. The most common rock types are gneiss, schist, phyllite, amphibolite, syenite and granite (Rachlewicz 2002). Geochemical analysis has not conclusively determined the origin of the basement, oceanic or crystalline. Some authors interpret the Hekla Hoek as oceanic origin, based on the abundance of basic rocks, whereas other authors base a continental origin on the existence of granitic and conglomeratic successions.

2. Devonian → The Devonian sediments typically lie in grabens in northern Spitsbergen (Figure 1.4). These strata are called the Old Red Sandstone of the Wood Bay Formation, and are only exposed in north-central Spitsbergen. The Wood Bay Formation consists of sandstone-mudstone cycles between bounding faults trending north south and delimited by the Caledonian fault belts (Friend 1996).

The outcropping geometry implies that the Devonian sediments were deposited in a narrow north-south basin between faults acting on both sides. This sedimentary basin was filled from Late Silurian to Late Devonian with clastic sediments derived from the rising Caledonian Orogen, affected by equatorial climatic conditions with great abundance of fauna and flora. Studies presented by Friend (1996) suggest three meandering to braided river systems draining from the south-west towards a northern area (Wisshak et al. 2004).

3. Permo-Carboniferous → The Central Basin, in which our study area lies, records lithologies ranging from Upper Permian to Carboniferous. The sediments were deposited after

the Caledonian movements and the so-called Svalbardian Deformation during a Carboniferous period of extension (Figure 1.3).

The Carboniferous-Permian rocks are represented by several sedimentary rock types: conglomerates, sandstones, mudstones, limestones, coal seams, gypsum, anhydrite and dolomites (Rachlewicz 2002). Vertical thickness variations in many of the deposited Members and Formations are noticeable. Such variations are caused mainly to tectonism rather than to sedimentological processes (McCann & Dallmann 1996 ; Harland 1997). The adjacent Billefjorden Fault Zone activity during the sediment deposition caused the apparent vertical thickness variations.

4. The Platform Areas east of Spitsbergen and on Barentsøya and Edgeøya → The geographical platforms are located north-east of Svalbard, mainly into the Nordauslandet region. The sequence is mainly pre-Devonian (basement exposure) though a condensed Permo-Carboniferous sequence is preserved (Harland 1997). The western boundary is not clearly defined due to the presence of a glacier covering the strata, though its eastern margin is delimited by the Lomfjorden Trough and the Lomfjorden Fault (Harland 1997).

5. The Tertiary Basin and fold belt along the western Spitsbergen coast → The Tertiary sediments of Svalbard are located on the Tertiary basin, which is rift-related and located in southern and central parts of Spitsbergen (Figure 1.4). The Tertiary sediments are clastic, mostly shales and sandstones, coal-bearing in the uppermost and lowermost parts representing delta-related shelf of Paleocene to Eocene age (Dallmann et al. 1999).

### 1.1.3 Regional tectonics

The tectonic events recorded in Svalbard are multiple and of varying intensity. The uplifting of the Barents Shelf was a consequence of late Mesozoic and Cainozoic crustal movements, the last of which is documented in the western fold and thrust belt of western Spitsbergen. Tectonics, stratigraphy and structure of the Svalbard archipelago are the result of a close interaction between these crustal movements. This interaction responds to the continuous northward displacement from Devonian equatorial latitudes to the current arctic situation. This northern drift has also imparted strong climate changes affecting the lithological composition of the sediments. The tectonic controls result from four main tectonic episodes:

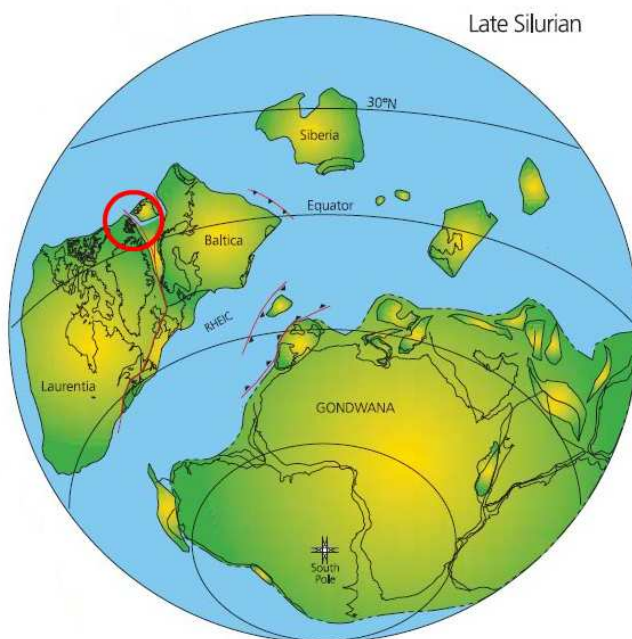
- a) Caledonian Orogeny (compression and metamorphism)
- b) Svalbardian Movements (transpression and compression)
- c) Variscan lateral movements and uplift
- d) West Spitsbergen Orogeny

The most prominent tectonic events are listed from Dallmann et al. (1999). The chronology of the successive tectonic regimes is here related based on Harland et al. (1974) and punctuated by other authors.

1. Pre-Cambrian basic volcanism recorded in the Hekla Hoek basement indicates crustal extension which might be oceanic and related to Proto-Iapetus, opened in Pre-Cambrian times (Harland et al. 1974).

2. Mid- Ordovician acid volcanic rocks indicate a relative proximity to a continent or to an island arc, first intruding and later on overlaying the basic Pre-Cambrian rocks. It is preserved 10-15 Km to the East of the Billefjorden Fault Zone.

3. Ordovician-Silurian tectogenesis as part of the Caledonian orogeny. The Pre-Cambrian sediments were subject to an intense metamorphism (Friend & Harland et al. 1997). It seems accepted by most of the authors that this event was mainly compressive E-W. It was characterized by crustal thickening related to the closure of Iapetus. The closure of Iapetus implied the collision between Greenland and Spitsbergen with Baltica. In detail the collision involved Baltica's north western area, today incorporated into the Scandinavian Shield (Figure 1.5).

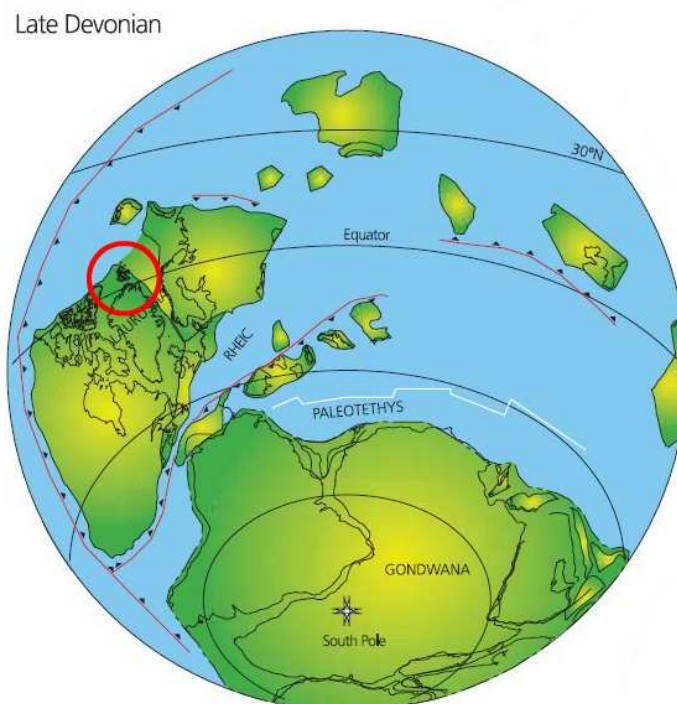


**Figure 1.5:** *Late Silurian Plate configuration. After the Caledonian orogenic event attributed to, a period of sedimentation started during an extensional Devonian stage, when Svalbard was located at equatorial latitudes. (Modified from Torsvik et al. 2005)*

4. Sinistral transpression following the Caledonian compression. The transpression was aligned N-S according to Harland et al. (1974) and NNW-SSE according to Friend (1997). The transpression occurred along the Billefjorden Lineament.

5 Late stage of orogeny in the Ny Friesland block, on the north eastern corner of the nowadays Spitsbergen island (See Figure 1.1). This orogeny has induced more severe erosion in the Ny Friesland block than in its western boundary, the Devonian basin.

6. Devonian continuous subsidence as the basin was infilled with the materials coming from the proximal Caledonian mountain range (Figure 1.6).

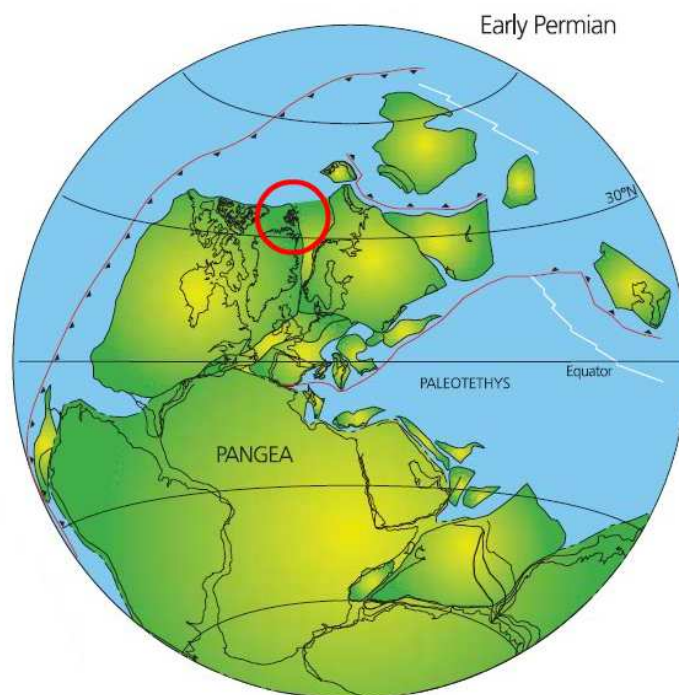


**Figure 1.6:** Late Devonian Plate configuration. The Devonian sedimentary deposition in half-grabens was followed by another period of major transcurrence between two tectonic plates, Baltica and Laurentia, during the Late-Devonian Early Carboniferous period. (Modified from Torsvik et al 2005.)

7. Transpression and compression (Svalbardian Movements) with dominantly sinistral transcurrence corresponding to major transcurrence between two major plates. A displacement of 200 Km is provable although there is external evidence of displacement up to 1000 Km along the central and northern areas of the nowadays Spitsbergen. Folding and thrusting appear to be secondary (Harland 1974 ; Buggisch et al. 1992). Buggisch et al. based

their arguments on the Old Red sediments in Blomstrandhalvøya, imbricated together with basement marbles. It would indicate that, after the Devonian deposition, the sediments were thrust, possibly during the Svalbardian Movements.

8. Carboniferous extensional vertical movements controlling the Carboniferous sedimentation (Figure 1.7).



**Figure 1.7** Early Permian Plate configuration. After the Upper Devonian transcurrent stage, Svalbard experiences subsidence and extension during the Permo-Carboniferous period with a northward tectonic drift into tropical latitudes. (Modified from Torsvik et al. 2005)

9. Upper Cretaceous deformation related to the Variscan orogeny (Dallmann et al. 1999 ; Buggisch et al. 1992). The Upper Cretaceous tectonic event included lateral movements, formation of a basin, uplift and erosion.



10. Mid Cainozoic (Tertiary) E-W compression and transpression to the west of Spitsbergen by continental collision. It involved cover and basement and it propagated eastward to the Billefjorden Fault Zone.

#### 1.1.4 Regional stratigraphy

The geological structures recorded on Svalbard, particularly on Spitsbergen, resulted from the tectonic control on deposition. The tectonic regimes create and diminish accommodation space, and preserve or expose the sediments. The climate influence on sediment deposition is also discussed in this Chapter. Figure 1.8 summarizes the main depositional events from Devonian to Tertiary, ages and paleolatitude. We distinguish seven main depositional events:

*Pre-Caledonian or Pre-Old Red rocks* → Sediments deposited before the Caledonian tectonic event and posterior metamorphism. Three different basement provinces are recognised (Dallmann et al. 1999), juxtaposed during the Caledonian period and structurally forming a regional geosynclinal (Ohta 1978). The metamorphic products consist of schist, gneiss, amphibolite, syenite and locally blue schist and even eclogite, indicating the intensity of the metamorphism.

*Old Red Sandstone* → Deposited in Devonian times between the Caledonian and Svalbardian movements. The Old Red Sandstone was deposited in a subsiding period of deposition from the Caledonian orogen erosion and weathering.

*Upper Paleozoic* → Following the shear and thrusting derived from the Svalbardian deformation between Devonian and Carboniferous, the Permo-Carboniferous period was characterized by a widespread intracratonic rifting and development of an immense post-rift carbonate platform (Worsley 2006). First tropical humid conditions led to the deposition of the clastics from the Billefjorden Group, followed by a shift to arid conditions, regional uplift and subsequent rifting. This led to fault-controlled subsidence and depocentres forming in local half grabens such as the Billefjorden trough (Worsley & Stemmerik 2005). During the lowstand accompanying the regional deposition of carbonate, some basins became isolated, precipitating evaporites under the dominant arid conditions. Carbonates and evaporites are represented by the Gipsdalen Group. The extension ended at Upper Carboniferous.

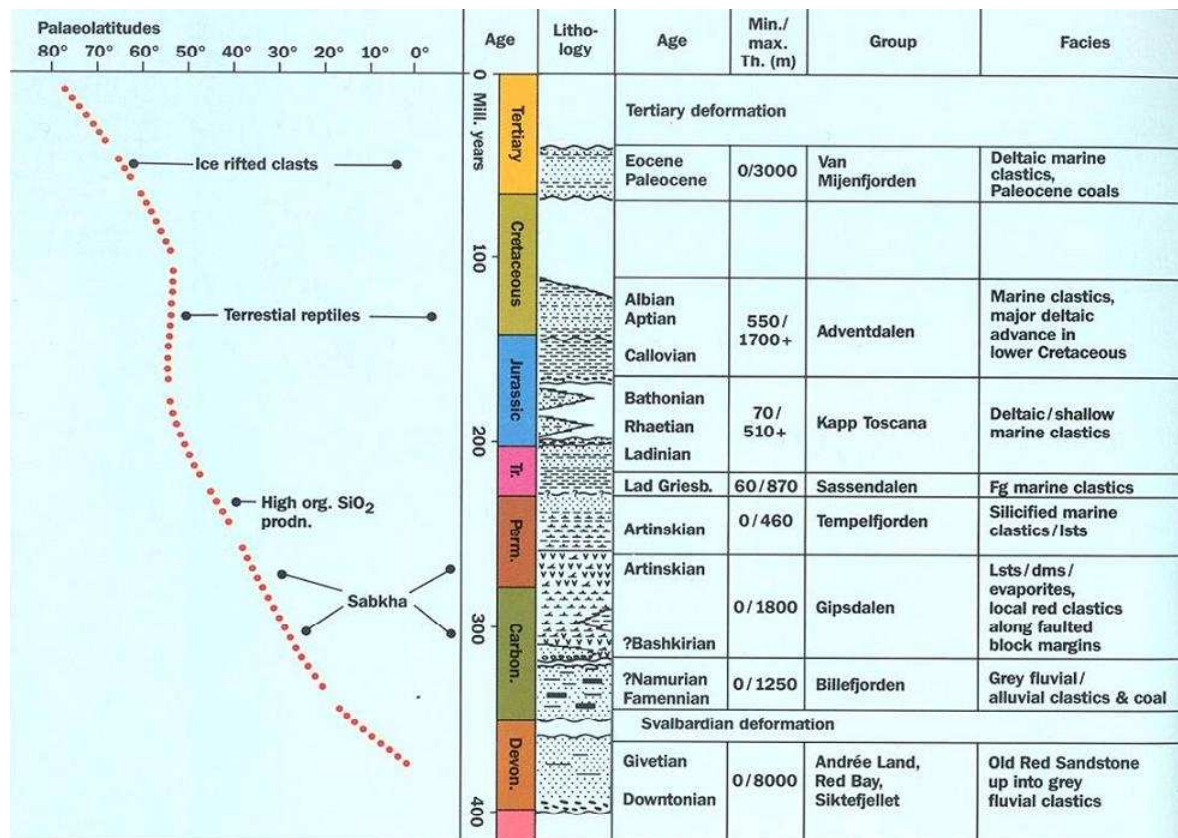
*Upper Permian to Early Triassic* → Beginning of a new clastic deposition of deep cold water siliciclastic sediments. Its fossiliferous contents indicate high organic productivity. Mudstones and organic-rich shales were deposited on the siliceous units, constituting a potential hydrocarbon source rock (Worsley & Aga 1986).

*Late Triassic to Late Cretaceous* → In general terms, the Triassic, Jurassic and Cretaceous period was dominated by mudstone, sandstone and siltstone deposition under temperate conditions. The Mesozoic clastic successions consist of delta-related coastal and shallow shelf sediments. No major tectonic movements are recorded but an overall uplift. A first sign of breaking between Greenland and Europe, with the subsequent opening of the Arctic and North Atlantic Oceans at the Lower Cretaceous, are the doleritic intrusions (Grogan et al. 1998), combined with first lateral movements.

*Tertiary* → It was a period characterized by transform and convergent movements, previous to the physical separation between Greenland and Svalbard. It starts the opening of the Polar

Basin or Arctic Sea and the North Atlantic Ocean. These convergent movements thrust the Mesozoic cover and part of the Basement, uplifting the western Svalbard and creating an associated foreland basin. It is known as the Tertiary Basin, where Paleocene and Eocene clastic sediments and peat were deposited (Dallmann et al. 1999).

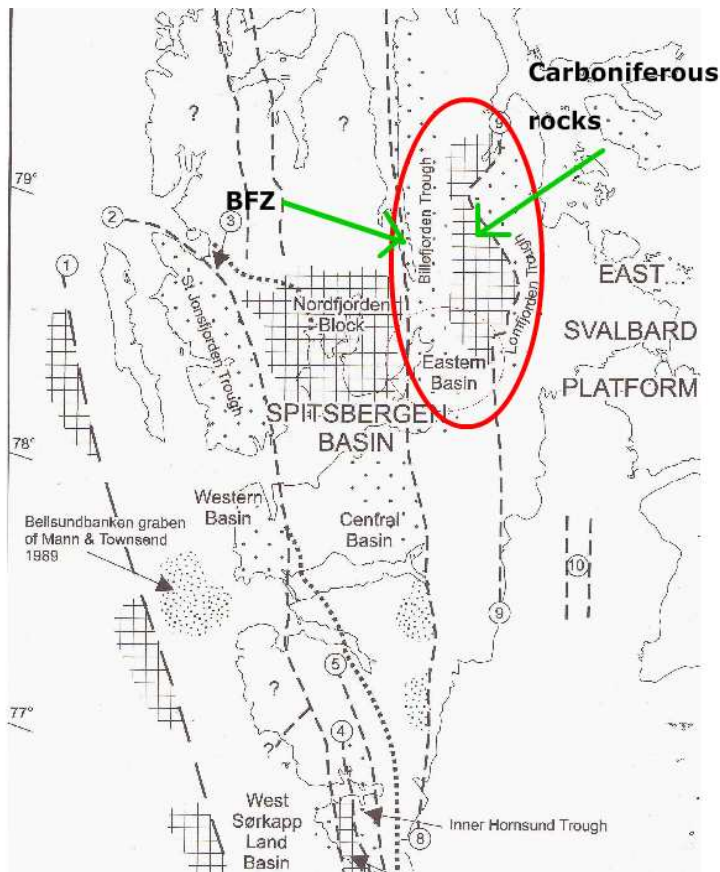
*Quaternary* → The Quaternary is the last stage in the geological history of Svalbard, marked by the Neogene glaciations and volcanic activity in NW of Spitsbergen. In present times, Svalbard and the Barents Shelf experience uplift from a post-glacial rebound (Dallmann et al. 1999).



**Figure 1.8** Summary of the sedimentological history of Svalbard together with its overall northward displacement. The table displays the lithology and depositional age of each formation from Late Silurian to Tertiary. The paleolatitude of the Svalbard archipelago through geological time is shown to the left side of the picture (Worsley & Aga 1986)

## 1.2 Focus on the Billefjorden Trough, Central Basin

We focus our attention on the Central Basin, particularly on the Billefjorden Trough, where Permo-Carboniferous sedimentation has been preserved until Recent. The most characteristic feature is the Billefjorden Fault Zone (BFZ). It is an area located in centre-west of Spitsbergen, with well-delimited western and eastern margins. The western margin is dominated by the BFZ, which controls the trough-shaped basin. It sets in contact Devonian rocks on the western side of the BFZ with the eastern Carboniferous rocks (Figure 1.9).



**Figure 1.9** Map of Spitsbergen where the boundaries of the several basins and main fault lineations are shown in dashed lines: the Central Basin, the Eastern Basin and the Western Basin. The Eastern Basin is the focus of our study Lomfjorden Fault in number 9. (Modified from Harland 1997).

### 1.2.1 Structural framework

Towards the north west of the Billefjorden Trough, the so Billefjorden Fault Zone emplaces a belt of Pre-Caledonian rocks between the Devonian and Carboniferous rocks. On

the eastern side, the Billefjorden Trough is limited by Carboniferous carbonates and evaporites (Figure 1.9).

Both sedimentary and igneous basement rocks, adjacent to the BFZ, underwent deformation mainly due to the Paleozoic transpressive movements of horizontal dislocation (Rackiewicz 2002 ; Witt-Nilsson 1997).

The metamorphosed basement rocks have a determinant influence on the deposition of the unconformably overlying Paleozoic cover. They influence differential deposition, erosion and deformation of the Permo-Carboniferous sequence, providing an inherited framework (Harland 1997).

Differential deposition and facies changes along the sequence are also fault-controlled. The Spitsbergen basin may be divided in blocks and troughs as well as into three Paleozoic depositional basins defined by N-S lineaments and separated by highs: the Central Basin, the Western Basin and the Eastern Basin (Figure 1.9). The currently eroded Mesozoic sedimentation on the Billefjorden Trough was mainly controlled by faults and basement. The Eastern Basin (the eastern member of the Central Spitsbergen Basin) can be divided into the Lomfjorden Trough and the Billefjorden Trough. The lastest is object of our more thorough analysis.

### 1.2.2 Local stratigraphy

The vertical column of sediments preserved in the Billefjorden Trough can be divided into four different sequences, occasionally separated by unconformities. The most noticeable

unconformities are:

- 1) Disconformity between the Lower Carboniferous Billefjorden Group and the Upper Carboniferous Wordiekammen Formation (hiatus on the Billefjorden Fault Zone)
- 2) Angular unconformity between the Minkinfjellet Formation and Ebbadalen Formation.
- 3) Nonconformity between the metamorphic basement rocks and the sediments of the Billefjorden Group.

We give special emphasis on the thick Carboniferous carbonate deposition.

#### 1.2.2.1 Hekla Hoek Pre-Cambrian to Silurian rocks

The Hekla Hoek basement is also present in Central Spitsbergen, in the Billefjorden Trough, as isolated outcrops of resistant dark rocks. Its formation was as consequence of the E-W collision between two continental plates: Laurentia-Greenland and the Fennoscandian-Baltica plates (Caledonian Orogeny), forming a huge mountain range. The lithologies exposed in the Central Basin consist of gneisses, schists, phyllites, quartzites, marbles and granites. They are separated from the Paleozoic sediments by an unconformity derived from the uplift (Stemmerik & Worsley 2005).

The basement is distinguished into Proto-Basement and Basement (Harland 1997). The Proto-Basement is referred to those rocks that existed before the E-W compression, transforming the pre-existing rocks into its metamorphic equivalents. It is therefore believed that the proto-basement rocks are Mesoproterozoic with Paleoproterozoic protoliths. The

basement rocks form a pronounced geoanticlinal structure underlying the Paleozoic sequence (Harland 1997)

#### 1.2.2.2 Devonian rocks

The Devonian Old Red Sandstone and fluvial sediments are found on the western side of the Billefjorden Fault Zone, in the Central Basin. It is not preserved in the Billefjorden Trough itself. The red sandstones, breccias and conglomerates of the Devonian Old Red Sandstone were generated by the uplift of the Caledonian range. They were deposited in extensional basins, and not according to a strike-slip basin model (McClay et al. 1986).

Devonian outcrops are located northwest from the Billefjorden Trough. Its location and preservation to the northwest is related to the BFZ. The Devonian Old Red Sandstone rocks are exposed northwest in a half graben similar to the Billefjorden half-graben with an active western margin. The Balliolbreen Fault is the principal feature of the BFZ separating Devonian to the west and Pre-Cambrian rocks to the north-east Spitsbergen (Lamar & Douglass 1995 ; Haremo et al. 1990).

The Devonian sediments are older than the Permo-Carboniferous sequence, well-developed in the west of the Billefjorden Fault Zone (BFZ), and located exactly adjacent but further north. The northern position is explained by the dextral Late Devonian - Early Carboniferous transpressive Svalbardian Movements which brought the terranes of the BFZ hundreds of kilometres to the north. However, the practical absence of Devonian sediments in the Billefjorden Trough exposures has its explanation on the control exert by the BFZ through lateral displacement.

The Old Red Sandstone was deposited in a half-graben with a western tectonically active margin and an inactive eastern margin. The absence of Devonian sediments in Ny Friesland (Figure 1.1, North Spitsbergen) and east of the BFZ can be explained because of a rapid eastward pinchout of Devonian Old Red Sandstone units (Lamar & Douglass 1995) , combined with a tectonic subsidence controlled by the BFZ (Balliolbreen Fault).

The Late Devonian to Silurian was characterised by reactivation of strike-slip along the BFZ with the formation of sedimentary basins. These basins accommodated the deposition of the Old Red sediments, grading up to fluvial and alluvial clastics, under arid environments since Svalbard was positioned close to the equator.

#### 1.2.2.3 Permo-Carboniferous rocks

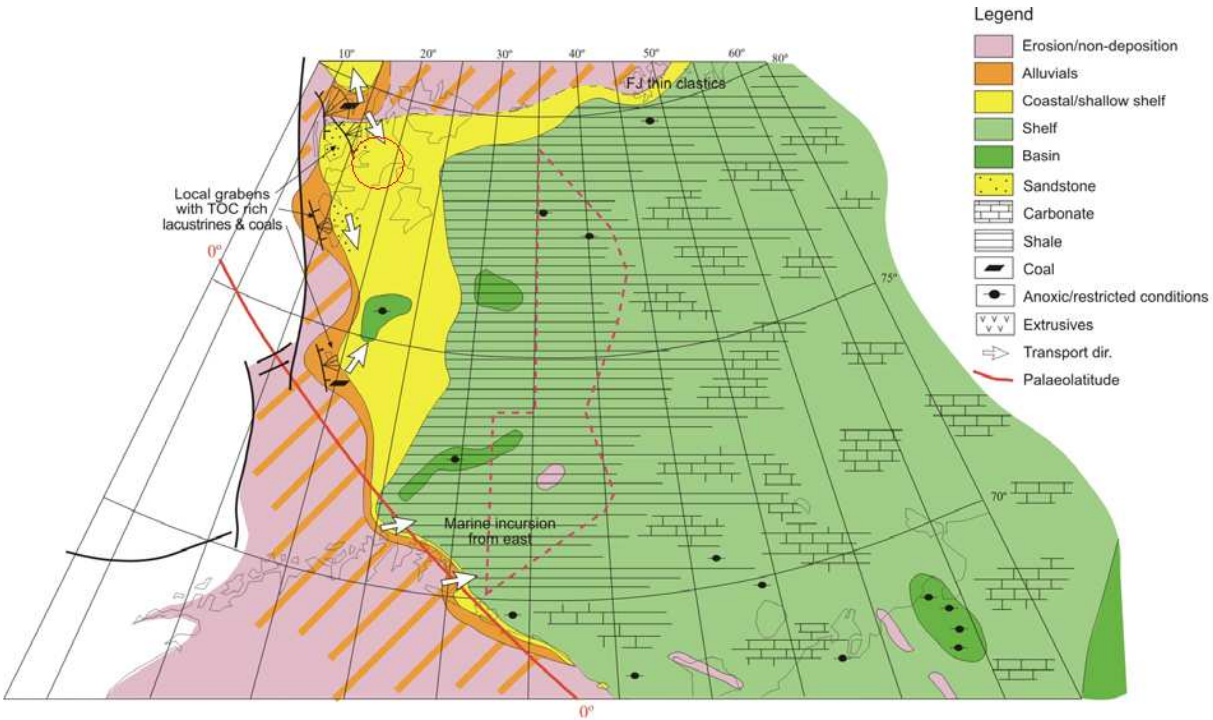
The Carboniferous sediments overlie the Devonian succession in an angular unconformity controlled by the BFZ deformational movements. On the eastern side of the BFZ, the Permo-Carboniferous strata lie directly unconformably over the basement. For clarity, we have divided the succession into Lower Carboniferous, Mid-Carboniferous, Upper-Carboniferous and Permian.

*Lower Carboniferous* → Accumulation during the Early Carboniferous period was controlled by basement features, especially in areas where Devonian sediments were absent (Figure 1.10).

Climate is a second factor controlling deposition. Due to the equatorial location of Svalbard during the Lower Carboniferous, climate was warm and humid, with a high water



table resulting in reducing conditions (Harland 1997). The water table was a control on the facies. The earliest Carboniferous sediments contain the Old Red Sandstone characteristics although the reducing conditions controled the deposition of deltaic facies such as coals, silt, shales and ironstones. The predominant reducing conditions where a key factor in order to preserve the organic matter which later became a regional hydrocarbon source rock in the Barents Shelf.



**Figure 1.10** N-S Paleo-geological map of the Barents Shelf showing paleo-environments and the lithologies deposited during Lower Carboniferous. The red circle shown on the northwestern corner corresponds to a terrigenous-dominated Lower Carboniferous deposition on Svalbard and Barents Shelf (Modified from Worsley 2006)

The lithostratigraphy consists of terrestrial sedimentation of continental sandstones shales and coals, as well as conglomerates, within a regressive depositional environment including swamps, flood plains, fluvial fans and lakes, typical of deltaic areas. All the Lower Carboniferous sediments were deposited in an elongated half-graben basin under tectonic control. (Harland 1997 ; Dallmann et al. 1999).

The deposition in the Billefjorden Trough was dominated by non-marine tropical humid clastics. They postdate the basement and lie immediately over the Upper Devonians are the Hørbyebreen and Mumien Formations of the Billefjorden Group (Steel & Worsley 1984 ; Worsley 2006).

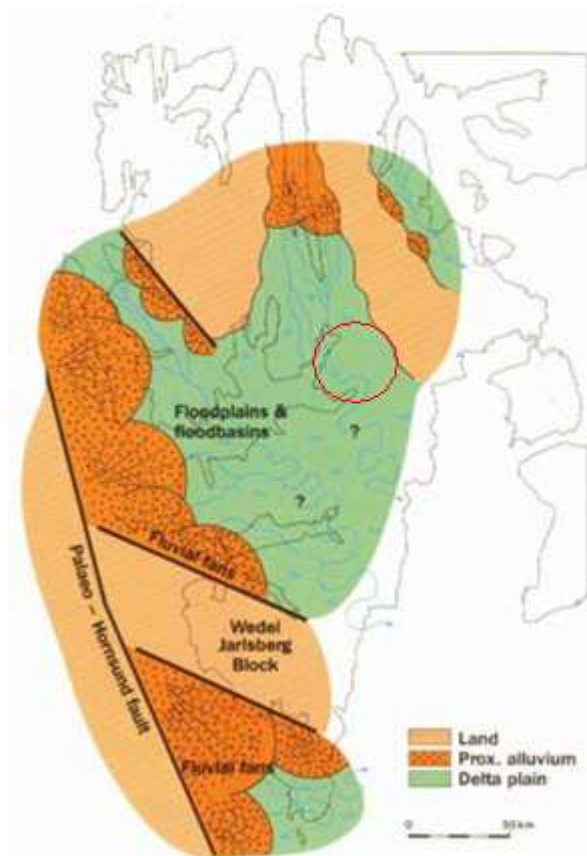
*Mid-Carboniferous* → The Mid-Carboniferous sediments were deposited during a period characterised by frequent sea level changes in warm and arid to semi-arid climate, reflecting the northern drift of Svalbard (Worsley 2006). After the Serpukhovian uplift (Lower Carboniferous), an extensional period of rifting begins. The extension was mainly concentrated along the BFZ and other adjacent faults, creating subsidence east of the structure (Harland 1974; McCann & Dallmann 1996).

The lithostratigraphy is dominated by sabkha evaporites and shallow marine carbonates coupled with a regional rise in sea level (Figure 1.11). Within the carbonate dominated sequence horizons of sandstone and shale are present (Eliassen & Talbot 2003). In the most distal parts of the recently-formed graben is where the carbonates, gypsum and evaporites started to precipitate. In the most proximal graben margins the sedimentation was still dominated by siliciclastics (Stemmerik & Worsley 2005). These sediments formed the Ebbadalen and Minkinfjellet Formations, further on referred as potential reservoir rocks in the study area.

This is a period dominated by extension concentrated along the BFZ, causing the formation of the Billefjorden Trough to the east (Serpukhovian uplift). Previous to the extension, regional uplift is recorded by a break in the deposition and angular unconformity at

the base of the Bashkirian-Moscovian. The unconformity controls the sedimentation by abrupt facies changes (Harland 1997).

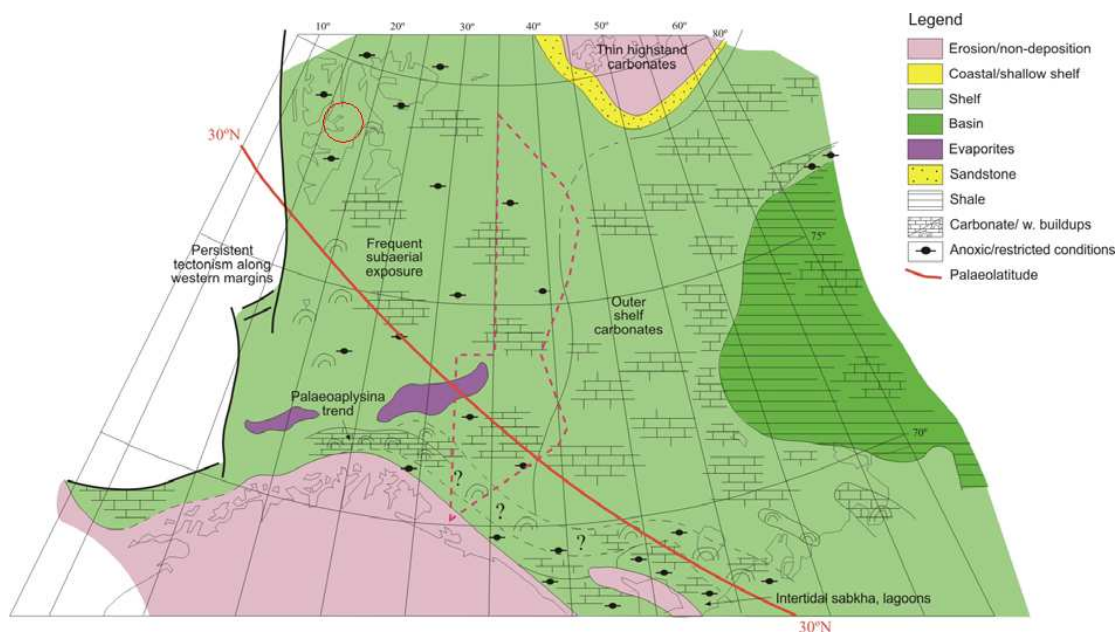
The marine sediments deposited during this period are the Ebbadalen and Minkinfjellet Formations (Gipsdalen Group). The marine syn-rift infill of the Billefjorden Trough is started by the deposition of the Ebbadalen Formation. It contains clastics from the uplifted Nordfjorden High, still not transgressed (Sundsbo 1982). The syn-rift Minkinfjellet Formation is more strongly transgressive. The deposition turned into purely carbonatic sedimentation once the structural highs, the source of clastics, were drowned (Eliassen & Talbot 2003).



**Figure 1.11** N-S Paleogeological map and legend of the lithologies deposited during Mid Carboniferous. The red circle on the northeastern corner, shows the paleogeography of the Billefjorden Trough. The clastic sedimentation is now restricted to the graben margins with deposition of sabkha evaporites within. (Modified from Worsley & Aga 1986)

*Upper Carboniferous-Early Permian* → This period starts with the establishment of humid temperate conditions with a renewed transgression towards open marine conditions.

The Carboniferous-Early Permian was a period characterized by carbonate build-ups in shallow areas, deposited together with some organic limestones. The repeated cycles of sub-aerial exposure and transgression continue along this period. During regression, sabkha plains developed in the basin margins (Figure 1.12). The dominant lithologies are carbonates, oftenly dolomitised, associated with evaporites (Stemmerik & Worsley 2005; Steel & Worsley 1984). A new flooding during the Early Sakmarian (Early Permian) determines the end of evaporitic sedimentation. The basins became better connected with the open sea and the weather changed into rather humid conditions.



**Figure 1.12** N-S Paleogeological map and legend of the lithologies deposited during Upper Carboniferous. The red circle on the north-western corner, shows the paleogeography of the Billefjorden Trough. It is a carbonate-dominated sedimentation. It represents an overall transgression, depositing carbonates and evaporites with eventual organic limestones when the anoxic conditions prevailed. (Modified from Worsley 2006)

A slight unconformity between Late Carboniferous and Early Permian strata indicates that the Nordfjorden block was sub-aerially exposed and eroded before the first Permian transgression. The Permian transgression resulted in moderate deepening with deeper shelf environments and periods of anoxic conditions (Sundsbø 1982).

The major faults were overlapped by sedimentation and started to hold a less important control on sedimentation. Consequently, the marine transgression was coupled by the shift into a more stable tectonic regime (Harland 1974,1997).

The Wordiekammen Formation records the transgressive event. It was deposited throughout this period of transgressive-regressive post-rift sediments in more opened conditions and lithologically constituted by carbonates, evaporites and minor shales (Eliassen & Talbot 2005).

#### 1.2.2.4 Quaternary Sediments

The most recent sediments are Neogen, though uplifting and glacial dynamics have removed an important part of them. The drainage of the western orogen brought sediments both into the western Greenland-Norwegian basins and east to the Central Basin (Harland1997).

In our location in the Eastern Basin of the Central Spitsbergen Basin, the Quaternary sediments consist of a cover of glacio-marine muds sands and gravels as well as glacio-fluvial sediments transported during the summer season when the ice partly melts down (Rachlewicz 2002). The most noticeable recent geological feature is the sedimentary cover of slope

sediments partly masking the outcrops, derived from weathering and denudation of the adjacent relief after the last glacial period and uplift.

### **1.3 The Løvehovden area**

The Permo-Carboniferous sequence of the Løvehovden area is located in northern Billefjord, east of Petuniabukta. The outcrop is delimited by the Ragnar valley to the north and the Ebba valley to the south, and features an excellent 3D exposure.

#### **1.3.1 History of investigation**

The first geological studies carried out on Svalbard are reported from the beginning of the 19<sup>th</sup> century. The aim was, in the very beginning, far from pure geological understanding but rather to prospect for coal and mineral deposits.

The first serious investigation for coal exploration was in 1926. Birger Johnson investigated the Bellsund, Pyramiden and Bûnsowland areas. Hoel and Orvin performed detailed studies on Carboniferous and Cretaceous sediments in 1937. At the same time, several British expeditions from Cambridge and Oxford enriched the geological knowledge of Svalbard. From 1948, annual scientific expeditions from the Norsk Polarinstitut widened the fields of research (Dallmann et al. 1999). All these initiatives contributed to divulgate the geology of Svalbard and to motivate further international research from the 1950's decade, enhanced by petroleum plays and prospects.

Works describing the geology of Svalbard from a structural and stratigraphic point of view were first carried out by Orvin (1940), Steel & Worsley 1984, Worsley & Aga (1986), McCann & Dallmann (1996), Harland (1997) and Dallmann (1999).

The Løvehovden area has been subject of multiple studies. Plenty of them applied to the Billefjorden Fault Zone and by extent to its control upon the deposition of the strata present in the Ebbadalen area. Many of the publications focused on sedimentology with emphasis in diagenesis, cementation and sequence stratigraphy of the carbonate deposition. Some of the most relevant publications are here listed showed as follows: Cutbill & Holliday (1972) first described in detail the Ebbadalen Formation followed by Johanessen (1980). In (1982) Sundsbø described the strata deposited between Lower Carboniferous-Lower Permian. A thorough description of the Minkinfjellet basin is given by Dallmann (1993) and Eliassen & Talbot (2002, 2003 (2) & 2005) who studied diagenetic, cementation and dissolution processes on the Minkinfjellet and Wordiekammen Formations. Samuelsen & Pickard (1999) offered a complete study of the regressive transgressive cycles recorded in the carbonate sequence.

Major structural studies applying to the Billefjorden Fault Zone are of especial interest for the geological reconstruction of the events recorded in the sequence exposed in Ebbadalen. The most relevant publications concerning structural descriptions of the Ebbadalen-Ragnardalen area are referred to Harland (1974). He studied the tectonic history of the Billefjorden Fault Zone. Further work was published by Lamar & Douglass (1982,1995), McCann (1993), Mandby (1994), and Friend (1997).

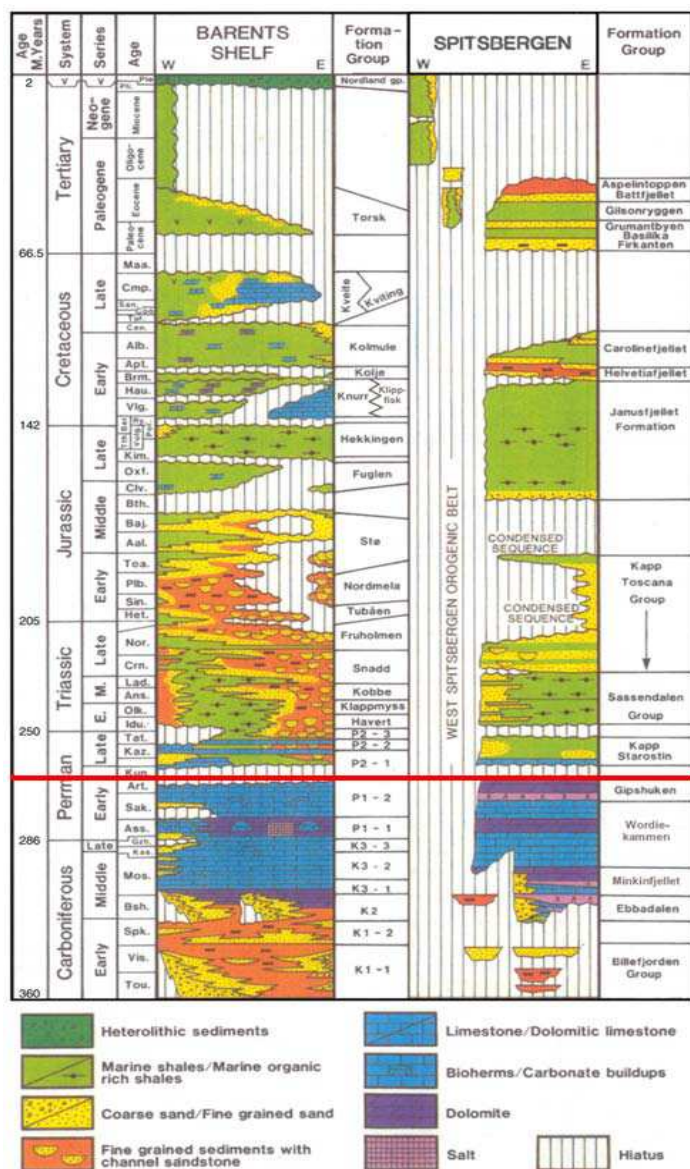
Also recent geophysical surveys have been made in the zone with the aim of modelling the physical properties of the reservoir and to export them into the Barents Shelf. Daslegg et al. (2005) executed a recent work in georadar and resistivity measurements.

### 1.3.2 Depositional sequence in the study area

In this Section, the depositional sequence preserved and eroded in the Ebbadalen-Ragnardalen area will be described in detail. Our area corresponds to Løvehovden, located on the eastern side of the Billefjorden Trough. At 78° 43'N and 16° 43'E, the area is located between two valleys, the Ebbadalen (south) and Ragnardalen (north). To the east it limits with the Billefjorden Fault Zone. The outcrop is dominated by the Løvhovden topographic high. The western boundary is the N-S Lomfjorden fault.

Stratigraphically, the succession may be divided into the rocks that belong to the Pre-Cambrian (Mesoproterozoic) basement and the Paleozoic sedimentary cover. The Paleozoic cover is represented by the Billefjorden Group, the Gipsdalen Group (Hultberget Ebbadalen, Minkinfjellet, Wordiekammen and Gipshuken Formations) and the Kapp Starostin Formation (Figure 1.13).





**Figure 1.13** Synthetic stratigraphic column comparing the stratigraphic record on Spitsbergen and its equivalent on the Barents Shelf. The strata below the red line represent the Permo-Carboniferous sequence that we observe in Ebbadalen and its equivalent analogues on the Barents Shelf (to the left of the picture). (Modified from Nøttvedt et al. 1993)

In the Løvehovden area, the strata are preserved from the Billefjorden Group to the Wordiekammen Formation. The Gipshuken Formation is preserved further south in Billefjorden and the Kapp Starostin Formation west of the BFZ (Dallmann et al. 2004).

Figure 1.13 shows the Mesozoic and Tertiary sedimentary sequence deposited over the Upper Permian Kapp Starostin Formation. The Mesozoic and Tertiary strata have been eroded in the study area although their equivalent analogues are present in the Barents Shelf and other parts of Spitsbergen.



#### 1.3.2.1.1 Basement rocks (*Paleo-Proterozoic to Meso-Proterozoic*)

The basement is poorly exposed in the Ebbadalen-Ragnardalen area, though at least five units are recognised from the Geological Map according to Dallmann et al. (2004):

Polhem unit (upper part) → quartzite and amphibolite

Polhem unit (lower part) → mica, schist and amphibolite

Smutsbreen unit → garnet mica schist, calcic-pelitic mica schist and marble

Eskolabreen unit → biotite gneiss, amphibolite and granitic gneiss

Distinct marble layers are also present.

#### 1.3.2.1.2 Paleozoic

The Paleozoic strata are represented by the Billefjorden Group and the Gipsdalen Group. From the Gipsdalen Group, the Gipsuken and Kapp Starostin Formations have been eroded at the Ebbadalen-Ragnardalen area, although they are preserved at the vicinity of the study area. The Mesozoic and Tertiary strata are eroded in the study area, although present into the Barents Shelf. A brief description of the eroded sequence will be given in this Section.

#### Billefjorden Group (*Upper Devonian-Early Carboniferous*)

The Billefjorden Group is constituted by the Hørbyebreen and Mumien Formations. The general lithology is terrigenous, with clastics and local coal seams (Dallmann et al.

1999). It was deposited in angular unconformity over the Mesoproterozoic basement, unconformably over Devonian strata to the west.

#### *Hørbyebreen Formation (Famennian-Tournassian)*

Lithology → The Hørbyebreen Formation consists of sandstones, conglomerates, shale and coal deposited in cyclic sequences. The sandstones and conglomerates form the lower part (Triungen Member). The upper part of the Formation consists of black/grey shales and mudstones interbedded with thin sandstones, coals and coaly shales (Dallmann et al. 1999). (See Appendix I for stratigraphic column)

Depositional environment → The terrestrial materials are interpreted as part of a continental setting within a small restricted basin (Harland 1997). Sandstones and conglomerates are of fluvial origin, interbedded with shales and coals. They are of lacustrine origin, representing the periodic flooding of the flood plain, controlling the mentioned cyclicity (Dallmann et al. 1999).

Lithology → The Mumien Formation consists of sandstone, shale and coal. The lower part (Sporehøgda Member) consists of massive coarse-grained sandstone and minor shale occurrences. The upper part (Birger Johnsonfjellet Member) is characterised by a change from sandstone to coal bearing shales, with abundant coal seams and siltstone (Dallmann et al. 1999). (See Appendix I for stratigraphic column)

Depositional environment → The deposition of this terrestrial unit was fluvial-dominated. It begins with sandstone units and evolves upwards into lacustrine and flood-plain deposits,

highly vegetated given that the coals are composed of lacustrine algae (Harland 1997; Dallmann et al. 1999).

#### Gipsdalen Group (Upper Carboniferous-Early Permian)

The Gipsdalen Group is the best exposed in the Ebbadalen-Ragnardalen outcrop. Early Gipsdalen Group deposition strata are characterized by Early to Upper Carboniferous clastic deposition. During Middle to Late Carboniferous and Permian time, carbonates and evaporites deposited in a fault-controlled subsiding graben.

The Gipsdalen Group lies unconformably over the Billefjorden Group, separated by a hiatus. The Group is comprised of five Formations, from top to bottom: Gipshuken, Wordiekammen, Minkinfjellet, Ebbadalen and Hultberget. The Campbellryggen Subgroup collects the Minkinfjellet, Ebbadalen and Hultberget Formations (Dallmann et al. 1999).

#### *Hultberget Formation (Late Serpukhovian)*

The Hultberget Formation marks a sharp depositional change from the coal bearing shales of the Mumien Formation into the red sandstones of the Hultberget Formation. The contact between both units is sharp (Dallmann et al. 1999).

Lithology → It is featured by red and purple shale, sandstone, siltstone and conglomerates. The sandstones are medium to fine grained in contrast to the massive package initially deposited in the Hørbyebreen Formation. The lithologies alternate each other in the sequence. (See Appendix I for stratigraphic column).

Depositional environment → The strata to represent stream and overbank deposits adjacent to alluvial fans (Harland 1997 ; Dallmann et al. 1999).

#### *Ebbadalen Formation (Bashkirian)*

The Ebbadalen Formation includes the Odellfjellet, Tricolorfjellet and Ebbaelva Members. Of these three, only the Tricolorfjellet and Ebbaelva Members are represented in our area of study whereas the Odellfjellet Member is only present west by the Billefjorden Fault Zone. The deposition of the Ebbadalen Formation was strongly controlled by the BFZ. Therefore lateral facies changes are common. The sedimentary sequence thins away from the fault and diminishes its thickness towards the western side of the graben (Harland 1997).

Lithology → Clastics, carbonates and evaporites are the main lithologies. The lower part of the Formation is constituted by sandstones and shales. The upper part presents carbonates and evaporites. The evaporites are diagenetic and the primary sulphate mineral is gypsum. Processes of solution and reprecipitation formed anhydrite (Eliassen & Talbot 2003 ; Shreiber & Helman 2005). (See Appendix I for stratigraphic column).

Depositional environment → It changes from continental to marine, including lagoons, lakes, mouth bars, fan deltas, braided systems and shoreface as well as sabkha playas (Dallmann 1999 from Johannessen & Steel 1992).

*Ebbaelva Member:* The Ebbaelva Member is constituted of grey and yellow sandstone interbedded with grey green shales and occasionally carbonates and evaporites, especially in

the uppermost part. The depositional environment is highly variable including lakes, lagoon, shoreface, mouth bars, braided streams, sabkhas and fan deltas (Dallmann et al. 1999).

*Tricolorfjellet Member:* The Tricolorfjellet Member contains gypsum and anhydrite interbedded with carbonates. To the west BFZ, the evaporites grade laterally into shales and sandstones from the Odellfjellet Member, only present west of the Billefjorden Fault Zone (Harland 1997). This interfingering with the Odellfjellet Member is interpreted as distal alluvial fans. The gypsum and anhydrite were accumulated in sabkha deposits (Harland 1997).

#### *Minkinfjellet Formation (Moscovian-Early Kasimovian)*

The Minkinfjellet Formation is represented only in the Billefjorden Trough. As well as the Ebbadalen Formation, it represents syn-rift deposition in a graben structure, controlled by the BFZ. In the Ebbadalen-Ragnardalen area the three members of the Minkinfjellet Formation are present. The lower member is the Carronelva and the upper is the Terrierfjellet Member. The boundary between these two Members is difficult to interpret in the outcrop since it is mainly covered by loose stones and rock debris (Dallmann et al. 2004). Laterally transitional with the Tricolorfjellet Member, the Fortet Member is well-exposed in the zone.

Lithology → The Minkinfjellet Formation consists mainly of carbonates, sandstones and evaporites. The Formation is characterized by lateral facies variations. More into detail, the lithology includes sandstones, limestones, dolomites, carbonate breccias and subordinate anhydrite/gypsum (Dallmann et al. 1999). (See Appendix I for stratigraphic column).

Depositional environment → The depositional setting is dominated by sabhka and shallow subtidal environments. The conditions range from shallow marine to open marine with several episodes of sub-aerial exposure, generating karst deposits (Eliassen & Talbot 2003).

*Carronelva Member (Early Moscovian):* Lithologically dominated by clastic and carbonate. It lies directly over the Tricolorfjellet Member of the Ebbadalen Formation. It evidences the transition from the evaporite-dominated deposition of the Tricolorfjellet into carbonate-dominated deposition of the Minkinfjellet. The base of the Carronelva Member contains coarse-grained conglomerates and sandstones (Harland 1997). The upper part consists of limestones, shale and marls. The deposition took place in peritidal to sub-tidal environments (Dallmann et al. 1999).

*Terrierfjellet Member (Moscovian - Early Kasimovian):* It is dolomite dominated, interbedded with minor marls and marly limestones (Harland 1997). The content of gypsum decreases upwards along the Minkinfjellet Formation leading the Terrierfjellet Member to rarely present gypsum levels. It was deposited in restricted marine deposits.

*Fortet Member (age ambiguous):* The Fortet Member consists of a thick succession of collapse breccia formed by the dissolution of the gypsum layers that originally lay within the Terrierfjellet Member (Eliassen & Talbot 2003). It presents high breccia porosity. The origin of these breccias has been widely discussed. The solution collapse origin theory is held by (Eliassen & Talbot 2003 ; Sundsbø 1982) though earthquake origin is also suggested (Dallmann 1993).



### *Wordiekammen Formation (Late Moscovian-Early Sakmarian)*

The Wordiekammen Formation consists of two Members, the Cadellfjellet and Tyrrellfjellet Members. The Cadellfjellet Member is not evident in the Ebbadalen-Ragnardalen study area.

Lithology → The base of the Wordiekammen Formation is characterized by a shift from the dolomite dominated underlying Minkinfjellet Formation into a more limestone-dominated sequence. The dominant lithology is limestone although bituminous matter is common. (See Appendix I for stratigraphic column).

Depositional environment → It was deposited in open to semi-restricted shallow sub-tidal marine and restricted inter-tidal to supratidal environments (Dallmann et al. 1999).

*Black Crag Beds:* The Black Crag Beds form the lower part of the Wordiekammen Formation in the study area. They are massive or thickly bedded black to grey fine-grained limestone interbedded with layers of fossiliferous, porous wackestone and packstone (Dallmann et al. 1999). They are characterized by the presence of breccia pipes cutting through the layering, interpreted as collapse breccia pipes (Nordeide 2008).

### *Gipshuken Formation (Late Sakmarian-Early Artinskian)*

The Gipshuken Formation has been eroded from the Ebbadalen-Ragnardalen area though is still present on topographic highs of the concomitant regions to the west of the BFZ. It is found in the Wordiekammen area, in south Billefjorden.

Lithology → Dominated by carbonates, evaporites and minor sandstones. Limestone/dolomite and gypsum/anhydrite were deposited in rhythmic sequences. The evaporitic strata are locally massive but in general shows lamination. The anhydrite deposits present karstic features. The sediments appear to have been completely dolomitised and the lower part of the Gipsshuken Formation contains carbonate breccias (Harland 1997).

Depositional environment → The Gypsshuken Formation was deposited in warm seas with restricted water circulation and arid climatological conditions that favoured the evaporitic chemical precipitation. Lagoonal, tidal flat and sabkha deposits are the typical environments where these sediments may be deposited (Harland 1997).

#### *Kapp Starostin Formation (Late Artinskian-Kazanian)*

Lithology → The Kapp Starostin Formation is dominated by biogenic chert deposition along with siliceous shale, sandstone and limestone (Dallmann et al. 1999).

Depositional environment → The sediments from the Kapp Starostin Formation were deposited in deep marine shelf conditions, with high biogenic productivity.

#### 1.3.2.1.3 Mesozoic-Tertiary

According to Michelsen & Khorasani (1991), 3900 meters of sediment were deposited on the study area, from which 2850 were Mesozoic and Tertiary strata.

Carbonate deposition prevailed during the Carboniferous and Permian periods, although from the Mesozoic era, a change into clastic deposition is recorded during the entire Mesozoic. All the Mesozoic sedimentary episodes led to sedimentation across Svalbard (Dallmann et al. 1999). The Mesozoic sequence is divided into three lithostratigraphic groups:

*Mesozoic:*

*Sassendalen Group (Lower Triassic)* → The lower unit is characterized by shallow marine grading to siltstones and sandstones deposited in coastal environments. The middle unit is shale and sandstone-dominated and the upper unit consists of phosphatic organic rich shales and minor sandstones (Dallmann et al. 1999).

*Kapp Toscana Group (Upper Triassic-Middle Jurassic)* → The lower unit (Storfjorden Subgroup) comprises shallow marine and coastal deposits of sandstones and claystones. The middle unit (Realgrunnen Subgroup) consists as well of sandstones deposited in coastal and shallow marine environments. The upper unit (Wilhelmøya Subgroup) is the condensed marine equivalent of the Realgrunnen Subgroup and consists conglomerates rich in phosphatic nodules (Dallmann et al. 1999).

In present times, the Tertiary rocks on Svalbard are confined to small isolated basins. The most outstanding of all is the Tertiary Basin. In Spitsbergen, the Tertiary sedimentary record is comprised by the Van Mijenfjorden Group.

*Tertiary:*

*Van Mijenfjorden Group (Eocene-Paleocene)* → The Van Mijenfjorden Group is basically a clastic sequence of sandstone, siltstone, shales and subordinate coals and conglomerates. The Tertiary strata represent delta-related shelf sedimentation.

#### 1.3.2.2 Carboniferous sequence stratigraphic framework

The Permo-Carboniferous sequence deposited and preserved in the Ebbadalen-Ragnardalen area is the result of regressive-transgressive cycles. The cycles are mainly controlled by climatic and tectonic processes, which regulate sediment supply and accommodation space through sea level changes (Coe et al. 2005).

The global climatic processes have been related to glacioeustasy and thermal expansion. This was locally modified by the extensional fault-controlled deposition for example in the Billefjorden Trough. The long term stratigraphic cycles would correspond to eustatic sea level changes and the short-term cycles by tectonic activity (Samuelsberg & Pickard 1999).

The stratigraphy in the Ebbadalen-Ragnardalen area records a syn-rift sequence except for the Wordiekammen Formation, which is a post-rift sequence. The deposition started in Lower Carboniferous with terrigenous shales, coals and sandstones in a delta setting during a period of regression (Billefjorden Group). Thickness variations within these continental strata document syn-sedimentary displacement on the Billefjorden Fault Zone (Sundsbo 1982). The sediments from the Upper Carboniferous and Lower Permian are instead characterized by an

increase in accommodation space during transgression (Hultberget, Ebbadalen and Minkinfjellet Formations). The sedimentation was mainly carbonatic and evaporitic with occasional terrigenous influence from subaerally exposed structural highs such as the Nordfjorden block, west of the BFZ. The overall major transgression, however, was also characterized by regressive phases. Four long term transgressive-regressive cycles have been identified in the Upper Carboniferous-Lower Permian rock succession (Samuelsberg & Pickard 1999).

The carbonate stratigraphy is cyclic; there is a vertical repetition of facies. The principal control is attributed to eustatic changes in sea-level affected by tectonic movements in the syn-rift sequence (Samuelsberg & Pickard 1999).

### 1.3.3 Structural features

The structural geology of the Billefjorden Trough, at the northmost end of Petuniabukta, reveals in a good degree of exposure the past tectonic history of Svalbard (Figure 1.15). Particularly, the BFZ records transpressional, contractional and extensional movements (Harland et al. 1974).

Following Dallmann et al. (2004) I discuss first the structures West of Petuniabukta, (Billefjorden Fault Zone) and the structures East of Petuniabukta (Ebbabreen Faults and Løvehovden Faults).



**Figure 1.15** Map of Petuniabukta, north Billefjord. The figure shows the structural lineation of the Billefjorden Fault Zone (N-S) and the axis of the Billefjorden basin. The color scheme is age-based. At the bottom-left corner, the legend shows the concrete age of the strata. (Modified from Dallmann et al. 2004)

### 1.3.3.1 The Billefjorden Fault Zone

The Billefjorden Fault Zone (BFZ) is one of the main lineations of Spitsbergen. The BFZ is located to the west of Petuniabukta, in parallel to the Løvehovden Faults. It is marked by a N-S trend, interpreted to be the result of plate interaction at least from Silurian to Tertiary times (Figure 1.16).

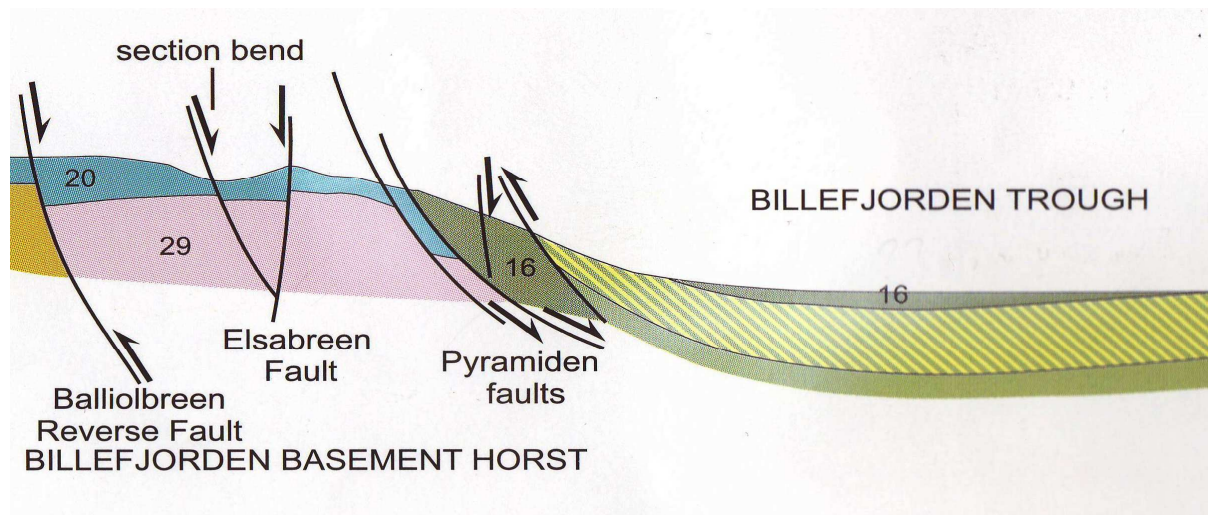
Harland et al. 1974 speculated that this lineament might have originated in a divergent context of ocean crust spreading before the closure of Iapetus. The first recorded activity

along the BFZ dates from the Silurian. In the Billefjorden area it coincides with a zone of retrograde metamorphism and shear in the Hekla Hoek basement. (Manby et al.1994). The same authors argue that the replacement of amphibolite by green schist in the shear zone suggests a maximum metamorphism achieved in Late Silurian to Early Devonian.

The first evidence of movement along the BFZ was due to strike-slip Caledonian movements. The Late Devonian to Early Carboniferous record renewed activity on the BFZ. That activity is related with the Svalbardian or Post-Caledonian movements. Sinistral strike-slip movements are interpreted by Harland et al. (1974). However, the obliqueness is not a conclusive argument to defend the strike-slip theory (Friend et al. 1994; McCann & Dallmann 1996).

Extensional normal displacements have also been recorded on the Billefjorden Fault Zone. A shorter extensional event in the Devonian age enabled the formation of the Devonian Basin and deposition of the Old Red Sandstone and fluvial clastics, controlled by the BFZ (Friend 1996). The history of activity of the Fault continues into the Mid-Carboniferous period. During the Mid-Carboniferous it was characterized by a major overall transgression and subsidence. The area east of the BFZ was down-faulted by 600-800 meters, forming the Billefjorden Trough (Sundsbø 1982). The preservation of sediment in the Billefjorden Trough has been strongly conditioned by its location on the down-faulted side. Therefore, the influence of the BFZ has conditioned sediment deposition in the Ebbadalen-Ragnardalen area.

Thicknesses measurements at the northern end of Billefjorden reveal a less pronounced down throw of approximately 150-200 meters (Sundsbø 1982).



**Figure 1.16** Cross-section across the Billefjorden Fault Zone on the west side of Petuniabukta. The Billefjorden Fault Zone is comprised by the Balliolbreen Master Fault, the Elsabreen Faults and the Pyramiden Faults. The stratigraphic units are shown in different colours: Billefjorden Group (20, blue); Old Red Sandstone (29, pink); Odellfjellet Member (16, dark grey); Tricolorfjellet Member (yellow) (Modified from Dallmann et al. 2004)

The Tertiary West Spitsbergen Orogeny has influenced in the Ebbadalen-Ragnardlen areaby stress transmission on the BFZ. Compressional Tertiary structures have been documented east from the BFZ as far as Storfjorden. That means that the BFZ has been under compressional stress.

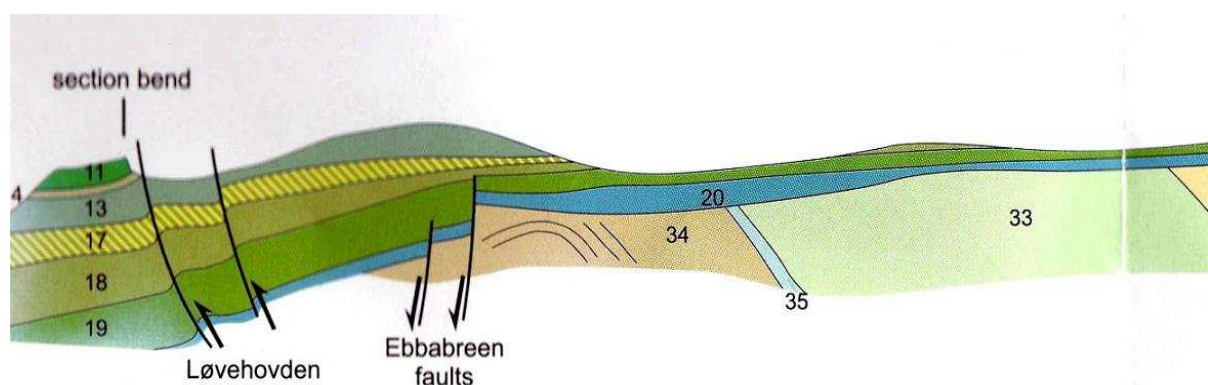
The transference of Tertiary W-E stress across Spitsbergen has triggered the formation of decollement zones in Paleozoic and Mesozoic shaly and evaporitic strata (Bergh & Andressen 1990). The stress affected the pre-Tertiary strata recognisable in the Billefjorden Fault Zone, where a decollement zone in the Ebbaelva Member formed (Figure 1.16). It is a minor thrust fault from the BFZ complex. The main faults of the BFZ are the Balliolbreen fault, the Odellfjellet fault and the Karnakfjellet fault (Manby et al. 1994).



### 1.3.3.2 The Ebbabreen and Løvehovden faults

The Ebbabreen faults consist of two steep west-dipping normal faults cutting through the basement, the Billefjorden Group and part of the Hultberget Formation (Figure 1.17). The Ebbabreen faults are located at the easternmost Ebbadalen and cut strata of Upper Devonian to Lower Carboniferous age. They predate the Permo-Carboniferous carbonate deposition. On the other hand the Løvehovden Faults date from the Mid-Carboniferous extensional period.

The Løvehovden faults have been interpreted by several authors, most recently as reverse faults by Dallmann et al. (2004) associated with Tertiary orogeny (Figure 1.17). The Løvehovden contractional faults overlie fold structures (Steffen 1999). Dallmann et al. (2004) show a map and cross-section with the Minkinfjellet, Ebbadalen and the Billefjorden Group appear to be affected by eastward-dipping reverse faults just east of the peak called Løvehovden. According to this interpretation, the faults would postdate the Permo-Carboniferous sedimentation. However, based on my fieldwork, I find only a minor E-dip Tertiary reverse fault and I interpret the Løvehovden Faults as a syn-rift fault system.



**Figure 1.17** Cross-section on Ebbadalen, east of Petuniabukta. The main faults present in the area are the Ebbabreen and Løvehovden Faults. The colours correspond to the following stratigraphic units: Metamorphic basement (33,34,35); Billefjorden Group (20,blue); Hultberget Formation (19,green); Ebbaelva Member (18,dark grey); Tricolorfjellet Member (17,yellow); Minkinfjellet Formation (13, grey); Fortet Member (4,brown); Wordiekammen Formation (11, green) (Modified from Dallmann et al. 2004)

The location of the Løvehovden and Ebbabreen faults has been described by Steffen (1999) & Dallmann et al. (2004). While the BFZ seems to have started its activity in Pre-Cambrian times, the Løvehovden and Ebbabreen faults are much more recent. The strata located east of Petuniabukta are affected by normal and reverse faults. According to Dallmann et al. (2004) they formed during the Permo-Carboniferous and Tertiary respectively.

The reverse Tertiary faults postdate most of the Carboniferous deposition. The extensional Ebbabreen Faults are overlain by the undeformed Ebbadalen succession (Dallmann 1993).

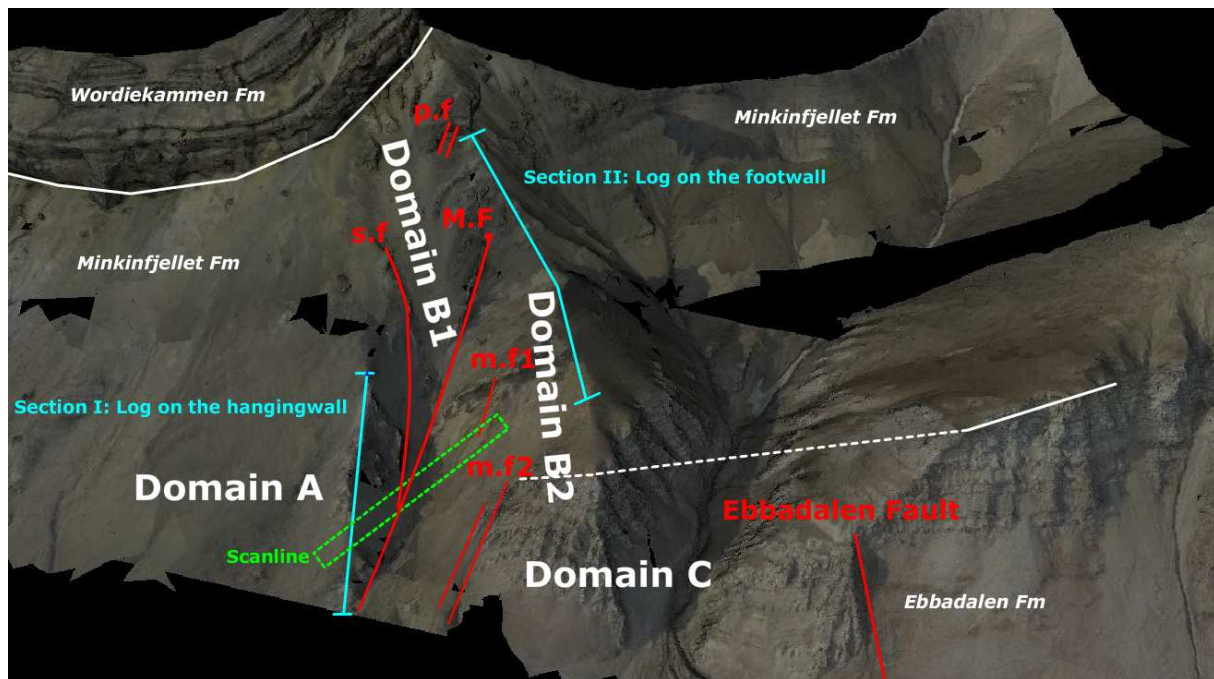
## **2. FIELDWORK DESCRIPTION AND DATA COMPILATION**

### **2.1 Methodology**

The carbonate and clastic strata were studied in two different scales: reservoir scale (approximately 2 Km) and detailed observation scale (centimetric). The first days were used on a first approach at reservoir scale, embracing the whole outcrop. This work was field-checked by several outcrop visits, both to gather new data and to verify the observations made from distance.

The second part was conducted to understand the complex Løvehovden Fault Zone, its mechanisms of formation and the relationship between the strata on both sides of the fault. In order to set up the connection between the layers from the hanging and footwall, two logs were recorded on the hangingwall and footwall respectively. The locations are shown in Figure 2.1. In addition, structural measurements of strike and dip were focused on the fault zone and strata immediately in contact with the faults.

The interpretation on the Lidar model referred as Figure 2.1 shows the distribution of the 3 different domains in which the outcrop is divided according to its relative position to the Løvehovden Fault Zone. The interpretation of the faults and stratigraphic units is performed on the Lidar data available from the area.



**Figure 2.1** Oblique view of the Løvehovden study area oriented SW-NE. The background image is a montage of photographs draped over the lidar digital topographic model. The black areas indicate no data. The red lines trace lineations here interpreted to result from faults. These lineations also define the structural domains discussed in the text. M.F = Master Fault ; s.f = secondary fault ; m.f = marginal fault; pf = propagation faults. The red dot on top of M.F indicates tip.

The location of the two logs recorded in the vicinity of the main fault and the scanline across the lowermost section of the zone complete the set of field data collection.

## 2.2 Outcrop data compilation

### 2.2.1 Domain A

Domain A lies west of the Løvehovden Fault Zone (Figure 2.1). It is characterized by a complete stratigraphic section and shows no structural complications.

*Observations:*

From base to top, Domain A starts with a non-faulted and complete carbonate and evaporitic sequence from the Minkinfjellet Formation, down to the lowest exposures in contact to the alluvial cones and the valley itself. As the strata approach an eastern lineament (“s.f” in Figure 2.1) the strata bend up. It is a feature especially obvious in the Wordiekammen Formation and the outcropping massive package of gypsum on the base of the Section I (Figure 2.1).

The base of the cliff is formed by the Black Crag Beds, the first depositional sequence of the Wordiekammen Formation, here preserved up to the top of Løvehovden. Field observations reveal that the lower Black Crag Beds are highly fractured and occasionally faulted. There are also heterogeneities at the base of the unit, where the layering is interrupted and cut through. The breccia bodies have conical to cylindrical shape.

#### *Interpretations:*

The strata present in this domain are essentially conformable and characterized by a normal drag in the vicinity of the fault zone (to the east). Interruptions in the basal Wordiekammen layering are here interpreted as breccia pipes (Sections 2.2.8.1, 2.2.8.2). There is a high degree of deformation associated to this contact. The lineament is interpreted as a normal fault called Secondary Fault (s.f).

#### 2.2.2 Domain B<sub>1</sub>

Domain B<sub>1</sub> forms a triangular area, from top to bottom, where the Master Fault and its associated secondary fault converge.

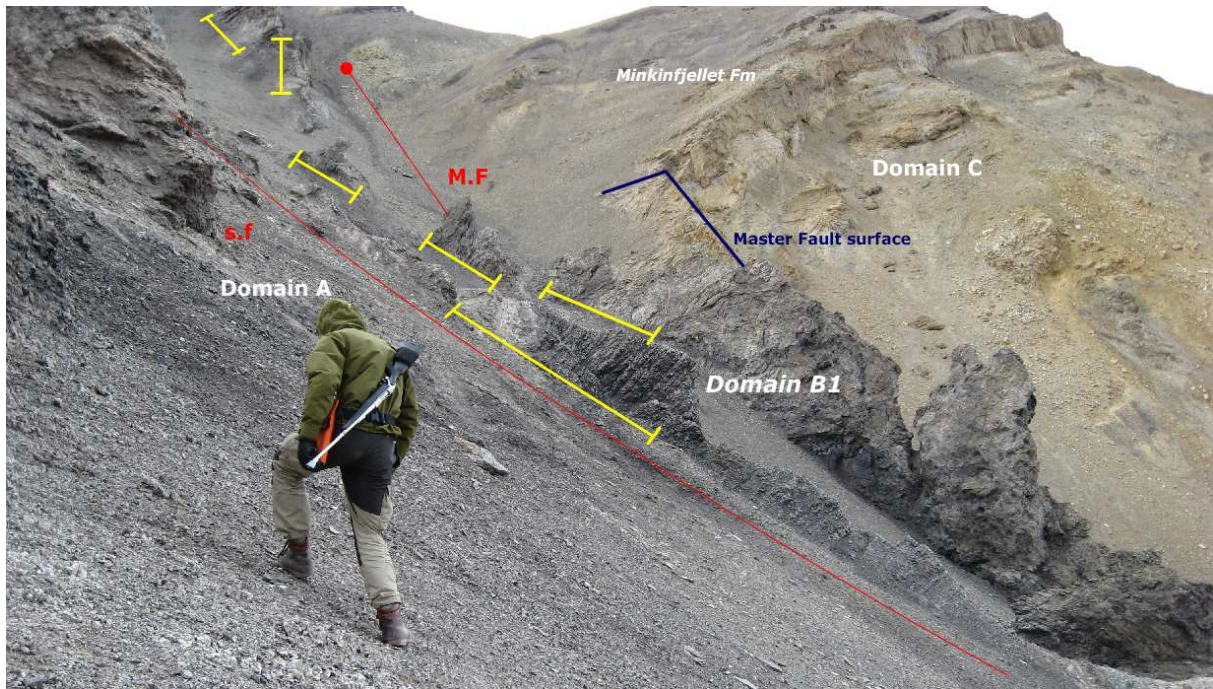
*Observations:*

The major lineament under the shortname M.F is the longest visible structure, located to the east in the B<sub>1</sub> domain. It juxtaposes the Tricolorfjellet Member evaporites with the Minkinfjellet Formation limestone as well as different levels within the Minkinfjellet Formation. Common rocks are yellow dolomites from the lower Carronelva Member of the Minkinfjellet Formation and grey shales and limestones from the upper Terrierfjellet Member (described by Harland 1997). A patch of the fault is seen as polished and striated surface oriented 310/43 SW.

In the following, the fault zone is the area encountered in Domain B<sub>1</sub>, where the beds of the Minkinfjellet Formation are rotated between the two main lineaments (M.F and s.f; Figure 2.1). Extensive rock damage is also found in Domain B<sub>2</sub>.

The fault zone is made of series of small lenticular outcrops characterized by repetition of dark highly brecciated porous limestone and dark oil-stained shales on top of white gypsum interbedded with micritic layers.

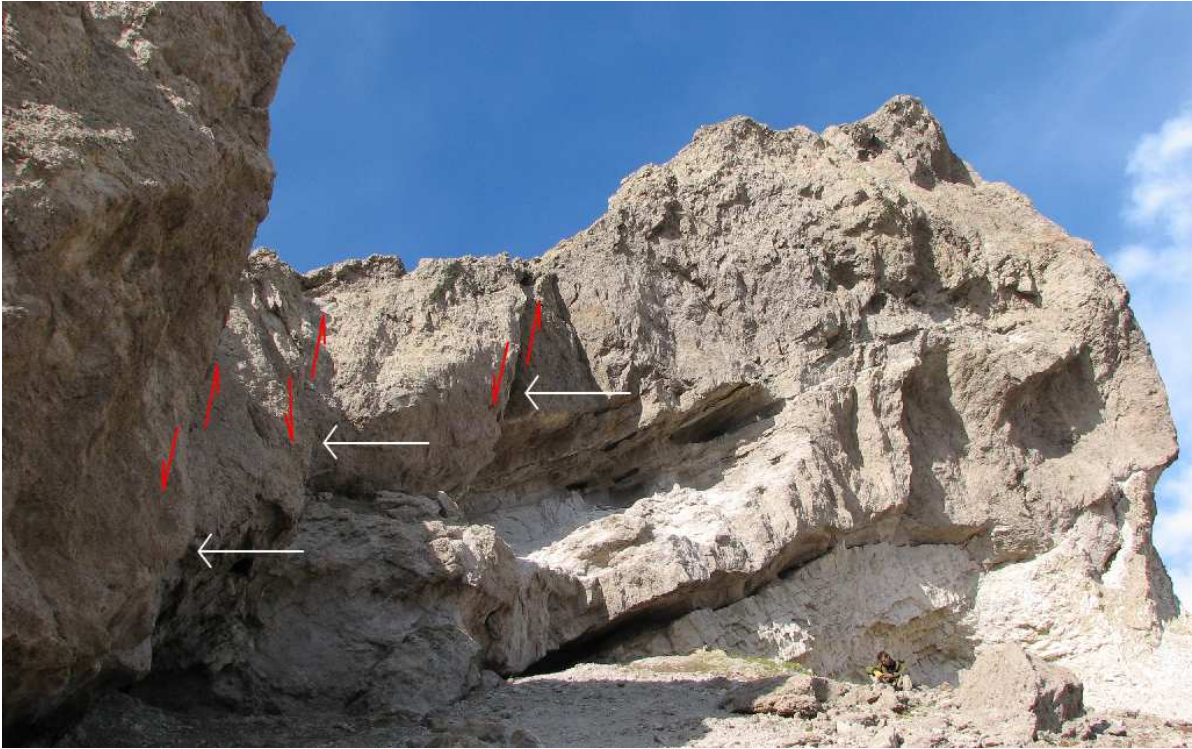
The distribution and truncation of the internal bodies of the fault zone set up a pattern nearly sub-parallel to the faults. The displacement between lenticular bodies ranges from meters to tenths of meters (Figure 2.2). Distance between the rock bodies increases close to where the M.F lineation and the Secondary Fault tend to converge.



**Figure 2.2** Løvehovden fault system, view towards east across s.f and M.F to footwall. The fault zone is characterized by constant repetition of materials from above the Master Fault tip to the lowermost part of the Domain B<sub>1</sub>. The fault zone breccias are inferred to be the fault core. The segments in yellow show the approximate extent of the repeated sequences of white gypsum, dark layered shale and breccia discussed in text. In blue, the exposed edge of the Master Fault surface. M.F = Master Fault ; s.f = secondary fault. The red dot symbolizes fault tip. The M.F extends behind the breccia outcrops.

The Secondary Fault (s.f) surface is not observed but it is seen as a lineament offsetting stratal units. Rocks marginal to the lineament show intense fracturing and deformation.

A tightly spaced set of short-displacement faults affect rocks above the tips of the M.F lineation and the s.f, higher in the slope. This is well expressed where it intersects a 30 meters thick layer of massive white limestone at the top of the Minkinfjellet Formation. The set of parallel faults has total displacements of around 20 m (Figure 2.3).

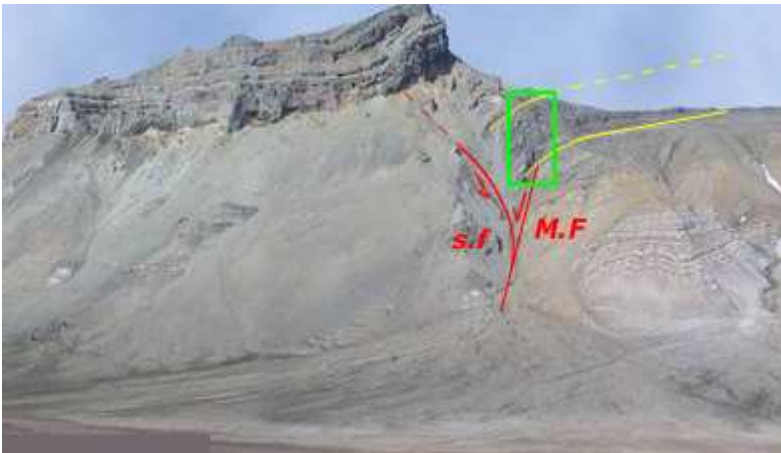


**Figure 2.3** Massive limestone from the upper Minkinfjellet Formation cut by normal faults. North-looking view oriented SW-NE near the Wordiekammen ridge on Figure 2.1. The parallel faults (delimited by the red half-arrows) are interpreted as normal faults resulting of propagation of the Master Fault. They are here named Propagation Faults, abbreviated p.f in Figure 2.1 Stereographic projection in Figure 2.13 (a-d).

Several smaller normal faults are also observed above the Master Fault (M.F). Figures 2.4-2.7 evidence short displacement faults both proximal to the fault zone and within the rotated bedding intrinsic to the fault zone.

Slickenside surfaces are rare. However, a good example is found close to the M.F. This surface is characterized by the presence of fined grained white stripe-like lineations (Figure 2.8). The slickenside surface is fairly shinny, polished and shows a preferential alignment.





**Figure 2.4** SW-NE oriented view of the Løvehovden area from Ebbadalen. Løvehovden (left side) and ridge to east. Monocline (yellow lines) related to Løvehovden Fault Zone (red lines) where several short-displacement faults were encountered. M.F (Master Fault); s.f (secondary fault).

(Source: Norsk Polarinstitut)



**Figure 2.5** Faulted carbonate breccia located in the monocline. The core is a few centimetres thick, made up of small fragments of dark micrite. Oil has flowed through, darkening the core.

The total displacement is estimated to be between some tenths of centimetres up to one meter. The pencil is located on the hangingwall. The sense of slip is SW, averaged in 60 degrees. Located in "12" in Figure 2.10.



**Figure 2.6** Normal fault interrupting the sub-horizontal layering of dark shales and carbonates (to the right side). The fault surface is represented by the red dashed line. The fault core is characterized by the presence of a white-yellowish breccia. The throw of this fault is about a few meters and dips approximately 45 degrees SW.



**Figure 2.7** NW-looking photograph of a W-dipping fault on layered carbonate rock interbedded with shale. This location is approximately along the upper yellow line in Figure 2.4. The sedimentary bedding is cut and offset by a 60 SW-dipping normal fault with a displacement close to 1 meter. Location in "13" in Figure 2.10



**Figure 2.8** Slickenside surface on the footwall block of the Løvehovden Master Fault. Location at “11” in Figure 2.10. Slickenlines, perpendicular to the pencil, are characterized by parallel white streaks and ridges several cm wide. Sense of displacement of the missing block is SE perpendicular to the pencil. Stereographic projection in Figure 2.13 (a-d).

*Interpretations:*

The observations suggest the presence of a large fault. The main lineament is regarded the Master Fault.

The repetition of rock sections in lenticular bodies is in good agreement with a relative down-W transport. Homogeneous evidence of smaller down-W extensional faults within the fault zone supports the view that the Løvehovden fault with associated breached monocline is a down-W normal fault zone. This contradicts earlier interpretations of contraction and basin inversion (See Discussion).

The striations of the Master Fault slickenside are not caused by scratches but they are chatter marks (Davis & Reynolds 1996). The surface looks quite striated and one of the mechanisms that could explain this observation would be the brecciation of the rocks with fault movement, creating the mentioned chatter zones (Figure 2.9).



**Figure 2.9** East-looking photograph beneath “17” in Figure 2.10. View of the Master Fault surface. The striated surface is exposed in a patch of 10 by 10 meters approximately. Weathering masked the original pattern over much of the exposure. Scale: photograph is about 1,5 meters in height. The strike and dip of the fault is 310/43 SW. The rock surface is broken and in places brecciated, attributed to fault slip. The fault slip may create the observed brecciation. Stereographic projection in Figure 2.13 (a-d).

### 2.2.3 Domain B<sub>2</sub>

Domain B<sub>2</sub> is made up of the area bounded by the Master Fault (M.F) and the so-called Marginal Faults (m.f) (Figure 2.1).

#### *Observations:*

The locally exposed unit of Domain B<sub>2</sub> is the Tricolorfjellet Member, consisting of the characteristic white gypsum, anhydrite and red shale. They are affected several Marginal

Faults (m.f2 in Figure 2.1). Immediately above starts the Minkinfjellet Formation. In this area, the sediments experience a manifest change in dip from the regional 8-10 degrees westerly dip of the basin to nearly vertical orientation towards the Løvehovden Fault Zone. The fold is that of the monocline above fault tips.

The Marginal Fault 1 (m.f1 in Figure 2.1) is seen in a yellow cliff of highly dolomitized and massive micritic carbonate overlaying a package of dolomitized carbonate breccia with clasts of chert and chalk. The throw is about 2 meters and its orientation parallel to the Master Fault towards the NW (p.f in Figure 2.1).

The Marginal Fault 2 is made up of two parallel small faults where only the eastern has significant throw. The fault core materials are protolith rocks dragged down along the fault. The fault throw was measured to 15 meters. These two faults do not propagate into the Minkinfjellet Formation.

#### *Interpretation:*

The SW dip direction and stratigraphic offset of the Marginal Faults identify them as normal faults. They are parallel to the Master Fault.

#### 2.2.4 Domain C

Domain C is in the footwall of the fault zone, east Domains B<sub>1</sub> and B<sub>2</sub>. Domain C is located to the area between two faults: the Marginal Faults and the Ebbadalen Fault (Figure 2.1).

### *Observations:*

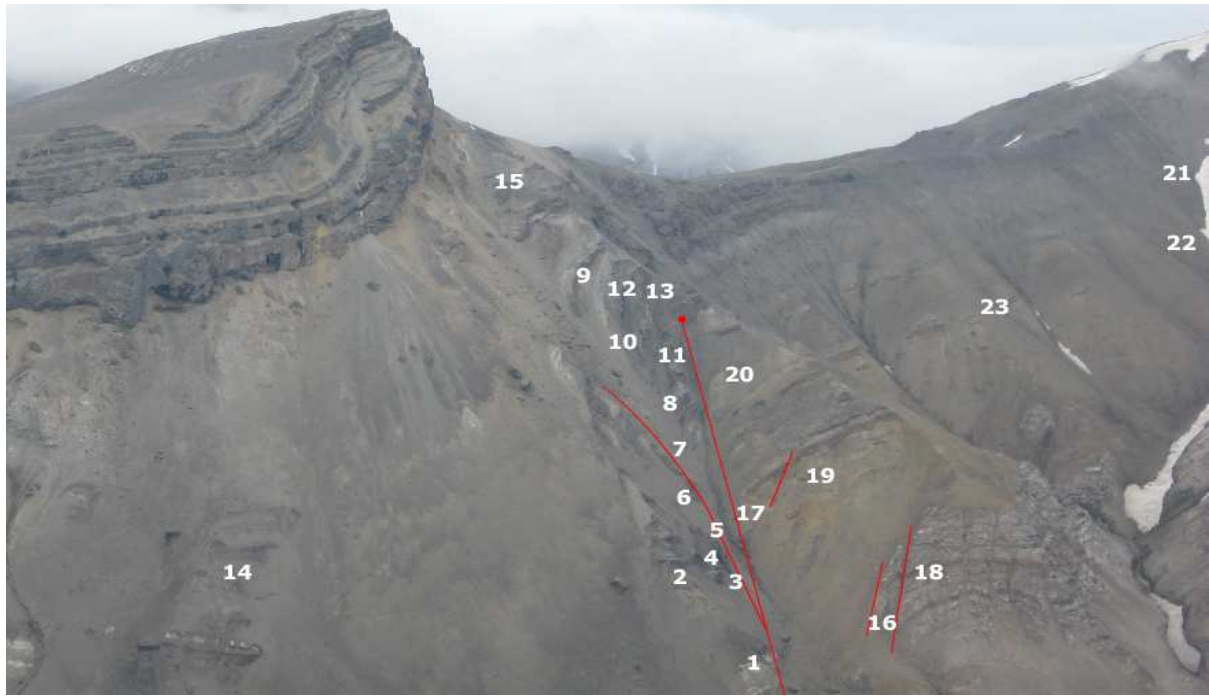
The Domain C rocks are basically unaffected by deformation. They dip to the W. The Ebbadalen Fault is almost vertical. The core is 2 meters thick, hosting a heterogeneous mixture of gypsum, sandstone and carbonates. The throw has been estimated to 70 meters based on field observations, and post-fieldwork correlation between the hangingwall and footwall gypsum layers on both sides of the fault on the Lidar data. It offsets the strata up to the base of the Minkinfjellet Formation.

### *Interpretation:*

The east-dipping orientation and the normal drag constitute the main evidences for the interpretation of the Ebbadalen Faults as a reverse fault. The formation of the extensional Marginal Faults and the compressional Ebbadalen Fault creates the characteristic gentle anticlinal to sinclinal shape on the Ebbadalen Formation between these two faults (See structural model in Figure 3.5 b).

#### 2.2.5 Structural data analysis

Strike and dip measurements have been collected across the area with special focus on the fault zone. The measurements cover layering, faults, joints and fractures (Figure 2.10). Table I summarizes all the structural data collected on the areas.



**Figure 2.10** North-looking view of the south side of Løvehovden and Hultbergfjellet taken from Wordiekammen. The numbers in white indicate the locations where structural measurements were collected, concentrated on the fault zone. The red lines define the boundaries between structural domains (Figure 2.1). The red dot indicates fault tip.

STRUCTURAL DATA							
Locality	X-UTM	Y-UTM	Strike	Dip	Plunge <sup>a</sup>	Type of surface	Area
1	536173	8739045	19	21		Layering	Hangingwall Master Fault
			29	26		Layering	Hangingwall Master Fault
2	536111	8739112	46	23		Layering	Hangingwall Master Fault
			8	30		Layering	Hangingwall Master Fault
3	536120	8739130	322	72		Joint	Løvehovden Fault Zone
			335	79		Joint	Løvehovden Fault Zone
4	536121	8739139	140	58		Joint	Løvehovden Fault Zone
			121	39		Joint	Løvehovden Fault Zone
5a	536149	8739179	330	59		Joint	Løvehovden Fault Zone
			340	68		Joint	Løvehovden Fault Zone
5b	536145	8739182	127	70		Joint	Løvehovden Fault Zone
			140	76		Joint	Løvehovden Fault Zone
6	536111	8739177	58	50		Joint	Løvehovden Fault Zone
			70	42		Joint	Løvehovden Fault Zone
7	536105	8739291	279	43		Joint	Løvehovden Fault Zone
			309	38		Joint	Løvehovden Fault Zone
8	536112	8739291	154	70		Joint	Løvehovden Fault Zone
			173	65		Joint	Løvehovden Fault Zone
9	536054	8739289	352	78		Layering	Monocline
			333	71		Layering	Monocline
10	536994	8739338	300	51		Layering	Monocline
			321	67		Layering	Monocline
11	536007	8739409	158	64	58 NW	Slip surface	Løvehovden Fault Zone
			150	67	59 NW	Slip surface	Løvehovden Fault Zone

12	536043	8739424	171	78		Fault surface	Monocline
			170	50		Fault surface	Monocline
			280	59		Fault surface	Monocline
13	536050	8739436	152	59		Fault	Monocline
			179	68		Fault	Monocline
			304	70		Layering	Monocline
			318	57		Layering	Monocline
14	535847	8739049	282	12		Layering	Hangingwall Master Fault
			298	18		Layering	Hangingwall Master Fault
15	535986	8739488	300	18		Layering	Hangingwall Master Fault
			291	80		Fault surface	Master Fault propagation
			317	79		Fault surface	Master Fault propagation
			334	82	82 W	Fault surface	Master Fault propagation
			342	79	79 W	Fault surface	Master Fault propagation
			242	41		Fault surface	Master Fault propagation
16	536217	8739025	19	70		Layering	Footwall Master Fault
			42	64		Layering	Footwall Master Fault
17	536139	8739192	303	39		Fault surface	Master Fault
			317	46		Fault surface	Master Fault
18a	536247	8739164	340	58		Fault surface	Marginal Fault 2
			333	60		Fault surface	Marginal Fault 2
			322	64		Fault surface	Marginal Fault 2
18b	536250	8739150	331	28		Layering	Hangingwall Marginal Fault 2
			20	30		Layering	Hangingwall Marginal Fault 2
			18	38		Layering	Hangingwall Marginal Fault 2
			320	24		Layering	Hangingwall Marginal Fault 2
			28	68		Layering	Footwall Marginal Fault 2
			80	18		Layering	Footwall Marginal Fault 2
			20	70		Layering	Footwall Marginal Fault 2
			3	48		Layering	Footwall Marginal Fault 2
			330	38		Layering	Footwall Marginal Fault 2
			30	14		Layering	Footwall Marginal Fault 2
			60	8		Layering	Footwall Marginal Fault 2
19	536232	8739285	8	24		Layering	Marginal Fault 1
			21	21		Layering	Marginal Fault 1
			298	44		Fault Surface	Marginal Fault 1
			302	44		Fault Surface	Marginal Fault 1
20	536128	8739229	317	41		Layering	Footwall Master Fault
			308	52		Layering	Footwall Master Fault
21	536540	8740007	326	18		Layering	Footwall Master Fault
			329	17		Layering	Footwall Master Fault
22	536532	8739948	1	21		Layering	Footwall Master Fault
23	536295	8739604	321	19		Layering	Footwall Master Fault
			355	23		Layering	Footwall Master Fault
							* Where measurable

**Table I** Summary of the collected strikes and dips of each of the measurement points shown in Figure 2.10

*Methods:*

The data analysis and comparison has been done by using the Stereowin program, which allows us to plot the measured planes as great circles and to calculate the poles (perpendicular lines to the planes). All the data is organized in strike and dip format according

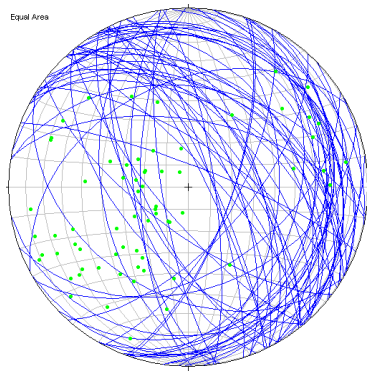


to the right hand rule. By having positioned the poles, we calculate the cylindrical best fit. It plots the plane contained in the poles as a great circle and give us an averaged perpendicular plane to the input data.

Another tool used in this analysis is the Kamb contour, which creates spaced contours from the poles array. The Kamb contours basically give us an account of how random is the point distribution. By contouring the poles, the statistical significance of the distribution can be counted. Finally, a rose diagram is made from each of the data sets in order to get a projection of the strikes of planes and to evaluate their mean orientation and by default the orientation of the structure. The data will be used to further determine the most accurate perpendicular section to the structure in order to build the structural models.

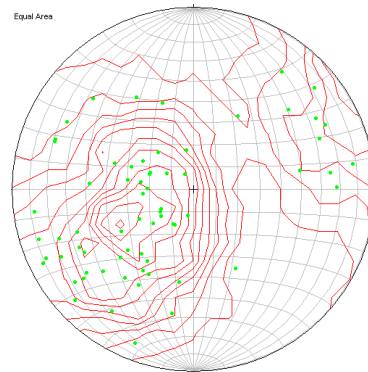
#### 2.2.5.1 Total structural data plot

By plotting the whole dataset, an estimation of the averaged orientation of the Løvehovden outcrop data is given by the dominant strike of the layers, faults and joints. The poles and hence the best cylindrical fit are fairly scattered. The scattering is caused by the structural complexity of the area. The rose diagram shows the main strike directions, which are concentrated along the NW-SE axis. The main outcome shown by the plots is the averaged strike of the Løvehovden zone, calculated to 341.2 degrees NW-SE (Figures 2.11 a-d).



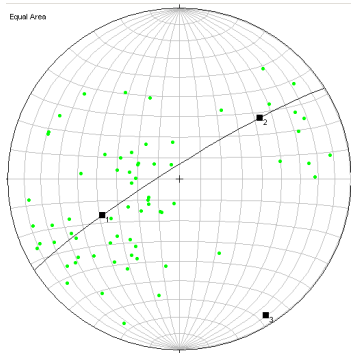
**Figure 2.11 (a):** Total data: great circles and poles

**Explanation.**  
Planes (n = 66):  
LINES SCATTER PLOT (n = 66):



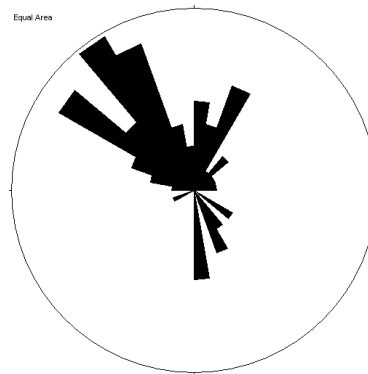
**Figure 2.11 (b):** Total data: Kamb contours from poles

**Explanation.**  
KAMB CONTOUR OF F-AXES (n = 66):  
Contour Int = 1.0, Counting Circle Area = 0.117  
Expected Number = 7.95, Significance Level = 3.0 sigma  
LINES SCATTER PLOT (n = 66):



**Figure 2.11 (c):** Total data: cylindrical best fit from poles

**Explanation.**  
CYLINDRICAL BEST FIT  
Eigenvalue Eigenvector (TSP) Confidence  
1. 0.6168 244.7° 69.7° Max = 15.1°, Min = 9.2°  
2. 0.2634 52.5° 40.7°  
3. 0.1198 147.8° 6.1° Max = 17.8°, Min = 8.2°  
LINES SCATTER PLOT (n = 66):

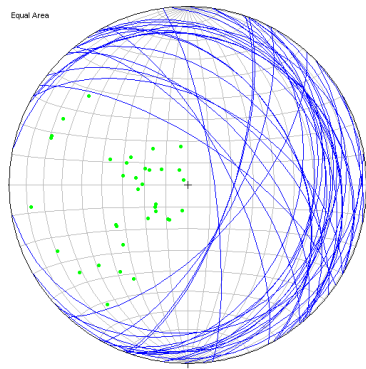


**Figure 2.11 (d):** Total data: rose diagram

**Explanation.**  
ROSE DIAGRAM  
Outer Circle = 12%  
Mean dir = 341.2, alpha95 = -1.0

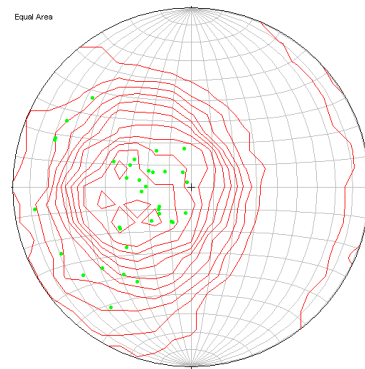
### 2.2.5.2 Layering

The layering is one of the main indicators to infer the structural orientation of the Løvehovden area. As we separate the measurements on the layers from the rest of the dataset, two main strikes are displayed in the rose diagram: a major NW-SE strike and a subordinate NE-SW. The great circles indicate a regional W to W-SW dip. The fit to the great circle is poor, which indicates that the structures are not cylindrical. (Figure 2.12 a-d).



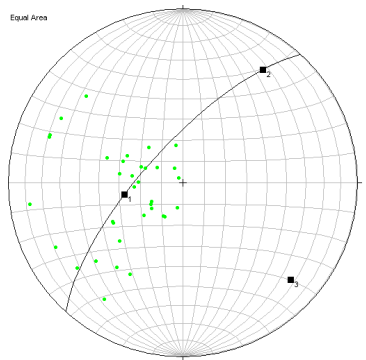
**Figure 2.12 (a):** Layering: great circles and poles

**Explanation.**  
LINES SCATTER PLOT (n = 35) •



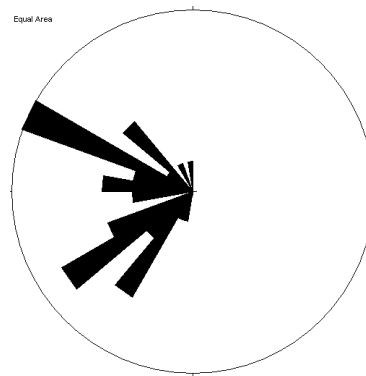
**Figure 2.12 (b):** Layering: Kamb contours from poles

**Explanation.**  
KAMB CONTOUR OF P-AXES (n = 35):  
Contour  $k = 1.0$ , Counting Circle Area = 0.205  
Expected Number = 7.16, Significance Level = 3.0 sigma  
LINES SCATTER PLOT (n = 35) •



**Figure 2.12 (c):** Layering: cylindrical best fit from poles

**Explanation.**  
CYLINDRICAL BEST FIT  
Eigenvalue Eigenvector (T&P) Confidence  
1. 0.7170 269.7° 61.5°, Max = 9.3°, Min = 6.5°  
2. 0.1187 35.1° 21.2°  
3. 0.1035 132.2° 17.6°, Max = -1.0°, Min = -1.0°  
LINES SCATTER PLOT (n = 35) •

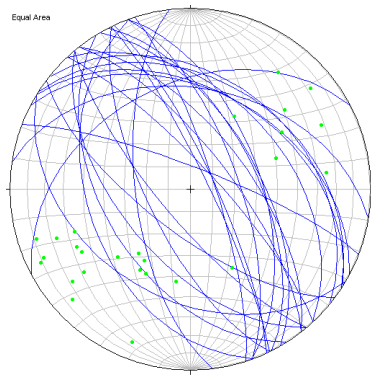


**Figure 2.12 (d):** Layering: rose diagram

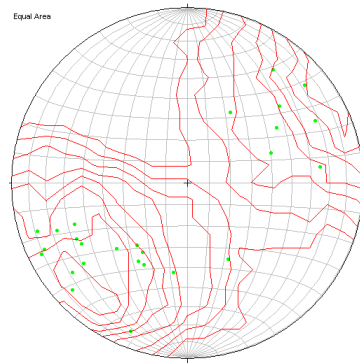
**Explanation.**  
ROSE DIAGRAM  
Outer Circle = 17%  
Mean dir = 262.7, alpha95 = 13.2

### 2.2.5.3 Faults

The great circles show that the faults are essentially perpendicular to the layering. On the other hand, the rose diagram indicates that the fault planes follow a main NW-SE alignment. They have parallel strike to the layering (Figures 2.13 a-d).



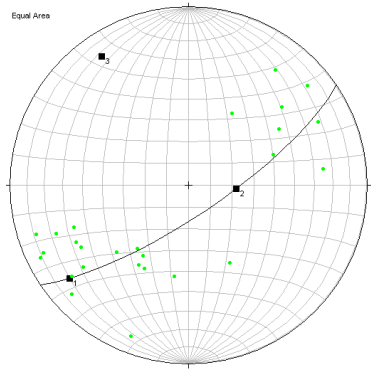
**Explanation.**  
 Planes (n = 26)  
 LINES SCATTER PLOT (n = 26)



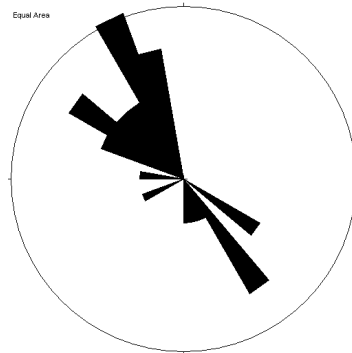
**Explanation.**  
 LINES SCATTER PLOT (n = 26)  
 KAMB CONTOUR OF PLACES (n = 26)  
 Contour Int = 1.0, Counting Circle Area = 0.257  
 Expected Number = 6.68, Significance Level = 3.0 sigma

**Figure 2.13 (a):** *Faults: great circles and poles*

**Figure 2.13 (b):** *Faults: Kamb contours from poles*



**Explanation.**  
 CYLINDRICAL BEST FIT  
 Eigenvalue: Eigenvector (T&P) Confidence  
 1. 0.6686 231.9° 16.4°, Max = 24.0°, Min = 8.3°  
 2. 0.2710 94.5° 56.2°  
 3. 0.0604 326.1° 13.9°, Max = 17.8°, Min = 8.3°  
 LINES SCATTER PLOT (n = 26)



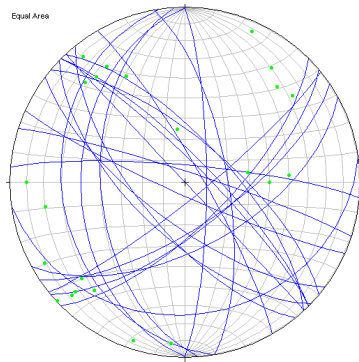
**Explanation.**  
 ROSE DIAGRAM  
 Outer Circle = 15%  
 Mean dir = 306.5, alpha95 = -1.0

**Figure 2.13 (c):** *Faults: cylindrical best fit from poles*

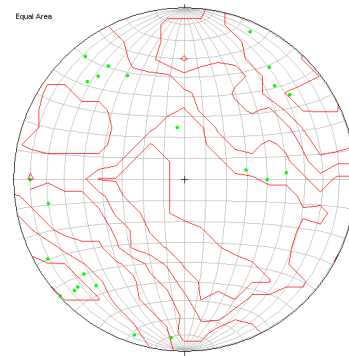
**Figure 2.13 (d):** *Faults: rose diagram*

#### 2.2.5.4 Joints

The results from plotting joint data do not show any particular trend. The wide orientation populations may be caused by the high fractured area enveloping the fault linkage area. The lack of trend could relate to the non-cylindrical monocline and fault zone geometry (Figures 2.14 a-d).



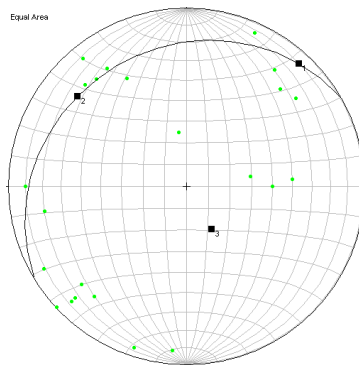
**Explanation.**  
 Planes (n = 23)  
 LINES SCATTER PLOT (n = 23)



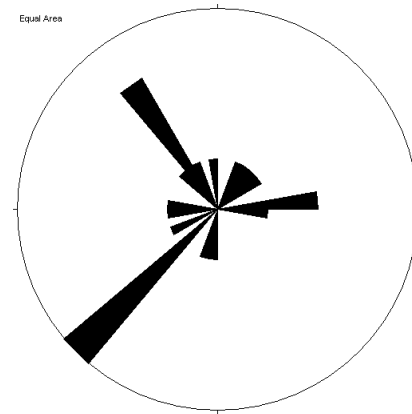
**Explanation.**  
 LINES SCATTER PLOT (n = 23)  
 KAMB CONTOUR OF P-AXES (n = 23)  
 Contour Int = 1.0, Counting Circle Area = 0.281  
 Expected Number = 6.47, Significance Level = 3.0 sigma

**Figure 2.14 (a):** Joints: great circles and poles

**Figure 2.14 (b):** Joints: Kamb contours from poles



**Explanation.**  
 LINES SCATTER PLOT (n = 23)  
 CYLINDRICAL BEST FIT  
 Eigenvalue Eigenvector (TSP) Confidence  
 1. 0.5415 42.2° 7.0°  
 2. 0.3022 309.6° 21.4°  
 3. 0.1563 149.5° 67.4°



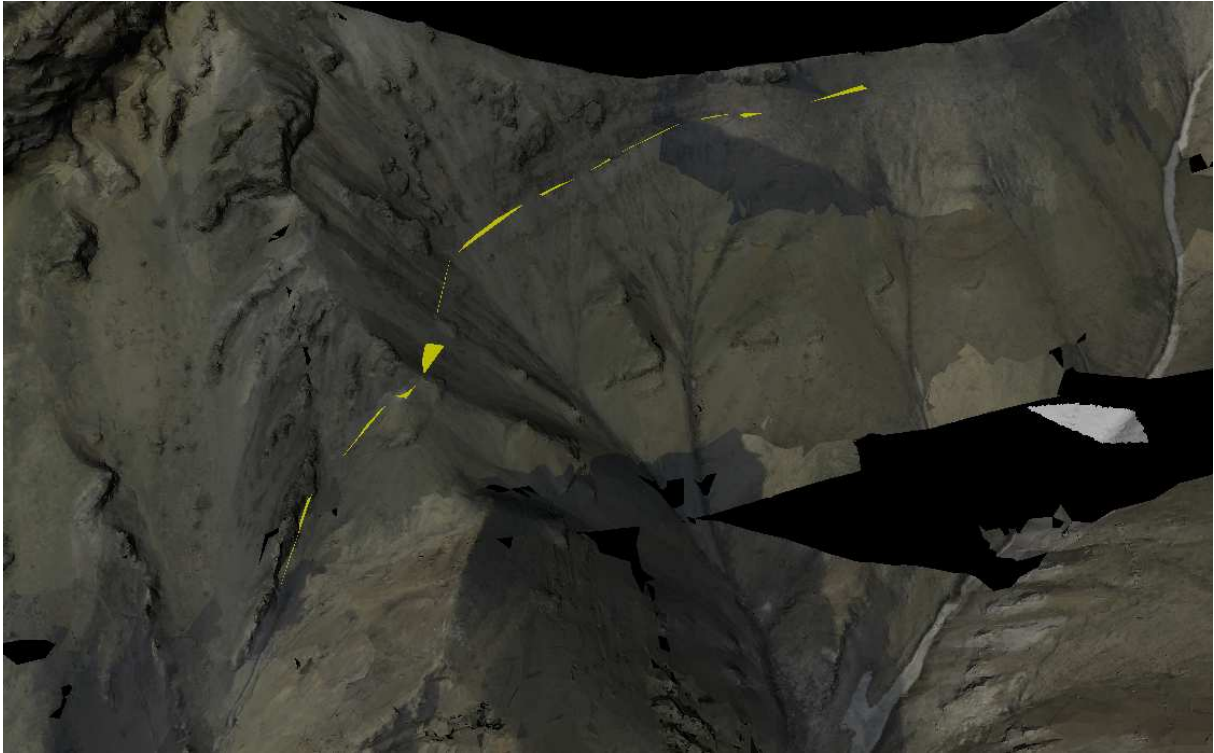
**Explanation.**  
 ROSE DIAGRAM  
 Outer Circle = 18%  
 Mean dir = 306.4, alpha95 = -1.0

**Figure 2.14 (c):** Joints: cylindrical best fit from poles

**Figure 2.14 (d):** Joints: rose diagram

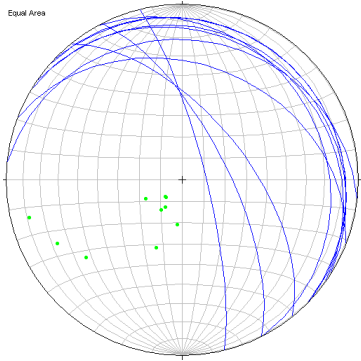
### 2.2.5.5 Lidar-based bedding data

In order to contrast the field and digital data, 10 planes have been created on the beds of the monocline by using the Lime software. Lime calculates the strikes and dips contained on the planes (Figure 2.15).



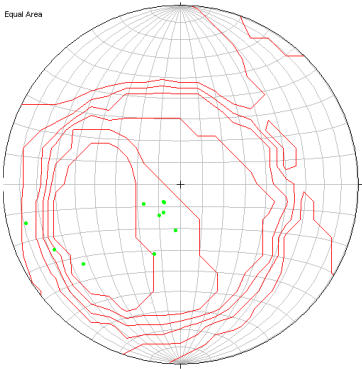
**Figure 2.15:** North-looking screen capture on the Løvehovden Lidar data. 10 planes (shown in yellow) define the monocline.

As observed on the plots, the orientation of the planes is parallel to the field measured layering and therefore confirms the field results, the NW-SE strike orientation (Figures 2.16 a-d).



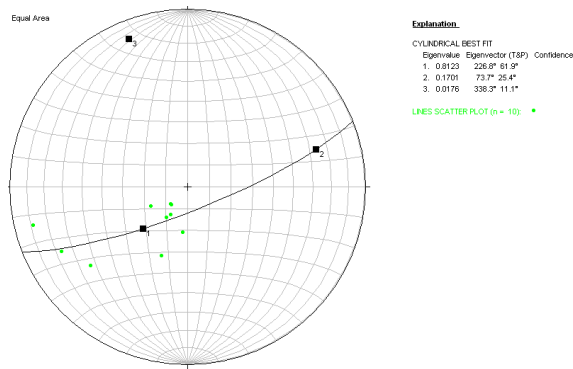
**Figure 2.16 (a):** Monocline: great circles and poles

Explanation:  
LINES SCATTER PLOT (n = 10):

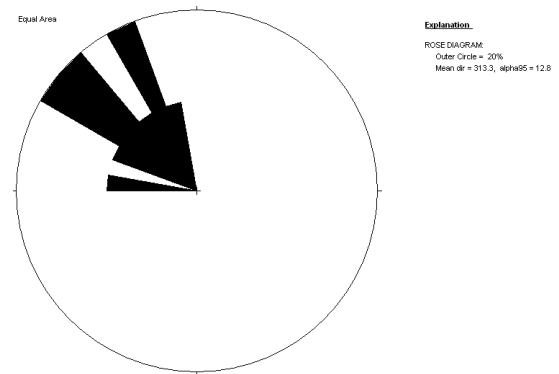


**Figure 2.16 (b):** Monocline: Kamb contours and poles

Explanation:  
KAMB CONTOUR OF PLACES (n = 10):  
Contour Int = 1.0, Counting Circle Area = 0.474  
Expected Number = 4.74, Significance Level = 3.0 sigma  
LINES SCATTER PLOT (n = 10):



**Figure 2.16 (c):** *Monocline: cylindrical best fit from poles*



**Figure 2.16 (d):** *Monocline: rose diagram*

### 2.2.5.6 Lidar-based fault throw data

In some instances, the fault surfaces were only recognisable in Lidar data. In such cases, fault throws are calculated on the Lidar data. Table II displays their averaged values.

		Strike	Dip	Fault Throw (m)	Input data
<b>Master Fault</b>		310	57	183	Field data
<b>Secondary Fault</b>	<i>Upper section</i>	174	45	not-measurable	Lidar data
	<i>Lower section</i>	162	76	not-measurable	Lidar data
<b>Marginal Fault 1</b>		300	44	2	Field data
<b>Marginal Fault 2</b>	<i>eastern fault</i>	332	61	15	Field data
	<i>western fault</i>	352	58	12	Lidar data
<b>Propagation Faults</b>		305	72	20	Field data
<b>Ebbadalen Fault</b>		167	69	70	Lidar data

**TableII:** *Faults orientation, throw and data source*

### 2.2.6 Logging

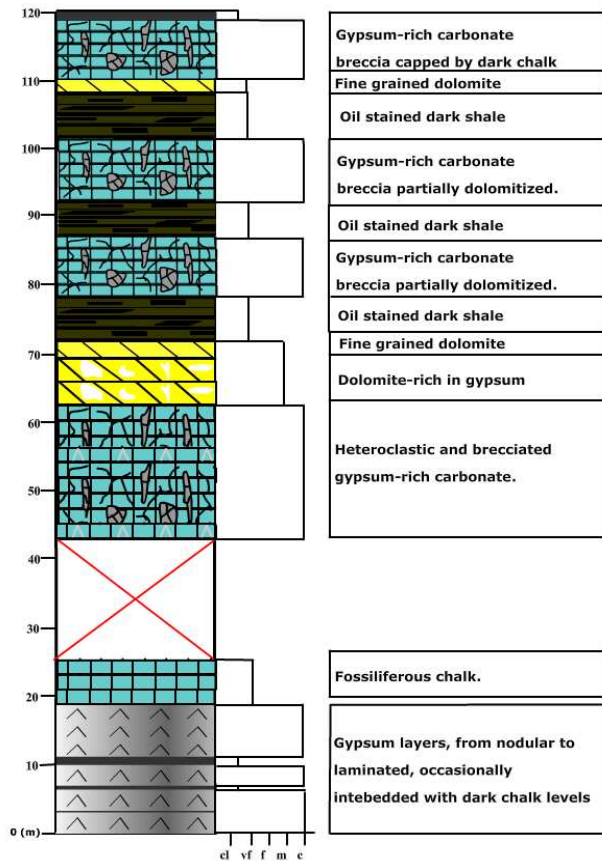
Two logs have been recorded in the footwall and hangingwall of the Løvehovden Fault Zone. The logs are located away from the damage zone, where the strata appear to be unaffected by deformation. The location of the logs can be seen in Figure 2.1. Apart from

providing detailed information of the stratigraphy, the logs assist in correlation across the fault. A common sequence in the logs constrains the stratigraphic offset across the Løvehovden Master Fault.

#### 2.2.6.1 Hangingwall log

The hangingwall log begins at the base of the first recognisable strata of the Minkinfjellet Formation. The log extends vertically in a continuous exposure and has stratigraphic thickness of 120 meters. It starts with a massive package of evaporites, consisting of gypsum and anhydrite with occasional layering of dark chalk. The facies are mostly nodular. The next unit is a homogeneous sequence of carbonate; a bioturbated fossiliferous chalk. After an area of poor exposure, the next section is a sequence of gypsum-rich carbonate with traces of dissolution. Some of the evaporitic clasts are still preserved, although most of them have been dissolved. Dissolution has left sub-rounded white voids in the rock covered by a white patina. The rock shows a high degree of brecciation. (Figure 2.17).



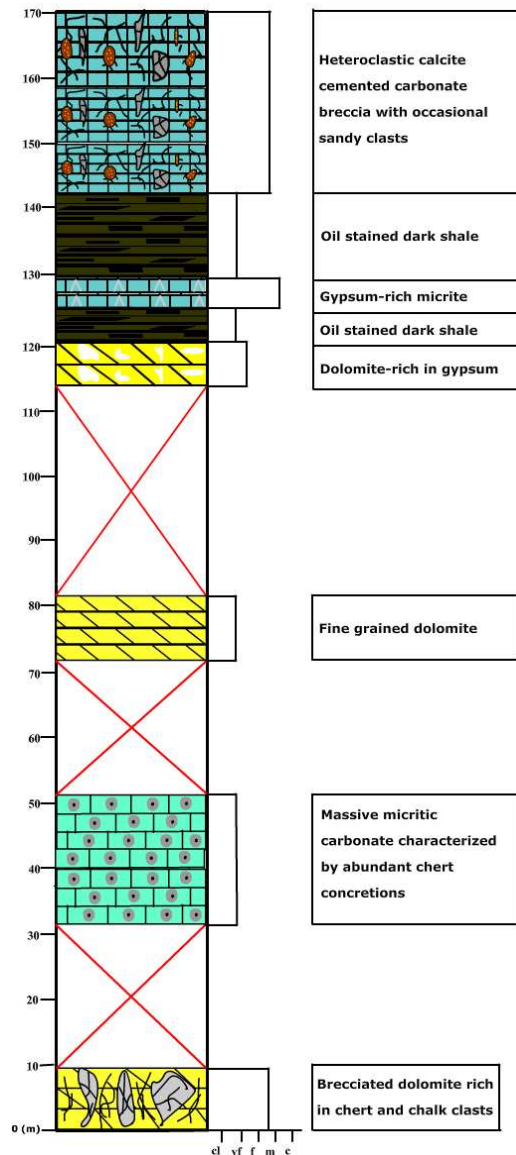


**Figure 2.17** Hangingwall stratigraphic log. The vertical scale is given in stratigraphic thickness. The *cl* = clay; *vf* = very fine; *f* = fine; *m* = medium; *c* = coarse

The carbonate breccias pass up into a very clear and highly dolomitized interval with a high content of evaporitic minerals. The uppermost layers are more finely grained and lack gypsum. Lying on top of the dolomite, we find three sequences of dark and oil stained shale interbedded with dolomite. The shale is lithologically homogeneous and presents stratification. The dolomite is highly brecciated. On the top of the third sequence of shale, we encounter a thin layer of very fine-grained dolomite. The log ends in a thin bed of dark shale.

### 2.2.6.2 Footwall log

The footwall log has been recorded from east of the fault zone and has stratigraphic thickness of 172 meters (Figure 2.18).



**Figure 2.18** Footwall stratigraphic log. The vertical scale is given in stratigraphic thickness. The cl = clay; vf = very fine; f = finje; m = medium; c = coarse

The exposure is in general good, around 40-50% of the section, but fragmentation of some parts made difficult to judge whether the strata were *in situ* or scree. The quality of the outcrop is especially poor along three different sections crossed out by a red “x”.

The section starts with a carbonate-based sequence characterized by a high degree of brecciation. It is a dolomitic rock which contains two types of clasts: chert and chalk clasts, trapped within the dolomitic matrix. This is our first observation of siliceous materials in the carbonate-dominated stratigraphy of the Minkinjellet Formation. The above laying micritic carbonate is massive and presents almost no fracturing. Chert nodules are homogeneously distributed within the strata. The sequence passes on, after a section masked by debris, into some layers of fine-grained dolomite with the consistence of dust. It does not present internal structures or heterogeneities.

On top of the dolomite, there is a package of white sediments, consisting of a dolomite very rich in gypsum. As well as in the hangingwall, the yellowish colour characteristic of dolomites is outmasked by its high content of evaporites, which confer its white colour. Immediately above the dolomite, there are some meters of dark shale, followed by a few layers of gypsum-rich micrite. The sequence continues with shale of the same characteristics than the previously described unit. The log ends with a carbonate breccia partially cemented, hereroclastic and heterolitic, since we encounter occasional clasts of sandstone. The whole outcrop tumes of hydrocarbons as we approach, evidencing past fluid flow.

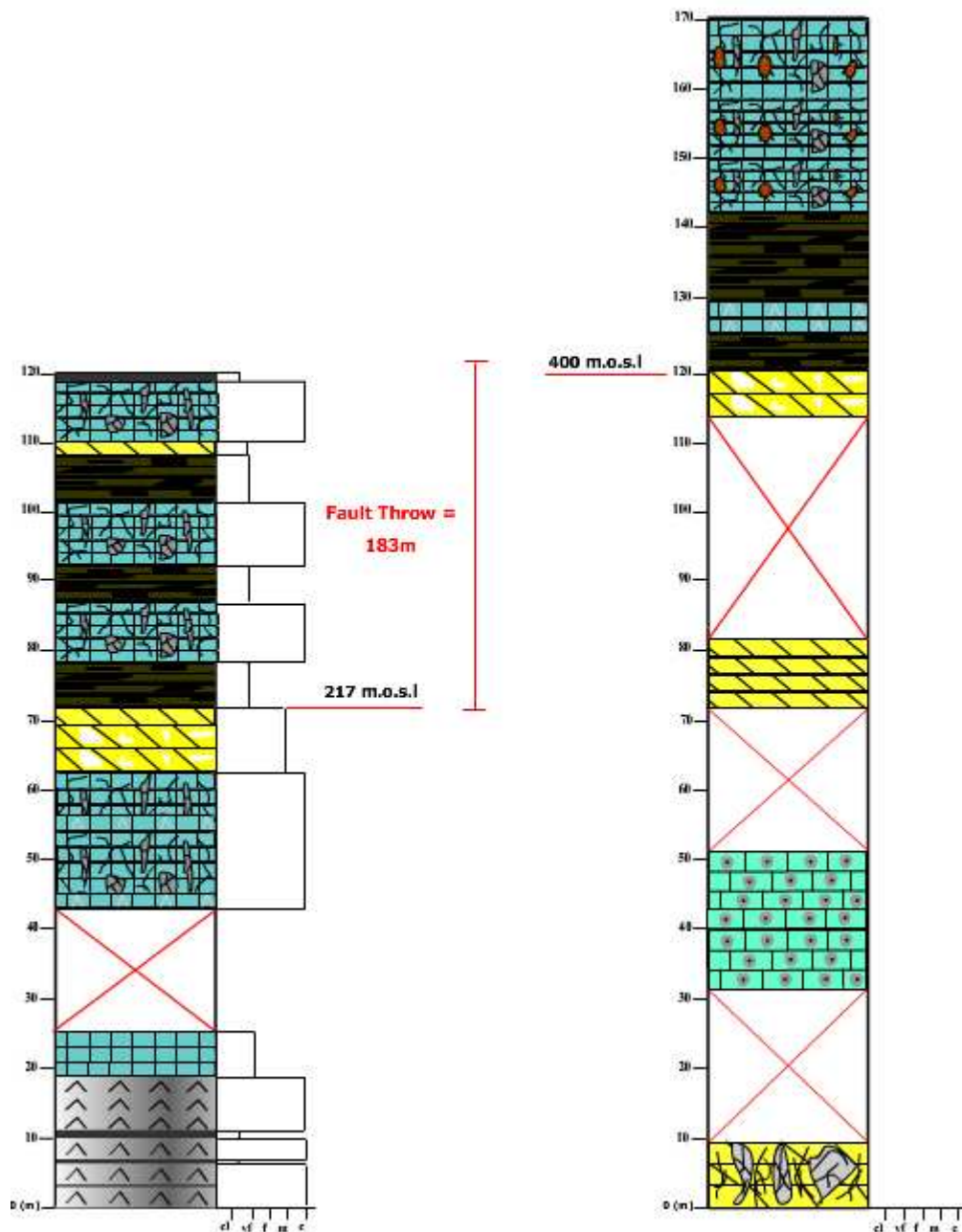
### 2.2.6.3 Comparison and discussion

The correlation between both log sections has been based on the identification of characteristic dark shale. Shale is found on the upper part of the footwall log and close to the

base of the hangingwall log, and in both cases is bounded by brecciated carbonates. The correlation could have been based as well on the gypsum-rich dolomite encountered on both sections at the same stratigraphic level, though its thickness is slightly different, while the first deposited package of shale is lithologically identical and equally thick. The shale can partially be traced across the fault zone, assisting in connecting the hangingwall and the footwall. Most of the fault zone is made up of shale and carbonate breccia, a fact that supports the log correlation.

The logs also reveal a possible connectable sequence of dolomite-rich gypsum right below the base of the shales. The dolomitization is more intense on the hangingwall side. The gypsum content instead is apparently higher in the footwall though the poorness of the exposure hampers an interpretation about the gypsum content.

The logs allow determination of the vertical extent fault throw, which can be precisely calculated from the Lidar data available from the area by distance between 2 points. The total vertical displacement is estimated to 183 meters (Figure 2.19)



**Figure 2.19** Log comparison. The vertical scale represents stratigraphic thickness. Both logs are recorded from different heights (see Figure 2.1). The matching point is shown by the red lines where the dark shale strata are found on both sides of the fault. The vertical displacement is given by the difference in height ( $z$ ) with respect to sea level.

The thickness of the Minkinjellet Formation can be measured on the Lidar data based on the logs. We measure from the top of the Minkinjellet Formation in the hangingwall to the base of the correlatable gypsum and shale levels. Moreover we should add the thickness from

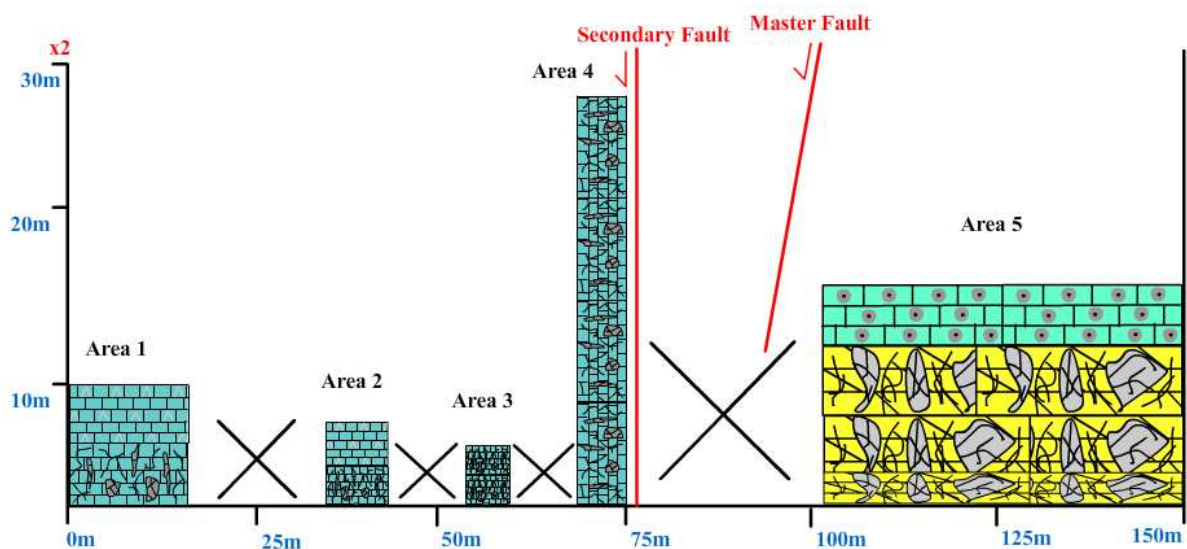
the same gypsum and shale levels of the footwall down to the base of the Minkinfjellet Formation. The maximum thickness calculated from the Lidar data is 470 meters.

### 2.2.7 Scanline across the fault zone

The scanline has been recorded across the Løvehovden Fault Zone, perpendicular to the faults. Areas 1, 2, 3 and 4 represent carbonate breccias occasionally rich in gypsum. Area 1 corresponds to the hangingwall and Areas 2, 3 and 4 belong to the fault zone. They are detached from each other. Area 5 represents footwall strata (Figure 2.20).

6

#### SCANLINE ACROSS THE LØVEHOVDEN FAULT ZONE



**Figure 2.20** Scanline shown as a schematic diagram across the Løvehovden Fault Zone. It shows the different intersected components and the projection of the major faults. The vertical scale is exaggerated x2 and the “x” marks show the intervals of no exposure. The lithologies of the strata are: Areas 1-2→ gypsum rich carbonate on top and carbonate breccia on the bottom; Areas 3-4→ carbonate breccia; Area 5→ chert rich carbonate on top and brecciated dolomite on the bottom (yellow).

From the data collected, we observe that the number of fractures increase towards the centre of the fault zone. The initial number of 30-40 fractures per meter of the area 1 gives place to more than 100 fractures per meter in Areas 3 and 4. This fact is actually coherent with the orientation of the fault core blocks with respect to the faults. The proximity of the areas 3 and 4 is shown by enhanced fracturing. The data is classified according to the lithologies. The number of fractures is higher in the gypsum-rich micrite. (Table III).

SCANLINE DATA							
Area	Dimensions	Material	UTM-X	UTM-Y	Layering	V	Fractures/m
1	14x10m	Carbonate breccia	536107	8739087	122/21	176/50	32
						180/40	39
						114/84	
						141/68	
						279/31	
		Micrite+gypsum	536106	8739106		288/85	87
						275/82	114
						330/82	
						315/78	
2	8x8m	Carbonate breccia	536158	8739138	340/50	45/70	75
						50/68	82
						134/65	
						127/71	
		Micrite+gypsum	536122	8739131	351/28	310/70	92
						315/81	96
						337/32	
3	5x6m	Carbonate breccia	536156	8739116	n.p	51/82	120
						56/69	131
						171/30	
4	7x30m	Carbonate breccia	536149	8739155	60/38	82/25	117
						61/59	105
5	13x15m	Carbonate chert	536192	8739260	188/24	350/70	1
						201/21	3
		Dolomite breccia				317/70	18
						317/90	

**Table III** Scanline data compilation, where V= fractures. The data is given by lithologies.

The brecciated heterolithic dolomite of the footwall is much less fractured than the fault zone. The chert rich carbonate lies on top and shows the lowest fracture density. In area 5, the number of fractures is here dramatically reduced; one order of magnitude, from 80-100 fractures down to 1-20 fractures per meter.

We can conclude that the lowest fracture density is given away from the fault zone. The carbonates forming the fault zone are highly brecciated and fractured. The centre of the fault zone is in comparison more fractured and crushed in Areas 3 and 4. According to my interpretation, it is at this point where the Master Fault and the Secondary Fault merge.

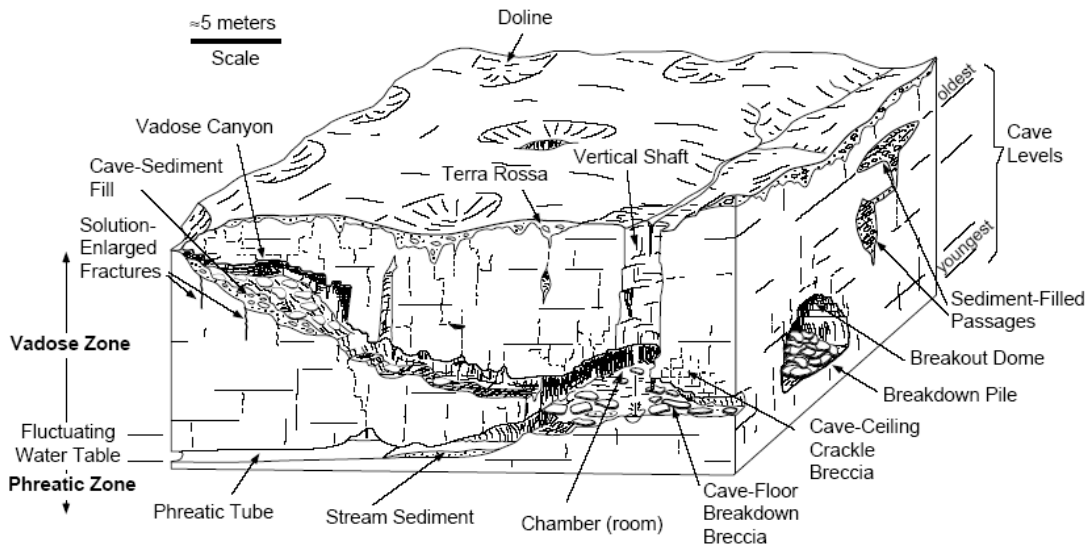
#### 2.2.8 Encountered breccia types, origins and implications

The Løvehovden area is characterized by high degree of brecciation. Two breccia types are collapse and fault breccias, located at the Løvehovden Fault Zone. A widely extended brecciation is found to affect mainly the Minkinfjellet Formation. The breccia pipes instead are located at the Wordiekammen Formation of the Løvehovden. The brecciated carbonates may provide good fluid flow paths, in paleokarst systems, due to its high permeability and porosity, when they are not cemented.

##### 2.2.8.1 Breccia pipes

The breccia pipes located within the paleokarst deposits of Wordiekammen. These breccia pipes are basically encountered in the Black Crag Beds of the Wordiekammen Formation and their vertical extent may reach up to 150 meters. They are relatively wide, from 12-170 meters and irregularly spaced (Nordeide 2008). They are characteristic of karstic environments where epigenic (surface waters) and hipogenic (underground waters) interact dissolving the calcite. The dissolution is especially intense along rock discontinuities such as fractures and faults. This process may create cavities where the mechanic strength of the rock is weaker. They tend to propagate upwards as the upper materials collapse into the cave and further drained out by underground waters (Figure 2.21).





**Figure 2.21** Illustration of a typical karst system with epigenetic and hypogenic waters dissolving the rocks and opening cavities in the subsurface. Caves collapse with time, and burial creates the nowadays known as paleokarst deposits. (Loucks 1999).

#### 2.2.8.2 Lidar interpretation of breccia pipes on Løvehovden

The breccia pipes that have been observed along the Black Crag Beds, at the base of the Wordiekammen Formation, can be accurately located on the available Lidar data of the area. The resolution of the dataset is high enough in order to display clearly objects of about 0.5 m<sup>2</sup>. The well exposed layering of the Black Crag Beds acts as guide. They contrast with the occasional bodies of rock cutting through the beds, which show a rather chaotic frame in comparison (Figure 2.22). The total number of encountered pipes is 11. They appear to be randomly spaced. The Lidar data shows three locations equally spaced where a number of 3 to 5 breccia pipes form clusters (Figure 2.22).



**Figure 2.22** Digital view of the Løvehovden ridge made of a composite set of screen captures around the ridge. The dashed white lines represent the boundaries of the breccia pipe bodies interpreted along the perimeter of the Wordiekammen Formation.

### 2.2.8.3 Fault Breccias

The Løvehovden Fault Zone consists of three basic elements: a major slip surface or Master Fault, the fault zone and a lateral damage zone. The Master Fault experienced most of the slip. The periferic damage zone, bounded by the Propagation and Marginal Faults carries part of the slip and part of the strain.

The scannline shows that the fault zone is especially crushed and fractured. The fault creates an area of brecciation, affecting the materials of the fault zone. This suggests that shear is localized along the brecciated zones, eventually ending up with the formation of fault gouges and the formation of slip surfaces within the fault zone (Rabitsch & Hausegger 2007).

The high amount of fractures and lack of cementation, converts the fault zone into a high permeable area prone to conduct preferentially fluid flow (Figure 2.23).



**Figure 2.23** *Crackle fault-breccia body in the Løvehovden Fault Zone. The white tones are gypsum contained in the carbonates. This is a clast-supported type of breccia, with non-cemented open fractures and some of the original layering still preserved. The crackle breccia type is a dominant feature of the Løvehovden Fault zone.*

#### 2.2.8.4 Collapse Breccia

This type of brecciation extends over larger extensions since it involves rock-fluid interactions at a more regional scale. There is intense brecciation on both fault walls (Section 2.2.6). It has a lateral continuity away from the Løvehovden Fault Zone, though less intense. The breccias are clast dominated and range from crackle to chaotic breccia with limited cementation. The micritic matrix is occasionally dolomitized.



### **3. STRUCTURAL MODELLING**

#### **3.1 Introduction**

The fieldwork data has been compiled and the sedimentary sequences interpreted along with the structural geology of the Løvehovden area in Chapter 2. The next step covered here, is modelling. The modelling workflow is intended to quantify several parameters: basin thickness variations, compaction, isostatic rebound, fault propagation and shortening. The goal of quantifying these parameters is first of all to provide accurate syn-rift geometry of the basin. Amount of compaction and possible effects on hydrocarbon migration, isostatic rebound and its impact on deformation are evaluated. Total Tertiary shortening on the basin is determined in the reconstruction workflow. Apex position, trishear apex, trishear angle and propagation of the Løvehovden fault are quantified in trishear models and tests.

The modelling uses algorithms integrated in the structural analysis and modelling program 2D Move. Although we have good 3D control on the stratigraphic surfaces, the faults, which control a great deal of the observed deformation, are exposed only in one of the sides of Ebbadalen (“Ebba valley”). Consequently, the fault surfaces can only be traced and interpreted in 2D. Therefore the modelling herein is two-dimensional modelling of a cross-section. The general 3D spatial geometry constrained by my field observations and Lidar data, adds accuracy to the 2D model.

The use of 2D Move let us project the structural features to the subsurface and to perform a structural reconstruction step by step. The principal operations carried out in 2D Move are: cross-section construction, structural reconstruction, and structural restoration by

sediment decompaction and isostatic rebound . These operations are aimed to test or discard my geological interpretations as well as to constrain new information about the structural evolution of the Løvehovden area.

### **3.2 Cross-section construction**

The cross-section is essentially constructed using the data presented and interpreted in Chapter 2. The map has been updated and digitized according to my observations and measurements. They include basically the fault interpretations, and strikes and dips of the eastern area (Løvehovden).

I have digitized for this purpose the “Geological Map of Billefjorden” from Dallmann et al. (2004), where unit contacts, topography, dip data and basement depth are specified. In order to determine thicknesses, I have used direct measurements on Lidar data and thicknesses presented on cross-section by Dallman et al. (2004). I I keep the Dallmann’s interpretation to the west of the Billefjorden Fault Zone (Svenbrehøgda) although I disagree on some interpretations on the Løvehovden area.

#### **3.2.1 Data preparation**

Prior to starting to build the cross section, a cartographic map of the area has been digitized and geo-referenced. The geo-referencing is done by setting up the UTM coordinates of 2 intersection points located on the top left and down right sides of the map. The map digitalization comprises three elements: horizons, faults and strikes and dips.

The strikes and dips have been located on the map from measurements collected during fieldwork. In the areas of difficult access, such as the top of Løvehovden, the strikes and dips have been calculated by using an algorithm built in the Lime program. It let us obtain strikes and dips by interpolating three measurement points in X,Y,Z. I use Dallmann's measurements on the easternmost side of the outcrop, especially measurements on basement rocks.

The location of the Løvehovden Master Fault (LMF) is the same as shown on the map, although I limit the vertical extent of the Ebbadalen Fault. According to the field observations I add Marginal Fault 2 (Figure 2.1) in the cross-section, since it is large enough to be recognised at the outcrop scale.

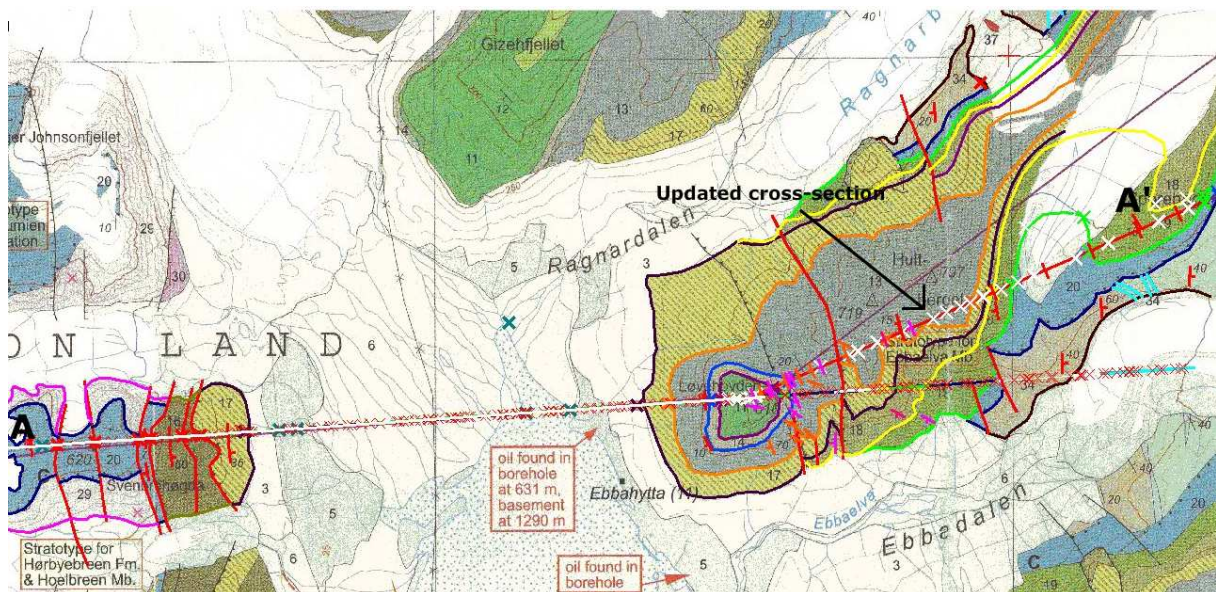
### 3.2.2 Orientation of the cross-section

A critical step before projecting the data and building a structural model, is the determination of the model orientation. Ideally, the model cross-section must be oriented perpendicular to the structure to record the true thicknesses, strikes and dips and minimize apparent false trends. This is the most important criteria although the cross-section must intersect the fault planes of the LFZ since it controls the displacement direction.

I have primary based the cross-section orientation on the results from plotting all the strike data collected from fieldwork in Stereowin. The program calculated that the average strike of the input data in 341.2 degrees (Figure 2.16 a)) with standard deviation  $\alpha_{95} = 1.0$ .

As an alternate method, I used the Lidar data to determine the strikes and dips at 10 points along the monocline using a well-defined horizon (Figure 2.15). The bedding attitudes were determined, using Lime (developed by Buckley 2008), to be 313,3 degrees (Figure 2.16 d) with an standard deviation  $\alpha_{95} = 12.6$ .

A reasonable section orientation should result from the perpendicular to the averaged strikes, obtained by direct measurements and computer-calculated measurements using the Lidar model. The average strike is 327 degrees. Figure 3.1 shows the orientation of the cross-section, which results from the perpendicular to the strike, in (057 NE-SW). It is preferable to trace a curved cross section to represent the true geometry since the orientation of the Billefjorden Fault Zone and strata is approximately E-W. By contrast the orientation of the Løvehovden sedimentary sequence and faults is NW-SE.

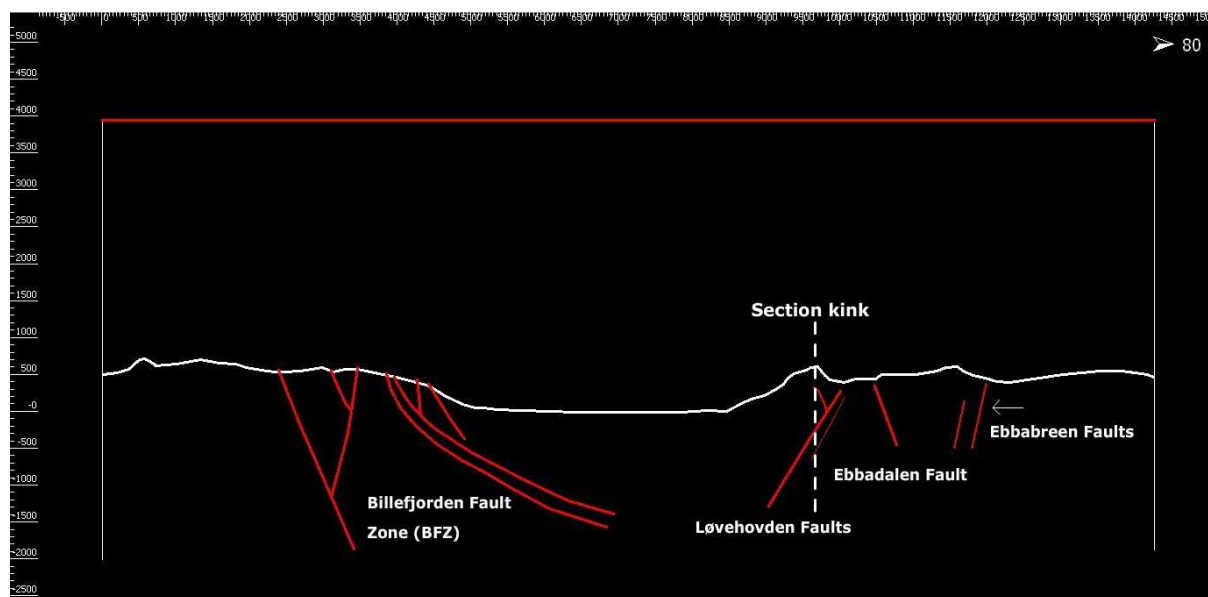


**Figure 3.1** Geological Map of Billefjorden from Dallmann et al. 2004 where the study area is digitized. It is used as input for the 2DMove section construction. Dips and intersections appear projected onto the A-A' section line.



### 3.2.3 Projecting data and building the section

As first step in the 2D Move cross-section construction, I draw a line from Svenbrehøgda (W) to Løvehovden (NE) (Figure. 3.1), which is converted into a cross-section. The next step is to collect all the intersection points, topographic points and dips onto the line. All the data is projected to visualize the dip data and its location on the cross section. The dips and points are displayed. In order to establish a relationship between the geology and topography, the topographic points are to be joined to result in a topographic profile. The faults are projected and drawn as shown in Figure 3.2.

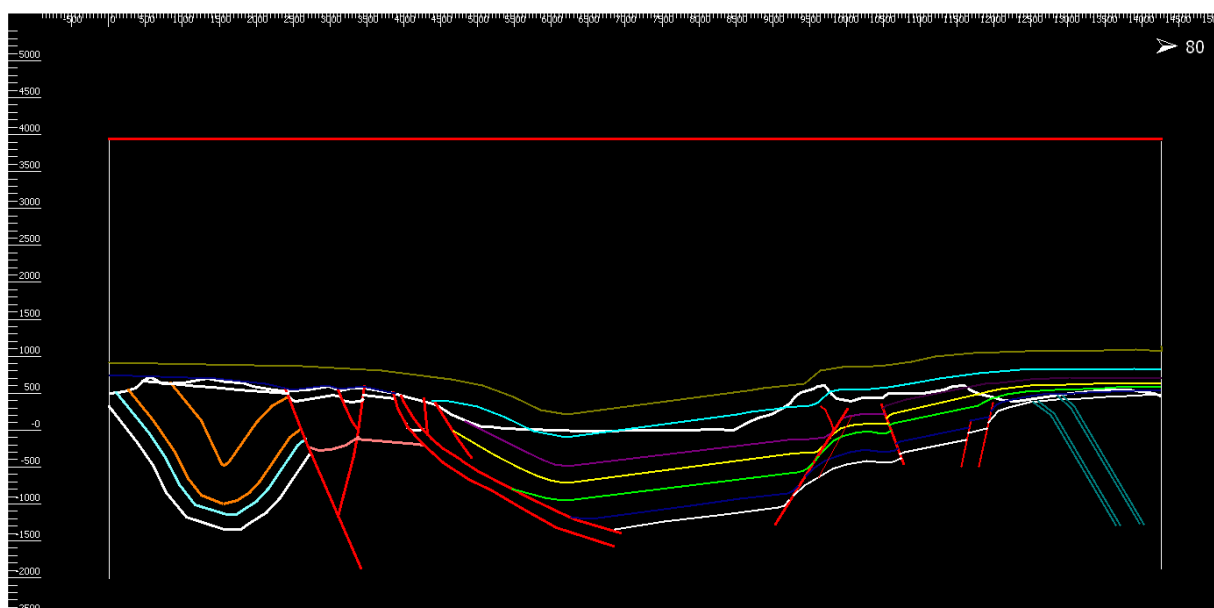


**Figure 3.2** W-E topographic profile and fault construction. The uppermost thick white line represents the topographic profile. The red lines are the faults. White line indicates topographic profile. The depth projection of the Billefjorden Fault Zone (BFZ) is more poorly constrained and interpreted in terms of syn-rift basin. The scale is given in meters, going from 0 to 14000 meters in the horizontal direction and from -2000 to -4000 meters in depth for the whole set of figures. The faults which throws are too small to be represented in this cross-section are drawn slightly thinner.

The construction of the stratigraphic horizons requires two basic steps. The first is the creation of a database containing information about each of the horizons such as name, thickness, lithology and age. The age number is used to arrange the strata from older to

recent. The higher the number, the older is the horizon. The absolute geological age is not required by the program. The database has space for P-wave velocities, porosity, permeability and porosity-depth coefficient, which are given by default. P-wave velocity and permeability are not used in the algorithms to create the stratigraphic sequence. The values of porosity and depth coefficient are entered further on when decompacting the sediments. The second step is to create a template horizon by projecting the dip data as well as considering how the faults will displace it up or down as it cuts through.

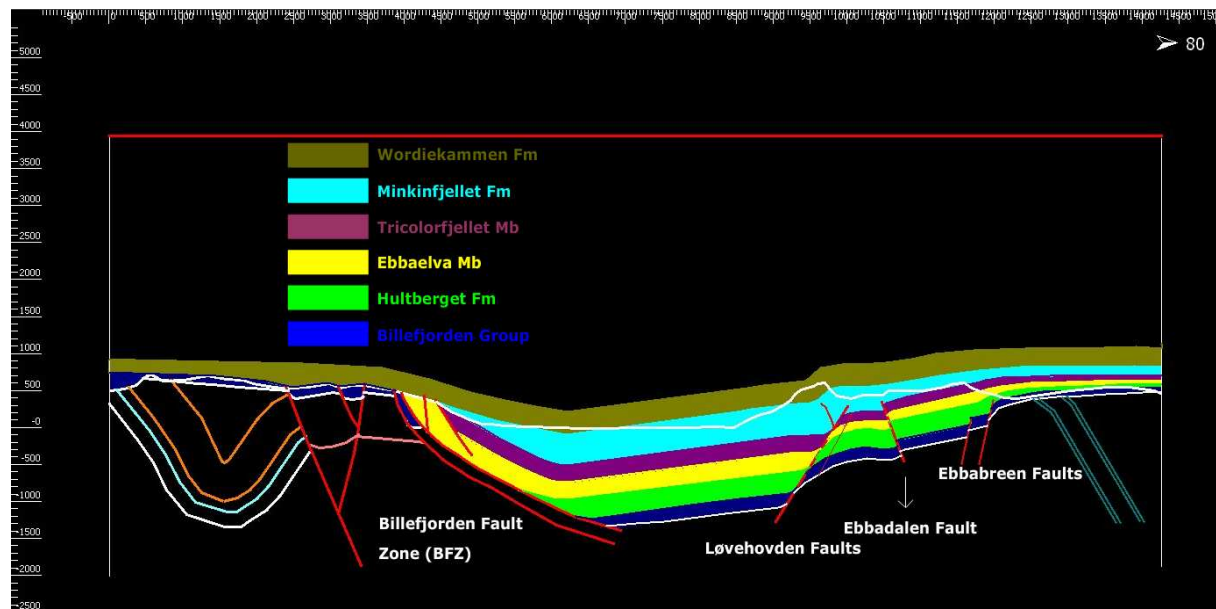
The “construct beds toolbox” is used to generate new beds above or below the template horizon based on the age and thickness data for each of them specified in the database. The horizons were edited to show syn-rift thickening towards the basin centre. Some bed thicknesses change along the section, where thickness is controlled by fault blocks. Hence, several sub-horizons have been created. New beds need to be generated from each of the fault blocks, which determine thickness changes in most of the cases. Figure 3.3 illustrates the complete section after bed construction.



**Figure 3.3** *Cross-section of the Svenbrehøgda (W) – Løvehovden (E). No vertical exaggeration. This western part of the cross-section is based on the data from Dallmann et al.*

(2004), interpreted by me in depth. The Billefjorden Faults are low angle listric faults and the Løvehovden Fault is interpreted by me as a normal fault. The sequence of beds is created for each of the different fault blocks since the geometry and thickness varies substantially within each of the blocks bounded by faults. The closely-spaced blue doubled lines to the east of the Ebbabreen Faults are marble layers belonging to the metamorphic basement strata.

Due to the listric geometry of the BFZ shown by Dallmann (2004), the thickness increase must be tiny. The listric geometry (Figure 3.4) does not leave enough space to accommodate much thickness increase. Figure 3.4 displays the section built with polygons as well as the legend for each of the units.

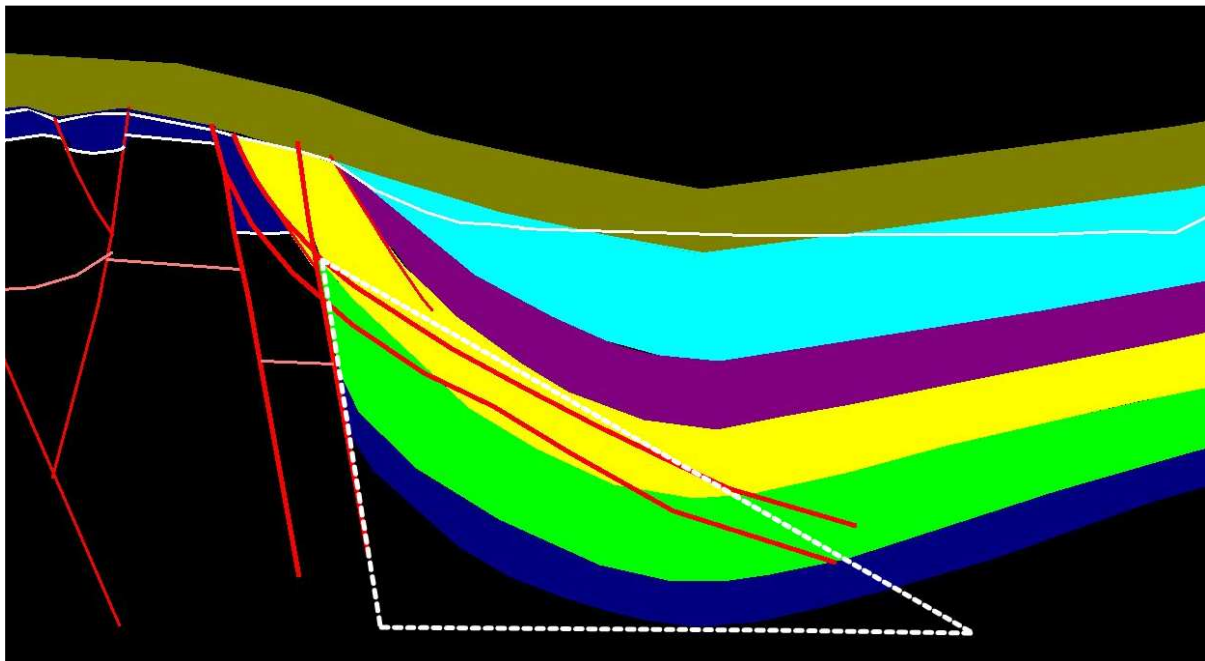


**Figure 3.4** Polygon cross-section across the Billefjorden Trough and respective legend. The polygons are created only for the Permo-Carboniferous stratigraphic sequence in order to highlight it with respect to the basement (in black) and the Devonian sandstones, siltstones and conglomerates appearing lined in orange, blue and white lines to the W of the BFZ. The purple lines west of the BFZ symbolize granitic gneiss. With respect to the structure shown in Figure 3.4, the interpretation of the Løvehovden Master Fault as a syn-rift fault allows the interpretation of the Billefjorden Trough as a syn-rif basin instead of a half-graben basin as shown in Figure 3.5 (b).

### 3.3 Testing the BFZ using syn-rift geometry

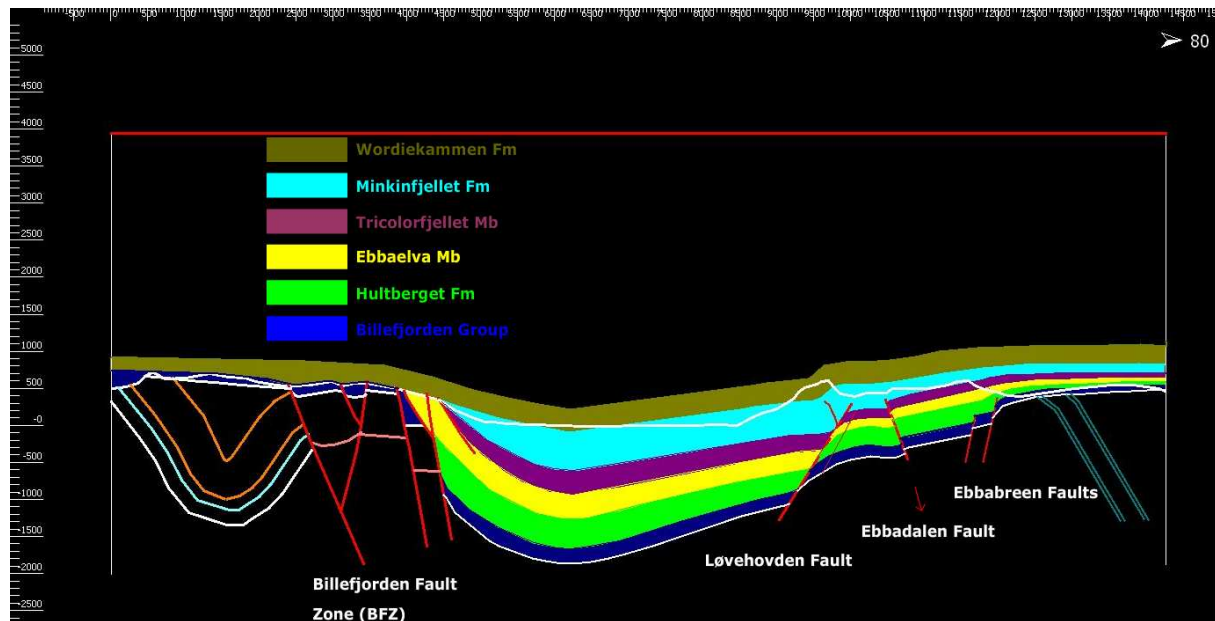
The re-interpretation of the Billefjorden Trough as a syn-rift basin, bounded by two sets of normal faults, changes significantly the disposition of the stratigraphic units in space. A significant increase in thickness must take place towards the basin centre, where the accommodation space is greater.

The BFZ listric and vertical geometries are juxtaposed for comparison in Figure 3.5 (a). The space occupied by the basement according to the listric geometry on Dallmann et al. (2004) can be used to accommodate syn-rift thickness increase. In order to fit the strata delimited by the white dashed-lined triangle above the listric faults, the units must be thinner, as shown in Figure 3.4.



**Figure 3.5 (a)** Cross-section of the north Billefjorden Trough where two sets of faults are juxtaposed for comparison: the listric fault geometry by Dallmann et al. (2004) and my sub-vertical fault geometry. The white dashed-lined triangle delimits the area occupied by the basement in Dallmann's cross section, which is required to accommodate a syn-rift thickness increase.

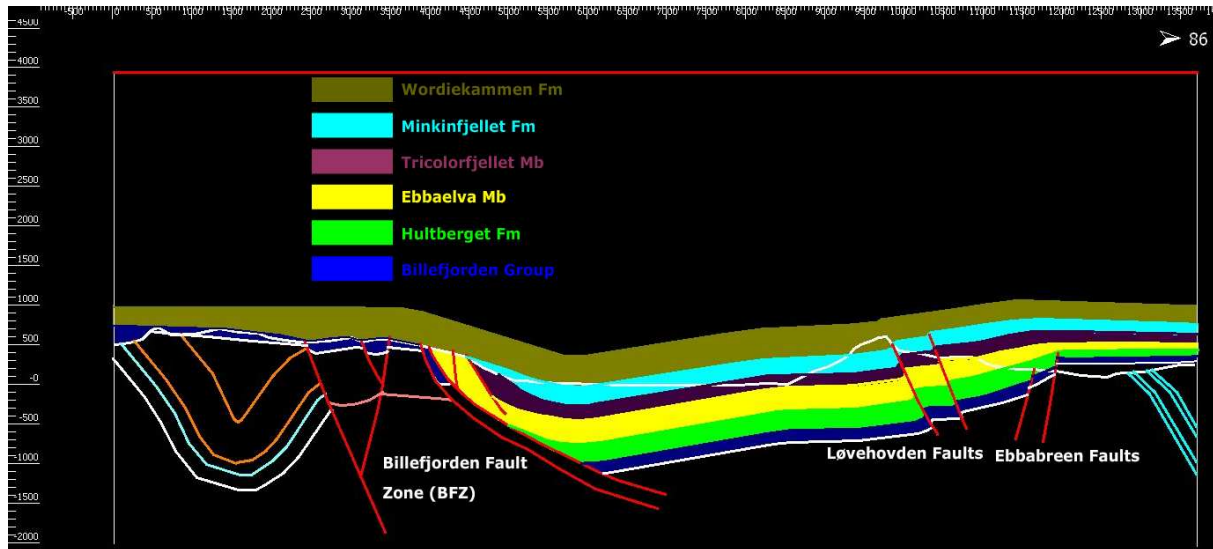
Hence, I propose a different geometry by setting the Billefjorden Faults more vertical. In this way, more space is created. The space used by the basement is now available for the syn-rift strata. I base the whole structural modelling on this geometry (Figure 3.5 b).



**Figure 3.5 (b)** *Cross-section of the North Billefjorden Trough showing thickness increase of the syn-rift sequence towards the basin centre. I interpret the two eastern faults of the BFZ to be sub-vertical in depth in order to create the necessary space to accommodate a syn-rift deposition. This is my final interpretation of the LFZ and BFZ and the geometry of the syn-rift basin.*

### 3.4 Comparison with a previous model (2004)

In 2004, Dallmann et al. published the “The Geological Map of Billefjorden”. The main difference between the Dallmann et al. (2004) section and the section here constructed, is the interpretation of the Løvehovden Faults. Here I interpret the Løvehovden Master Fault to be W-dipping and normal. Dallmann et al. (2004) interpreted it as a thrust fault, with eastern dip and reverse offset. Dallmann’s et al. (2004) cross section is here presented in Figure 3.6.



**Figure 3.6** Cross-section of the North Billefjorden Trough based on Dallmann et al. (2004). The Løvehovden Faults are interpreted to be reverse faults, and shows regional thickening across the basin. This is Dallmann's interpretation of a Carboniferous half-graben overprinted by Tertiary shortening.

I use the strikes and dips as well as the bed thicknesses available on the Dallmann's map. The Løvehovden Master Fault is considered to be a Tertiary thrust fault. Stratal thicknesses do not change across the fault since the fault movement is post-depositional. In my interpretation (Figure 3.5 b), the LMF is syn-depositional Carboniferous normal fault and hence affects the strata deposited during the Carboniferous period. Thicknesses changes on the outcropping strata have been in fact confirmed by my field observations and Lidar data interpretation.

The east-dipping Løvehovden Fault shown by Dallmann et al. (2004) would intersect the Minkinfjellet Formation. My model retains the easternmost "Ebbadalen Fault", but it does not cut through the Minkinfjellet Formation. The fault offsets the strata up to the Ebbadalen Formation, without propagating into the Minkinfjellet Formation.

### **3.5 Reconstruction and thickness variations**

The reconstruction workflow is designed to unfold the fold geometries, re-connect the different fault blocks and restore the regional tilt. 2D Move has built in several algorithms to restore sections depending on the amount of deformation, its origin, the type of fault and the strata involved. These algorithms are: “Flexural Slip Unfolding”, “Move”, “Trishear”, “Restore” and “Rotate”. The reconstruction is conducted in reverse chronological order. For this study, reconstruction steps are applied to the deformation created for the tectonic processes affecting the area from Carboniferous to Tertiary.

The strata are restored to a configuration with no deformation, where the Permian-Carboniferous strata lie horizontally. I infer quantitatively thickness changes in sediment deposition on the hangingwall of the LMF and along the section after restoring the fault throws and related deformation. The reconstruction provides a depositional profile on which to measure differences in sediment deposition.

#### **3.5.1 Flexural slip (1): Removing Tertiary shortening on the BFZ**

In 2D Move, the unfolding can be carried out by using two algorithms, called flexural slip and line length unfolding. Both are designed to unfold structures folded by contraction although they operate differently. The flexural slip maintains thickness variations. It also keeps the line length of the template horizon. Therefore, in order to maintain line lengths there needs to unfold each layer individually. Since one of the aims is to evaluate quantitatively thickness variations and shortening across the Løvehovden area it is more desirable to use the flexural slip algorithm.

In line length unfolding algorithm, thickness thickness variations are not maintained although it maintains a constant line length. Since we need to keep the original thickness changes across the basin, this algorithm has been discarded.

Flexural slip is a geological process, occurring during folding by contraction, where beds slip past each other as they are bended. Given the shaly nature of the Billefjorden Group and the high amounts of evaporitic minerals of the Ebbadalen and Wordiekammen Formations, a slip on the bedding planes may have occurred during the Tertiary uplift. This fact would make this algorithm the most suitable to unfold the strata deposited on the Billefjorden Trough.

The flexural slip unfolding algorithm controls the unfolding by using a pin which intersects the axial plane of a fold, keeping layer thicknesses. The algorithm is applied in two stages: the first one applied to the Wordiekammen and the Minkinfjellet Formations and the second applied to the rest of Formations. The slight curvature of the axial plane requires the use of two pins in order to describe the curve of the axial plane

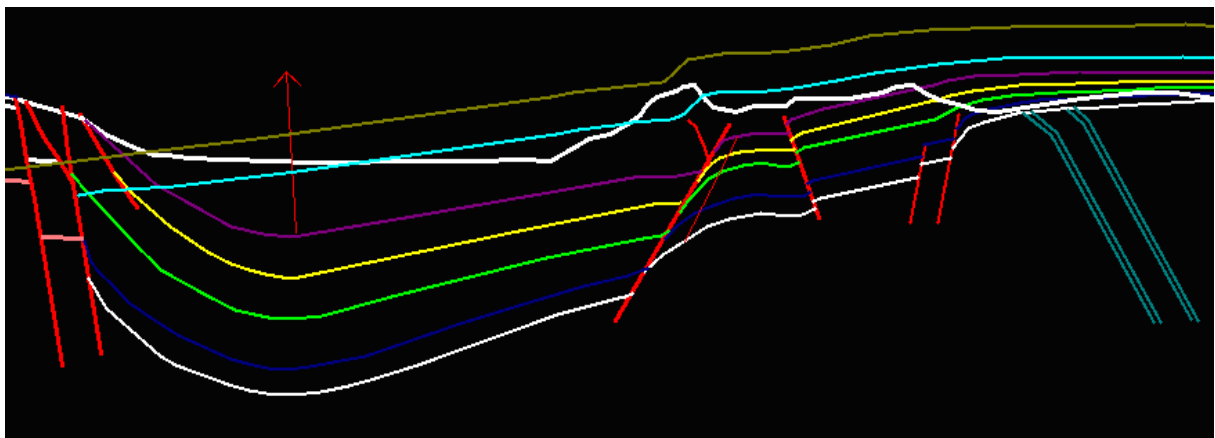
The algorithm works by inserting a pin across the fold axis. The fold has two limbs, the eastern and western limb. The Tertiary shortening on the BFZ is the consequence of the formation of the east-dipping western limb of the Billefjorden Trough. We select the beds of the western limb. The algorithm let the beds to will be unfolded with respect to the axial plane (pin), restoring them to the dip of the eastern limb.

The cross-section (Figure 3.5 b) shows that all the beds describe a syncline in the basin centre. The amplitude of the syncline is less pronounced in the Minkinfjellet and



Wordiekammen Formations since they are late-rift and post rift sequences, less affected by the BFZ and the LFZ. Most in concrete, the Wordiekammen Formation lies sub-horizontally over the BFZ.

Figure 3.7 displays the model with the Tertiary shortening strain across the BFZ removed for only the Minkinjfellet and Wordiekammen Formations.

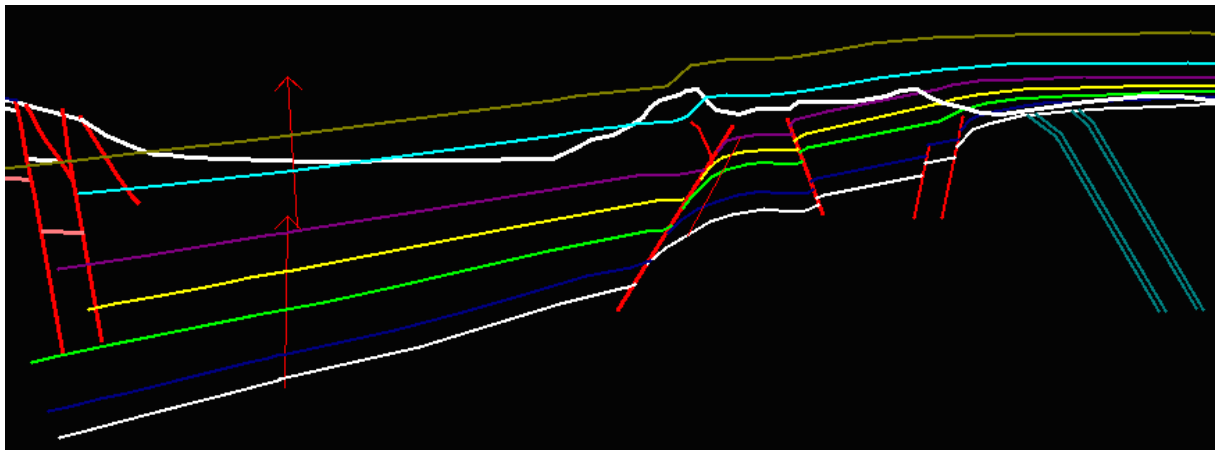


**Figure 3.7** Flexural slip unfolding of the Minkinjfellet and Wordiekammen Formations. The process removes shortening across the BFZ attributed to Tertiary thrusting. The result is the unfolding of the two uppermost strata, the Minkinjfellet and Wordiekammen Formations. The red arrow is the pin used to intersect the fold axial plane for the Wordiekammen and Minkinjfellet Formations, with vertical shear angle. Figure 3.8 shows the same process to unfold the rest of the beds since the fold axial plane is not straight and requires of two steps to unfold the sequence.

### 3.5.2 Flexural slip (2): Removing Tertiary shortening on the BFZ

In the second stage of applying the flexural slip algorithm, we define a slightly different second axial plane for the remaining strata of the hangingwall of the Løvehovden Master Fault. They are the Ebbadalen Formation, Hultberget Formation and the Billefjorden Group units. The second pin intersects these formations, completing the axial plane of the fold.

The results from the model shown in Figure 3.8 (a) demonstrate that, by employing a two-stage unfolding process, the beds are unfolded, keeping thicknesses. The line length is also maintained. Even though the basin is wider at shallow levels, the length of the beds is longer at the deepest levels (Base and Top of the Billefjorden Group and top of the Hultberget Formation).

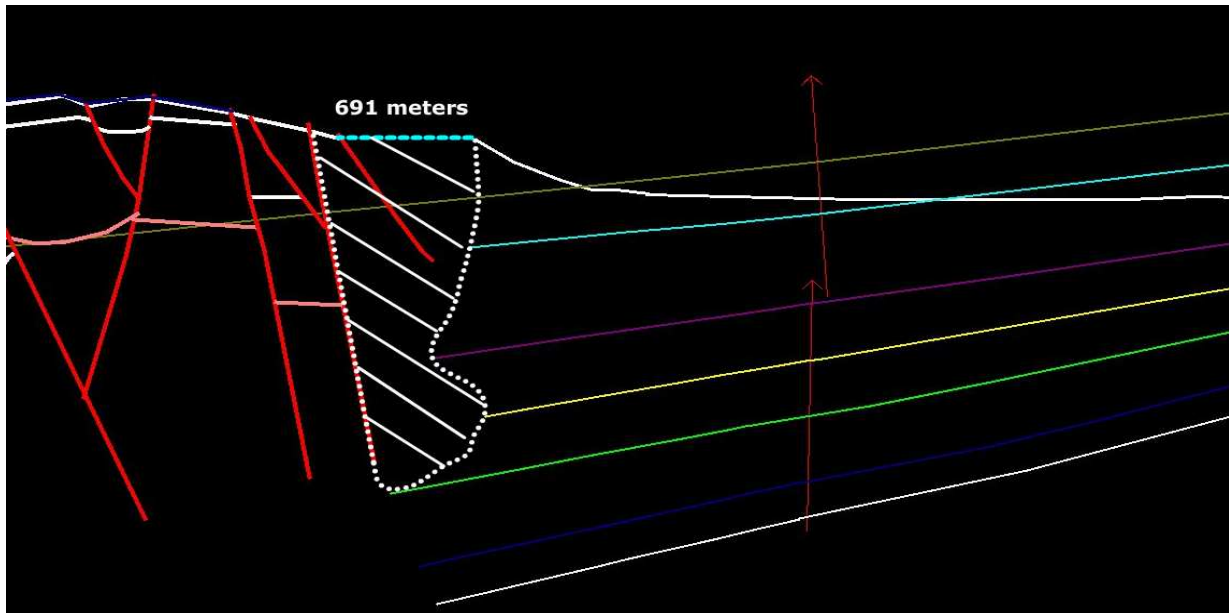


**Figure 3.8 (a)** *Flexural slip unfolding of the Løvehovden Master Fault hangingwall. The process is as well applied to remove shortening across the BFZ attributed to Tertiary thrusting. After applying the algorithm, all the beds are unfolded. The shear angle used to unfold the sequence is vertical once more since it has to be parallel to the axial plane of the fold. The red arrows show the orientations of the axial plane.*

The flexural slip restoration reveals that the lowermost beds of the stratigraphic sequence have been dragged at the Billefjorden Faults along a greater distance with respect to the rest of the syn-rift beds. The longest horizons are the upper and lower limits of the Billefjorden Group and the top of the Hultberget Formation. Since the Billefjorden Group and Hultberget Formation are the first syn-rift units, longer bed lengths may be caused by rift extension stretching the units over the whole Carboniferous period.

We can estimate shortening on the Billefjorden Fault Zone by measuring the distance into the gap created by extending the section. In Figure 3.8 (b) we observe that the section has

been extended. The aim is to match the longest beds to the faults to measure the amount of shortening. In order for the longest beds to match the faults, the section must be extended 691 meters, which is the maximum shortening across the BFZ (Figure 3.8 b).



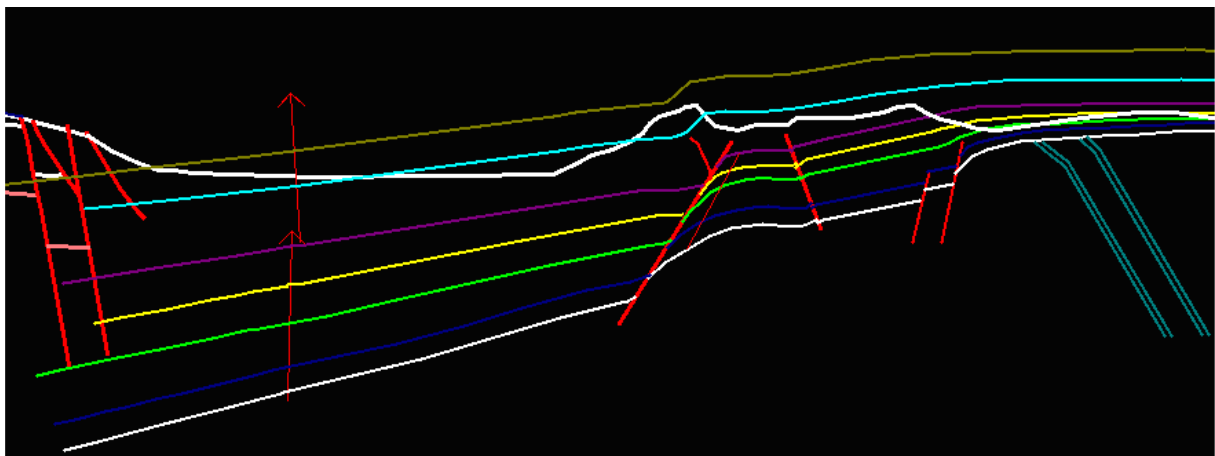
**Figure 3.8 (b)** Shortening estimation at the Billefjorden Fault Zone. Strata lying west of the BFZ are moved westwards. The lowermost (longest) beds are aligned with the Billefjorden Faults. The gap created in between (constrained by the dotted line) is the space contracted by Tertiary shortening. The maximum horizontal distance is measured to be 691 meters.

### 3.5.3 Move: Removing Tertiary shortening on the Ebbadalen Fault

It is the final step in the restoration of thrust-fault-related strain. The Ebbadalen Fault has been interpreted as a Tertiary thrust fault by Dallmann et al. (2004), possibly affecting the basement and the sedimentary cover from the Billefjorden Group up to the top of the Ebbadalen Formation. The vertical extent of the fault is inferred by my field observations where the fault core is clearly darkened by hydrocarbon circulation. Since hydrocarbons are sourced by the Billefjorden Group and stored in the same Billefjorden Group sands and Hultberget sands, it is likely that the Ebbadalen Fault extends down close to the Basement.

To restore the throw, we use the function “Move” to return the strata to reconnect the footwall and hangingwall. This operation reveals that the Tertiary shortening carried by the Ebbadalen Fault is 20 meters.

The deformation associated with the Ebbadalen Fault is limited to a zone less than 20 meters wide. Thus, the “Move” operation is sufficient because the fault-zone deformation is negligible at the scale of the cross-section. For this reason, we can use the “Move” tool to reconnect the horizons by removing the offset. The results are shown in Figure 3.9, where the strata are returned to their pre-shortening relative position along the fault plane.

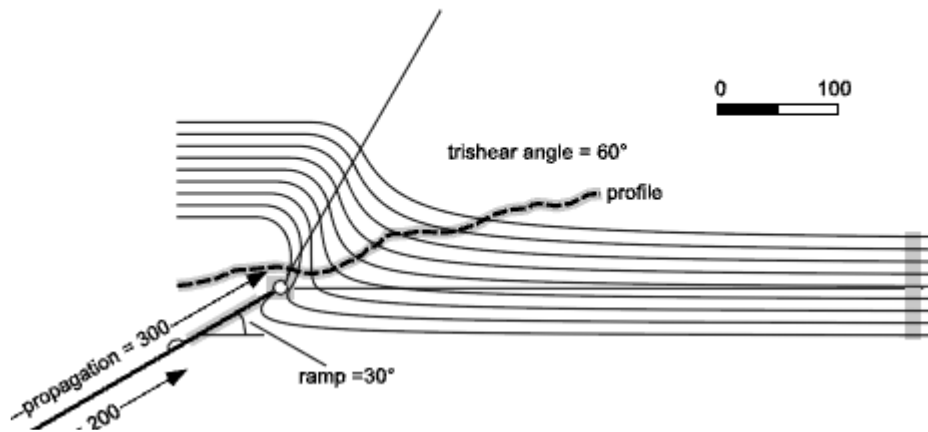


**Figure 3.9** *Ebbadalen Thrust Fault restoration. We use the “Move” function to remove Tertiary shortening across the Ebbadalen Fault. The result is the restoration of the Ebbadalen Fault hangingwall to its initial position and reconnection of the beds involved in thrusting. We have continued the restoration with the Ebbadalen thrust Fault since it is as well, a Tertiary feature.*

#### 3.5.4 Trishear: Removing the Carboniferous LMF-related deformation

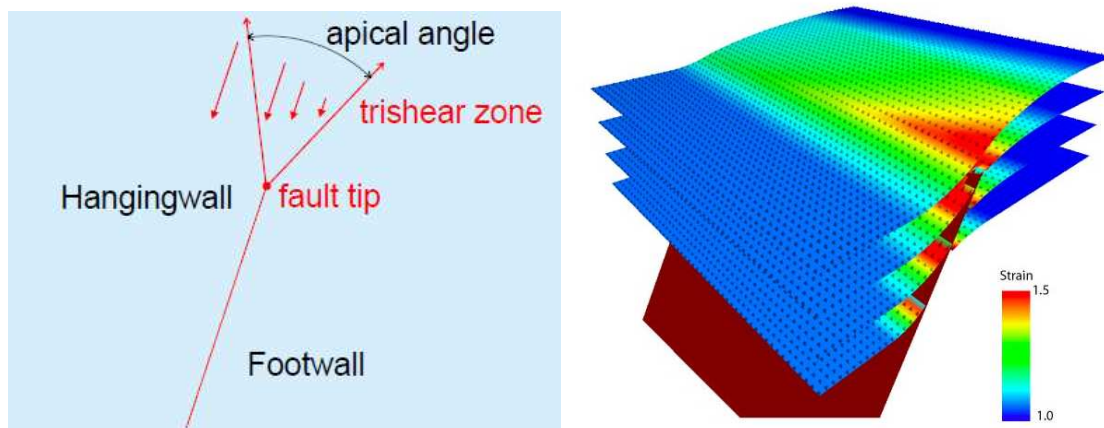
Trishear is a strain-compatible shear in a triangular shear zone, forming a triangular zone of penetrative deformation focused on the tip of the propagation fault (Erslev 1991). When the fault propagates, the strata lying above will fold above the fault tip.

A trishear zone is a kinematic model used in structural geology to define and explain the deformation observed enclosed in triangular zones of shear which can be related to fault propagation folds (Guohai et al. 2005). Figure 3.10 shows a simplified representation of a trishear zone.



**Figure 3.10** Deformation associated to fault propagation. The black line (in bold) represents the propagation of a west-dipping fault into the overlying strata at 60 degrees, which creates a triangular area of deformation. (Modified from Cardozo 2005)

When an extensional fault propagates, it creates a triangular zone of intense strain above the fault tip. This triangular zone consists of two limbs defined by the apical angle. As the fault propagates, the strain propagates as well into the overlying strata, which becomes offset. Strata fold above the fault tip, creating a monocline form on the footwall (Figure 3.11).



**Figure 3.11 (left)** Sketch showing the concept of triangular zone of strain propagation defined by the apical angle (Modified from Pelz et al. 2006) **(right)** 3D model showing in red where the strain from the propagation of an extensional normal fault is concentrated. Above the fault tip, the strata are bended into a gentle anticline-syncline form (Modified from Cardozo 2008).

The strata bend down over the hangingwall as more weight is added on the structure (Erslev 1991). A monocline forms above the fault tip when the rate of fault propagation is slow with respect to the rate of fault displacement. This creates a trishear zone, or area of distributed shear in a triangular zone, where the apex is located at the tip of the fault (Guohai et al. 2005). The monocline structures may act as a structural trap for hydrocarbons because of its convexity. With increasing strain or displacement, the overlying fold is cut by the fault as it propagates upwards (Stuart & McClay 1999).

The strata close to the surface are deformed by frictional drag into folds (Davis & Reynolds 1996).

The Løvehovden Master Fault may have initially stopped at some point within the Minkinfjellet Formation. However, the preferential deposition of sediments on the hangingwall led to a differential compaction. The differential deposition of sediments triggers the propagation of the Løvehovden Master Fault, creating a fault propagation fold as the strata bended over the fault tip (Figure 2.4).

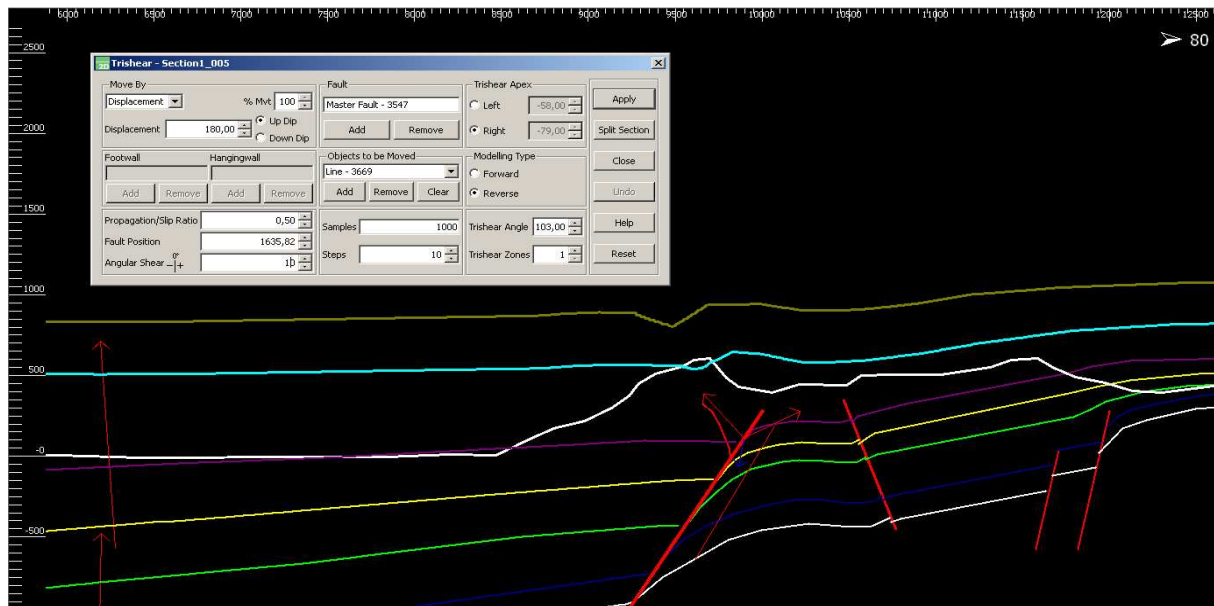
#### 3.5.4.1 Final model

The final trishear model results from having tested the fault position, trishear angle and trishear apex (Sections 3.5.4.2, 3.5.4.3, 3.5.4.4). I consider the fault throw and angular

shear as stationary values, since they are measured from field observations. The angular shear or regional dip was measured in fieldwork to be 10 degrees. The fault throw is calculated from log data and equal to 180 meters. The deformation associated to the trishear zone affects mainly the Wordiekammen and Minkinfjellet Formations.

Tests on the Løvehovden trishear zone create artifacts and unrealistic geometries when entering parameters that do not represent the deformation observed in field and on lidar data. The trishear-associated deformation is restored by trishear angles between 100 and 110 degrees, trishear apex between 70 and 80 degrees and 200-250 meters of fault propagation according to tests results. Further tests carried out at finer intervals of +/- 1 degree and +/- 1 meter (not shown in Sections 3.5.4.2, 3.5.4.3, 3.5.4.4 for practical reasons) conclude that the most suitable parameters to define the Løvehovden trishear zone are; trishear angle equal to 103 degrees, trishear apex equal to 79 degrees and fault propagation of 200 meters.

Figure 3.12 illustrates the final result of the trishear modelling after testing the location of the apex and trishear angle. The model shows two deformation limbs associated with the monocline formed above the Master Fault tip. Figure 3.12 shows the trishear zone along with a table containing the trishear input parameters. The displacement direction is specified to be “updip” since we work with an extensional normal fault with 180m of throw (calculated in section 2.3.6.3). I toggle “reverse” in “modelling type” since we are restoring the section to undeformed position.



**Figure 3.12** Detailed view of the Løvehovden trishear zone reconstruction. Fault propagation-associated deformation to the Carboniferous Løvehovden Master Fault is removed. This process has restored the LMF throw as well as the deformation related to the LMF propagation. The trishear zone is enclosed by the thin red arrows. The displayed dialogue box shows the parameters used in the trishear reconstruction.

The rest of the parameters are explained as follows:

*Propagation/Slip Ratio* → It is the amount of fault propagation and it ranges from zero to infinite. A Slip Ratio equal to zero means no fault propagation. A Slip Ratio of 1 will propagate the fault the same amount as the displacement. In this particular case, we know that the fault has actually propagated and the deformation associated to the fault propagation should at least be equal to half the displacement amount. Hence, I use the value 0,50.

*Apex Position* → The fault position sets the apex of the trishear zone, defined by default on the tip of the fault. After running several tests, I conclude that the apex zone must be located 200 meters below the fault tip, at 1635 meters, in order to minimize the deformation after restoration. This parameter is highly significant since the model does not work if we consider restoration from the actual fault tip. The results from testing the model indicate a possible



200 meters of fault propagation. By placing the paleo-fault tip 200 meters down-fault, the deformation associated with the Løvehovden Master Fault propagation is minimized when removing the effects of the trishear fault propagation folding.

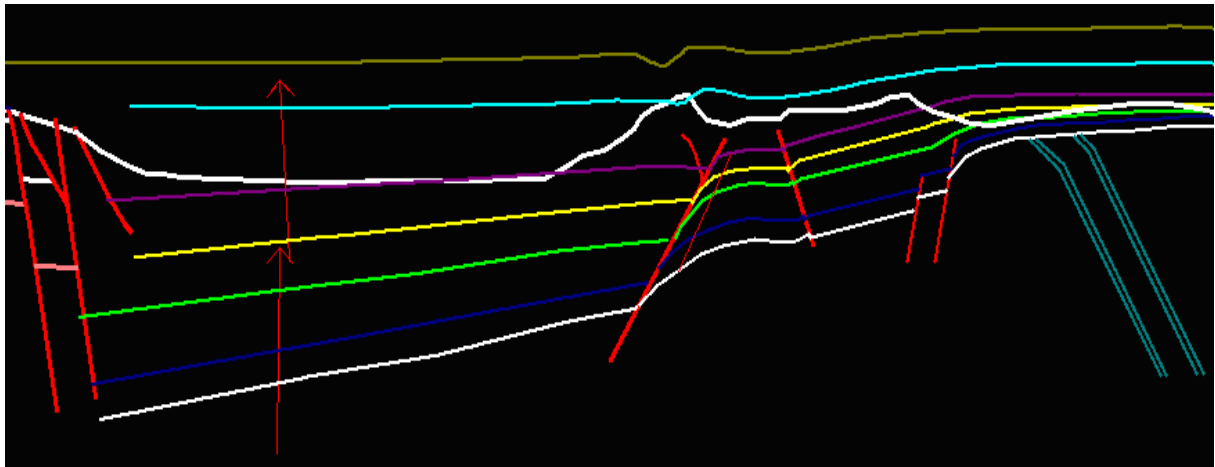
*Angular Shear* → It is the angle of shear of the beds affected by the trishear area, equal to the fault dip. The hangingwall beds dip approximately 10 degrees to the west at the vicinity of the LFZ.

*Trishear Angle* → It is the angle formed by the forelimb and backlimb (the red arrows in Figure 3.12) and it is also called apical angle. It defines the lateral extension of the trishear zone. After running several tests, 103 degrees is found to be the most suitable angle. An opening of 103 degree between the eastern and western limb of the trishear zone let us comprise the limits of the deformation created by the LMF propagation and to define the internal triangular area of deformation.

*Trishear Apex* → The trishear apex is the orientation of the bisector of the trishear zone or, in other words, the angle of the trishear zone with respect to the fault plane. By convention the angle is negative since the apex is rotated 79 degrees anticlockwise.

Finally, the *samples* and *steps* have been left as default (recommended by the 2DMove developers in the manual). The values have not any specific geological meaning but to divide the displacement into components and to animate the sequence of trishear restoration. In Figure 3.13 the results, intended to unfold the section by removing the strain caused by the Løvehovden Master Fault propagation, are shown. The same algorithm enables the restoration

of the hangingwall beds to the depositional horizontal position removing the effects of the throw and fault propagation.

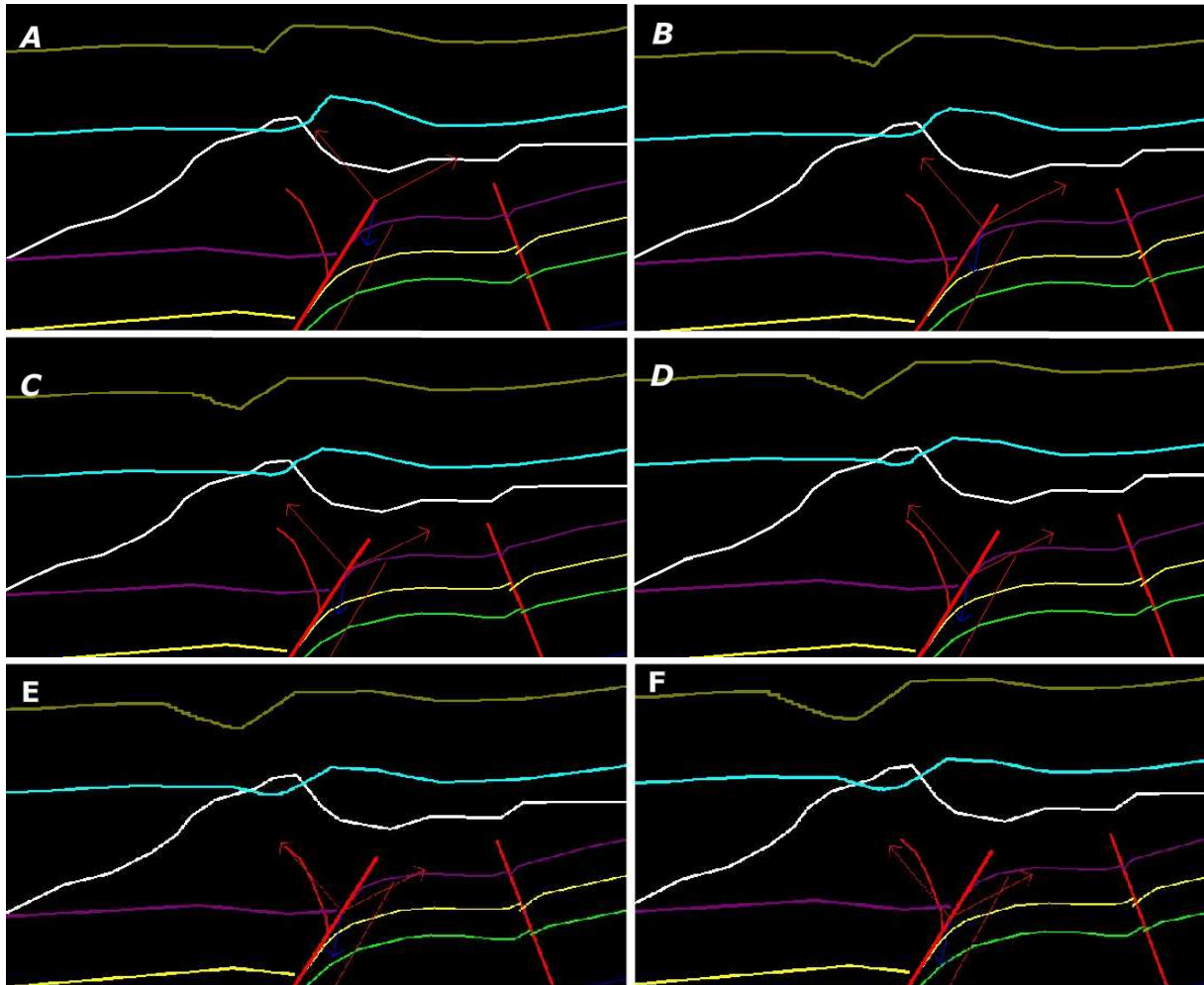


**Figure 3.13** *Regional view across north Billefjorden after trishear reconstruction.*

#### 3.5.4.2 Tests on the fault position

Tests on the location of the trishear apex let us quantify the amount of fault propagation. In case of no fault propagation the apex would be located on the present fault tip of the Løvehovden Master Fault. Differently, fault propagation requires relocating the apex to the point where the fault started to propagate into the overlying strata.

Figure 3.13 (a) shows the results of modifying the apex zone position on the Løvehovden Master Fault.



**Figure 3.13 (a)** Tests of trishear zone apex position (fault tip). In each test only the apex of the trishear zone is changed. Thick red line indicates Løvehovden Master Fault. Thin red lines with arrows indicate area of trishear. Tip of discrete fault and base of trishear lie at intersection of thin red arrows. The apex of the trishear zone is: (A = at top of the fault; B = 100 meters below top of the fault; C = 150 meters below top of the fault; D = 200 meters below top of the fault; E = 250 meters below top of the fault; F = 300 meters below top of the fault).

From A to F the apex of the fault is progressively moved down along the LMF. Models A and B revert the dip of the monocline, creating an anticline above the fault tip. Models E and F show a syncline formed on the Wordiekammen and Minkinfjellet Formations. This pattern was not observed in fieldwork. This unrealistic geometry suggests that the Løvehovden Master Fault must have propagated from deeper levels in the stratigraphy. The results of the model show that between C and D the deformation of the two

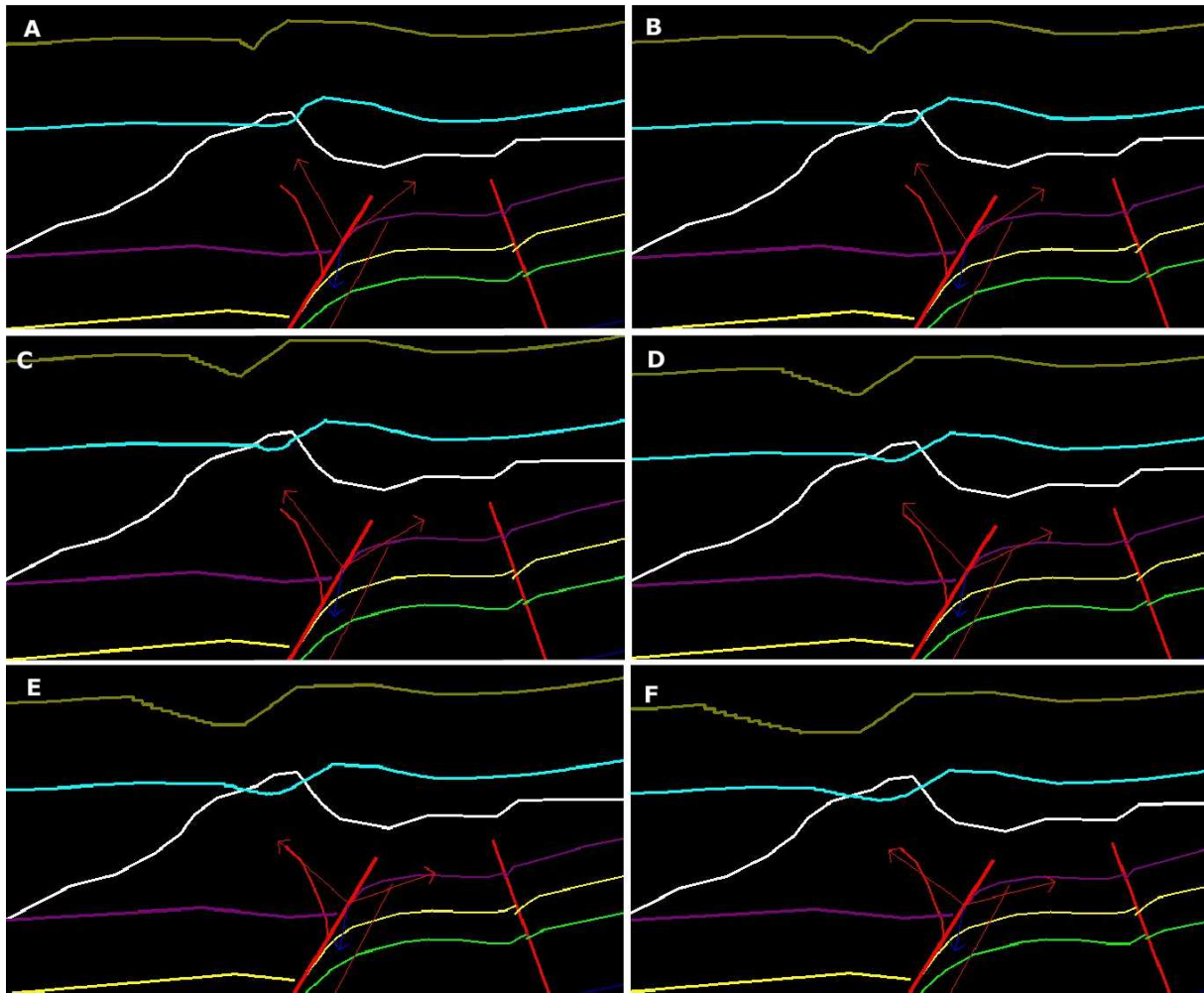
upper units is minor. The throw along the units is diminished and the horizons tend to be more horizontal after restoration. On C and D the apex is located between 200 and 250 meters with respect to the fault tip. According to the models, it is reasonable to expect 200-250 meters of fault propagation. The test results show 200 meters as the most likely amount of propagation (Section 4.5.4.1).

### 3.5.4.3 Tests on the trishear angle

The trishear angle controls the width of the trishear zone. The trishear angle must be able to comprise the forelimb and backlimb of the trishear zone, defining an area of fault propagation-related deformation in between.

Figure 3.15 (b) shows a case scenario where trishear angles from 80 to 130 degrees are chosen. Models A and B show the formation of a kink-shaped fold on the Wordiekammen Formation for trishear angles of 80-90 degrees. The Minkinfjellet Formation is by contrast less offset. The angulosity of the offset should smooth at higher stratigraphic levels. Hence, models A and B are not realistic.

Models E and F show the results of choosing obtuse angles. A long-waved syncline offsets the Wordiekammen, Minkinfjellet and Ebbadalen Formations. The restoration process creates more deformation than the originally observed. The angle is too open in order to embrace the trishear zone, producing undesired artifacts in the model. Even when some angulosity is still observed, models C and D reproduce more accurately the geometry observed on the Minkinfjellet and Wordiekammen Formations. Hence, a trishear angle of about 100 to 110 degrees is the most suitable input (Section 4.5.4.1).



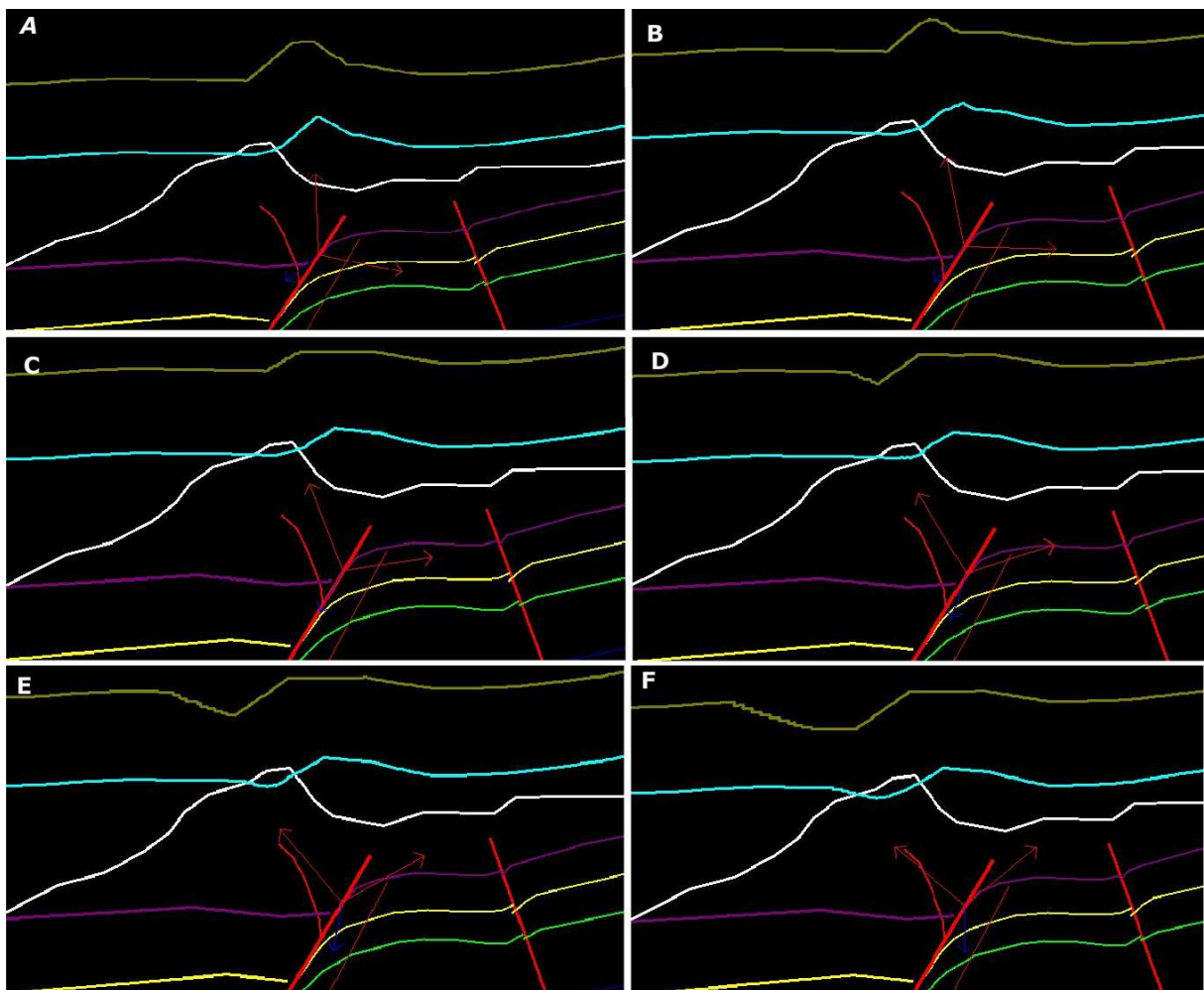
**Figure 3.13 (b)** Tests of trishear angle. In each test only the trishear angle is changed. Thick red line indicates Løvehovden Master Fault. Thin red lines with arrows indicate area of trishear. The trishear angles are: (A = 80 degrees; B = 90 degrees; C = 100 degrees; D = 110 degrees; E = 120 degrees; F = 130 degrees).

#### 3.5.4.4 Tests on the trishear apex

The trishear apex defines the orientation of the trishear zone bisector. The orientation of the lateral limits of the trishear zone must exclude the non-deformed areas.

Figure 3.13 (c) shows the results of modelling the trishear apex. In models A and B the trishear apex is mostly oriented to the East. The restoration algorithm creates an unrealistic dome over the fault tip on the Wordiekammen and Minkinfjellet Formations.

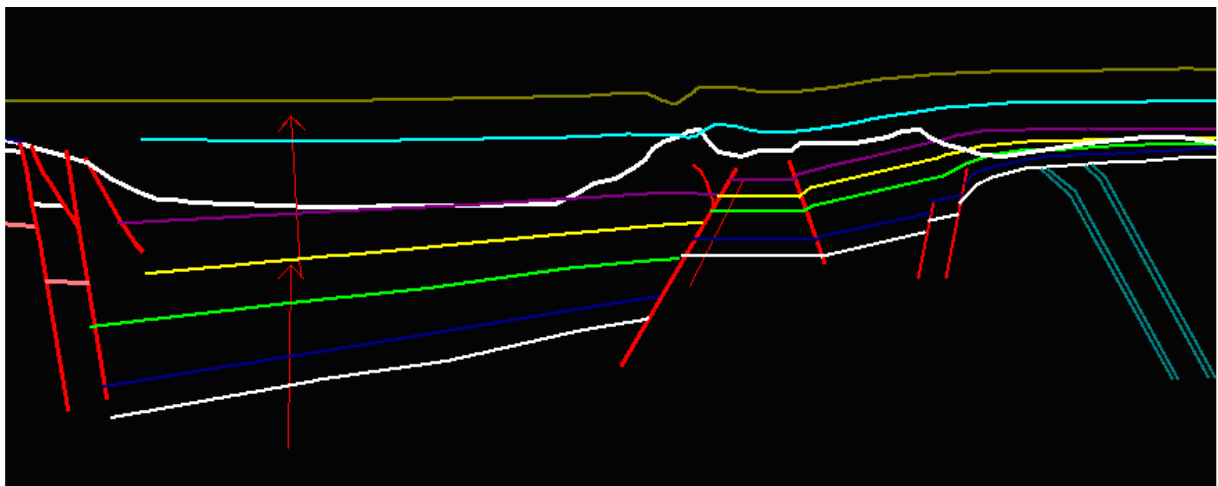
Oppositely, model F displays a broad asymmetric syncline to the west side of the LMF tip. Models C and D show a smoother geometry. However, the orientation of the trishear apex is not constrained to the observed area of deformation. The trishear apex orientation on model E represents the observed geometry on the Minkinfjellet Formation and is better constrained to the trishear zone. Hence, a proper input for the trishear apex would be 70-80 degrees (Section 4.5.4.1).



**Figure 3.13 (c)** Tests on the trishear apex. In each test only the trishear apex is changed. Thick red line indicates Løvehovden Master Fault. Thin red lines with arrows indicate area of trishear. The trishear apex are: (A = 40 degrees; B = 50 degrees; C = 60 degrees; D = 70 degrees; E = 80 degrees; F = 90 degrees).

### 3.5.5 Restore: restoring the central block

Between the Løvehovden Master Fault and the Ebbadalen Fault (central block), the strata are slightly curved in a smooth syncline-monocline form caused by the extensional and compressional stresses exerted by the bounding faults: the LMF and Ebbadalen Fault. The restore algorithm is a tool used to flatten gently dipping horizons. It is based on a reference datum, which can be either another horizon or a given height. The reference level I have used is a reference flat horizon. Strata are restored back to horizontal removing the fold caused by normal fault propagation. Figure 3.16 shows the results.

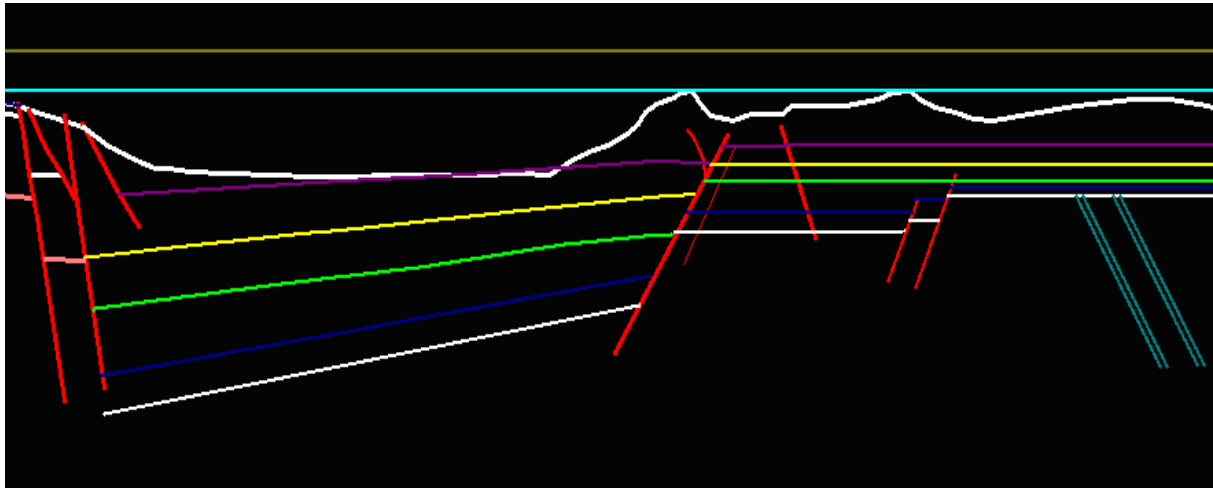


**Figure 3.16** Restoration of the Central Block (bounded by the LMF and Ebbadalen Fault). In this area, the strata are bended by the drag exerted by the LMF. The line length is not maintained since the deformation is not associated to shortening but to normal drag. The result is the removal of the offset caused by the bounding faults. I assume that they were horizontally deposited before being deformed.

### 3.5.6 Rotate: removing Permo-Carboniferous-related deformation

In general terms, the basin strata dip gently towards the centre of the basin defined by the LFZ to the east and BFZ to the west. The fault bounded block situated to the East side of

the Ebbadalen Fault is restored up to the top of the Ebbadalen Formation by rotating the whole block 11 degrees (Figure 3.17). The tilt of the strata in this area is the result of bed drape above the syn-depositional Ebbabreen Faults which creates a topographic depositional profile of 11 degrees.



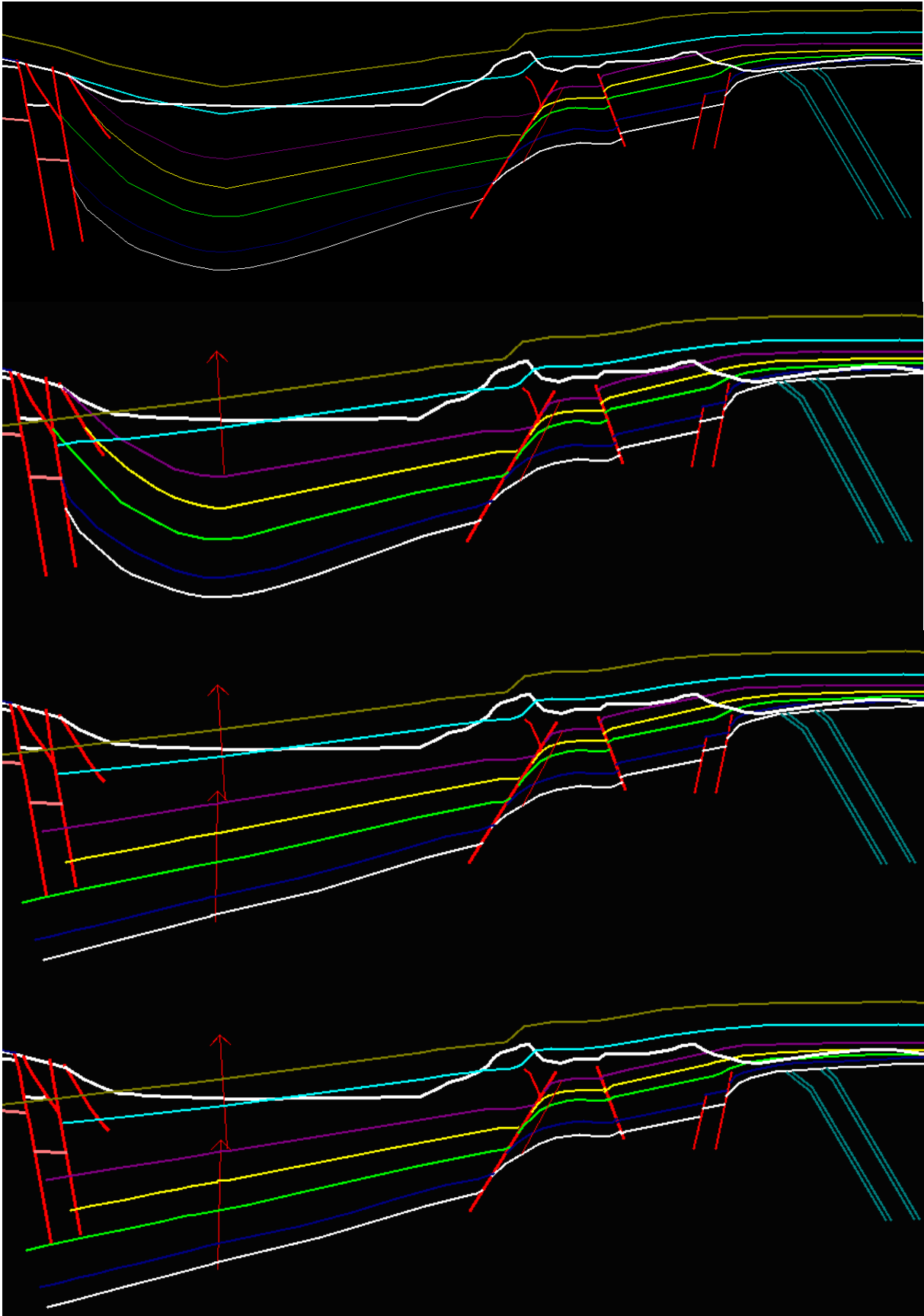
**Figure 3.17** *Result of the final stage of the restoration process. In this last step the block rotation and forward and editing operations are concluded. The block rotation restores the effects of drape over the Ebbabreen Faults. Sediment deposition over the syn-depositional Ebbabreen Faults caused the strata to bend over the fault tips, creating a stratigraphic monocline.*

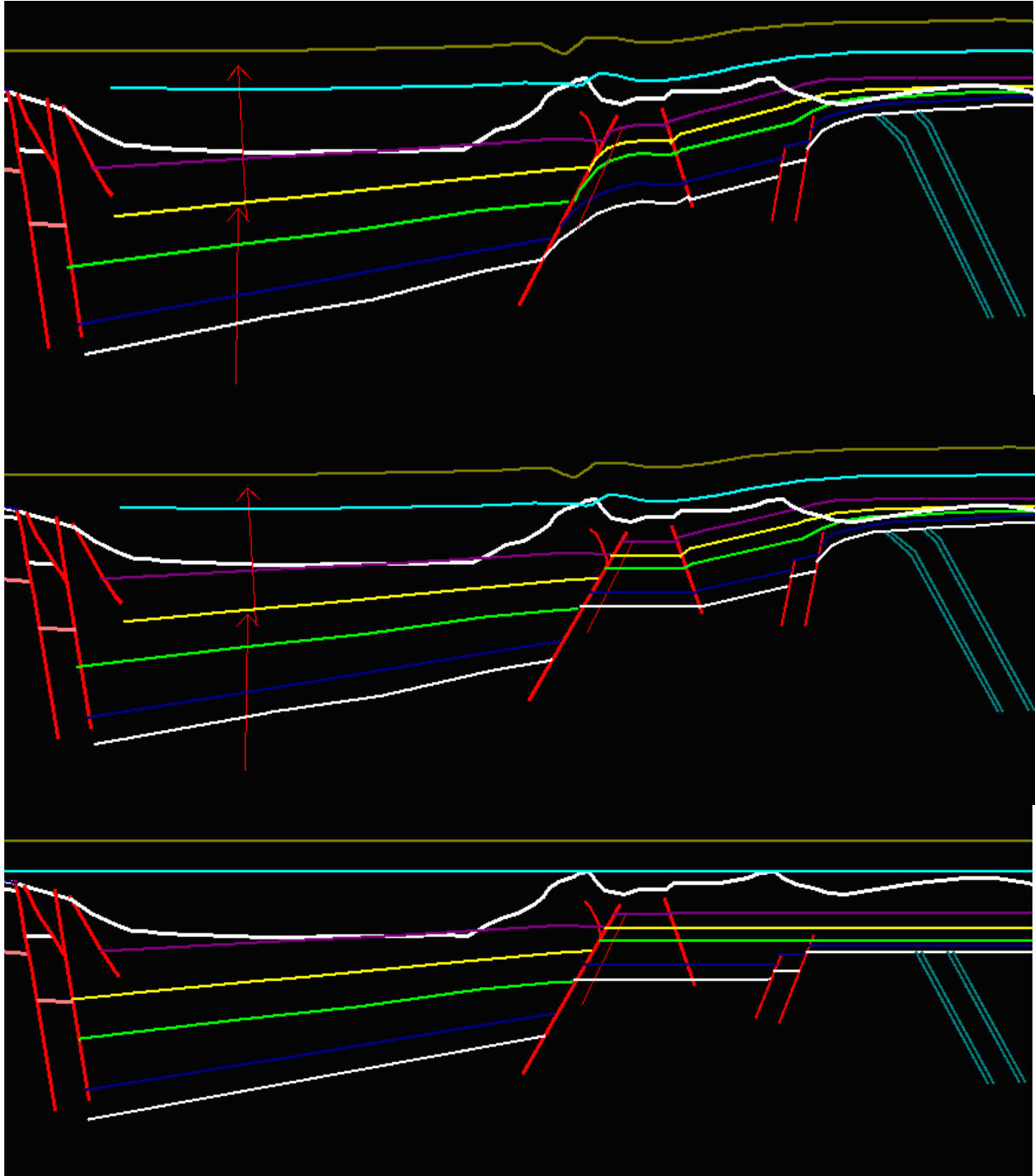
As a final step in reconstruction, the section should be edited and the imperfections smoothed. The results from the previous modelling steps are not perfect and leave some not residual deformation. Levelling the horizons will help measuring thicknesses accurately.

### 3.5.7 Structural reconstruction summary

In this Section, the retro-deformation sequence is summarized in a set of seven figures, which correspond to each of the steps of structural reconstruction (Figure 3.18).







**Figure 3.18** Summary of the structural reconstruction of the basin. The Figure is a set of 7 cross-sections which show each of the steps carried out in the retro-deformation process (See Figures 3.7; 3.8 (a); 3.9; 3.13; 3.16; 3.17). The first cross-section (on top of the Figure) shows the basin previous to the implementation of the restoration algorithms.

### 3.5.8 Thickness variations discussion

Thickness variations across the section determine the location of the basin depocentre. A progressive thickening from east to west was observed in the field on the strata outcropping in Ebbadalen, particularly on the Ebbadalen and Minkinfjellet Formations.

In my synthetic cross-section (Figure 3.5 b) all the normal faults (Ebbabreen faults and Løvehovden Master Fault) control thickness variations. There is no variation of thickness across the Ebbadalen reverse Fault. The normal faults present in the section controlled the sediment accumulation, leading to preferential accumulation of sediments on the hangingwall sides. Both the Billefjorden Group and the Hultberget Formation are thicker on the hangingwalls of the Ebbabreen faults, which can hence be catalogued as syn-depositional faults.

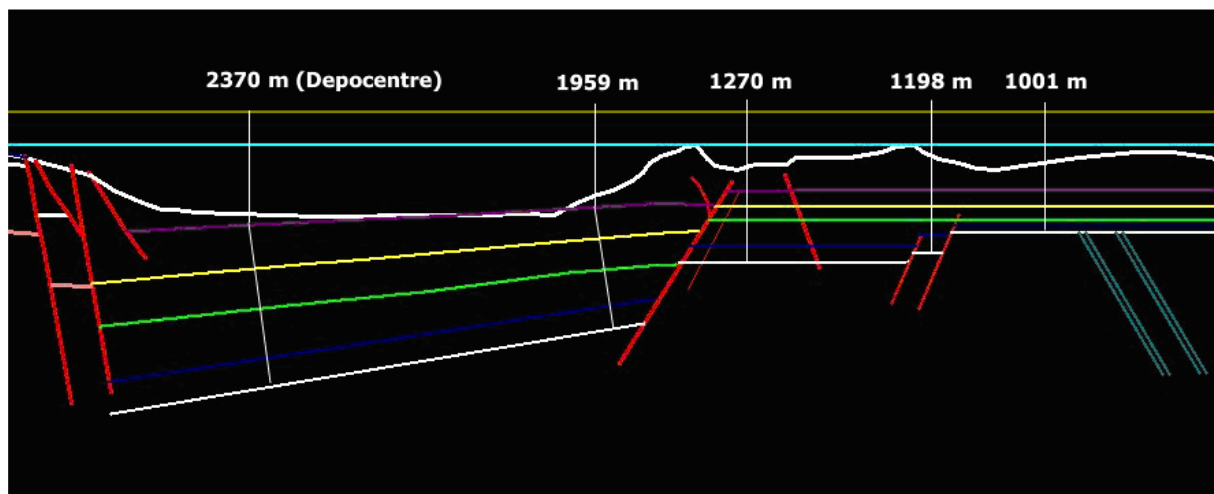
The syn-rift strata are thicker in the hangingwall than in the footwall, especially in the Ebbadalen, Minkinfjellet and Hultberget Formations. I construct the cross-section also taking in account the information regarding the basement depth provided by a Russian well displayed in “The Geological Map of Billefjorden” by Dallmann et al. (2004).

Since the LMF is leaking oil, the LMF would have vertically extended down at least into the Tricolorfjellet Member, which is the regional seal rock, allowing oil to flow upwards.

We do not know where the bottom LMF tip is located, though it could be anywhere between the Billefjorden Group and the Tricolorfjellet Member. I here interpret, that the

LMF affects the whole Permo-Carboniferous strata and in the models I locate the bottom LMF tip in the Billefjorden Group.

This fact implies that in the models I show thickening across the LFZ in the Billefjorden Group, Hultberget, Ebbadalen and Minkinfjellet Formations, since deposition would occur simultaneously with fault growth. These considerations along with the basement depth, constrains the thickness variations shown in Figure 3.19.



**Figure 3.19** *Thickness variations after restoration and quantification of the differential deposition of sediments across the basin.*

After measuring sediment thicknesses across the basin, I locate the Carboniferous depocentre between the BFZ and LFZ, at the vicinity of the BFZ. The maximum thickness would be about 2370 meters by considering a general uniform thickening.

An example of the important control of these faults on sedimentation is the maximum thickness differential across the LFZ. The thickness in the footwall is 1270 meters and a maximum of 2370 meters on the hangingwall. The development of the LMF controls the net

deposition of 1100 meters of sediments. This difference may have important implications in differential sediment compaction, porosity loss and fluid expulsion.

### **3.6 Decompaction**

In this section, the decompaction algorithm of 2D Move is applied on each of the units. In order to apply the algorithm we need to estimate several parameters, which are: initial porosity of the sediments, final porosity after burial and compaction, maximum paleo-depth and porosity-depth coefficient. Once these parameters are known a database is created, based on the mentioned values entered for each formation. The decompaction process can therefore be carried out.

Deposition of sediments throughout geological time causes subsidence and general compaction of the previously deposited units. The total vertical thickness of sediments plays an important role on basin subsidence and nature of the depositional units. The compressibility varies from lithology to lithology and the compaction processes may be physical or chemical. Mechanical compaction caused by the overburden weight is on this case not the only compaction mechanism. At local scale, evidences of extensive dissolution are recorded within the rocks of the Minkinfjellet Formation. This dissolution resulted in karstification in the past enhancing compaction by collapse along with burial dolomitization (Eliassen & Talbot 2005). In the sequence stratigraphy there is a complete record of a great variety of depositional environments. Basically I have encountered five lithologic groups: evaporites (gypsum and anhydrite), sandstones, shale, limestone and dolomite-dominated sequences.

Each of these sediments has a particular relationship between burial depth and compaction. In 2D Move this value must be entered individually for each lithology along with initial porosity values at depositional time. The most compactable are the evaporitic minerals, followed by limestone, shale and sandstone. When the sediments compact, the porosity loss generally describe an exponential on Athy's Law, which calculates the final porosity using initial porosity and depth as input data for sedimentary rocks ( $\phi = \phi_0 e^{-az}$ , where  $z$  = depth in km;  $\phi$  = final porosity and  $\phi_0$  = initial porosity).

The mechanical compaction is typically considered to be the principal mechanism but, in the study area, there is evidence of chemical compaction such as gypsum dissolution in the Minkinfjellet Formation. The mechanical compaction is derived from the accumulation of more than 4 Km of sediments (Appendix II). The average expected porosity for sediments buried more than 4 Km varies between 5% to 15%, applying Athy's Law. As an exception, I have considered the Minkinfjellet porosity to be 20% because of the high secondary porosity volume related to paleo-karst porosity enhancing processes. The Minkinfjellet Formation has undergone important processes of dissolution, collapse breccia and dolomitization, which converted it into a highly porous and permeable formation. The average porosity of a limestone compacted under more than 4 Km of sediment should not exceed 5%.

The proposed final porosity values are listed as follows, considering the dominant lithology of each of the formations. Porosity values are based on the standards from Mavko et al. (1996).

Porosity:

Billefjorden shale 10%

Hultberget sandstone 15%

Ebbaelva sandstone 15%

Tricolorfjellet evaporites 5%

Mininfjellet limestone and dolomite 20%

Wordiekammen limestone 5%

Overburden (mainly sandstone and carbonate units) 15%

The overburden is made up of the eroded units of the Upper Paleozoic (Gipshuken and Kapp Starostin Formation) and eroded Mesozoic to Tertiary units, which basically consists in carbonates and evaporites (Section 1.3.2.1.2 & 1.3.2.1.3). A porosity value of 15% is chosen from Mavko et al. (1996) based on standard values for carbonate and sandstone.

The second parameter that controls the decompaction workflow is the term called “porosity-depth coefficient” which is the change of porosity with depth, calculated from the following equation:

$$F = F_0 (e^{-cz}) \quad \text{where;}$$

$F$  = present day porosity at depth  $z$ ;  $f_0$  = initial porosity ;  $c$  = porosity-depth coefficient in km;  
 $z$  = depth in meters.

The initial porosity values are extracted from Mavko et al. (1996) and Allen et al. (1990), who give an account of initial porosities after deposition:

Shale →  $\phi = 0.6$

Sandstone  $\phi = 0.5$

Limestone  $\phi = 0.4$

Dolomite  $\phi = 0.4$

Evaporites  $\phi = 0.4$

In order to apply the equation we need to know the maximum depths of the sediments. We know from Michelsen & Khorasani (1991) that west of the BFZ at Pyramiden, the stratigraphic thickness was 3.9 km (Appendix II). This thickness does not include the Hultberget, Ebbadalen and Minkinfjellet Formations, not deposited west of the BFZ. The stratigraphic thickness of the Minkinfjellet Formation is estimated to be 470 meters from the logs in Section 2.2.6.3. The stratigraphic thicknesses of the Ebbaelva and Tricolorfjellet Members are measured on lidar data and equal to 125 and 150 meters respectively. The stratigraphic thickness of the Hultberget Formation is measured on the cross-section presented by Dallmann et al. (2004), equal to 250 meters. The total thickness of the Hultberget, Ebbadalen and Minkinfjellet Formations is 995 meters. The paleo-depth will be inferred by subtracting the thickness of each unit from the maximum burial depth, 4895 meters (3900 + 995). The thickness of the Wordiekammen Formation is measured in 300 meters from Dallmann et al. (2004).

Base of the Billefjorden Group →  $z = 4895 \text{ m}$  (4895-0 m)



Base of the Hultberget Formation → z = 4745 m (4895-150 m of the Billefjorden Group)

Base of the Ebbaelva Member → z = 4495 m (4745-250 m of the Hultberget Fm)

Base of the Tricolorfjellet Member → z = 4370 m (4495-125 m of the Ebbaelva Mb)

Base of the Minkinfjellet Formation → z = 4220 m (4370-150 m of the Tricolorfjellet Mb)

Base of the Wordiekammen Formation → z = 3750 m (4220-470 m Minkinfjellet Fm)

Overburden (eroded sequence from top of Wordiekammen to Tertiary strata) → z = (total 4895 – (995 m + 150 m Billefjorden Group + 300 Wordiekammen formation) = 3450 m

By entering the depth values related to each Formation we calculate the porosity-depth coefficient from:

$$C = \left( \frac{\ln \frac{F}{F_0}}{z} \right), \text{ where } F = \text{present day porosity at depth; } f_0 = \text{initial porosity; } z = \text{depth in (Km)}$$

$$C_{\text{Billefjorden Group}} = 0.36$$

$$C_{\text{Hultberget Formation}} = 0.25$$

$$C_{\text{Ebbaelva Member}} = 0.27$$

$$C_{\text{Tricolorfjellet Member}} = 0.48$$

$$C_{\text{Minkinfjellet Formation}} = 0.16$$

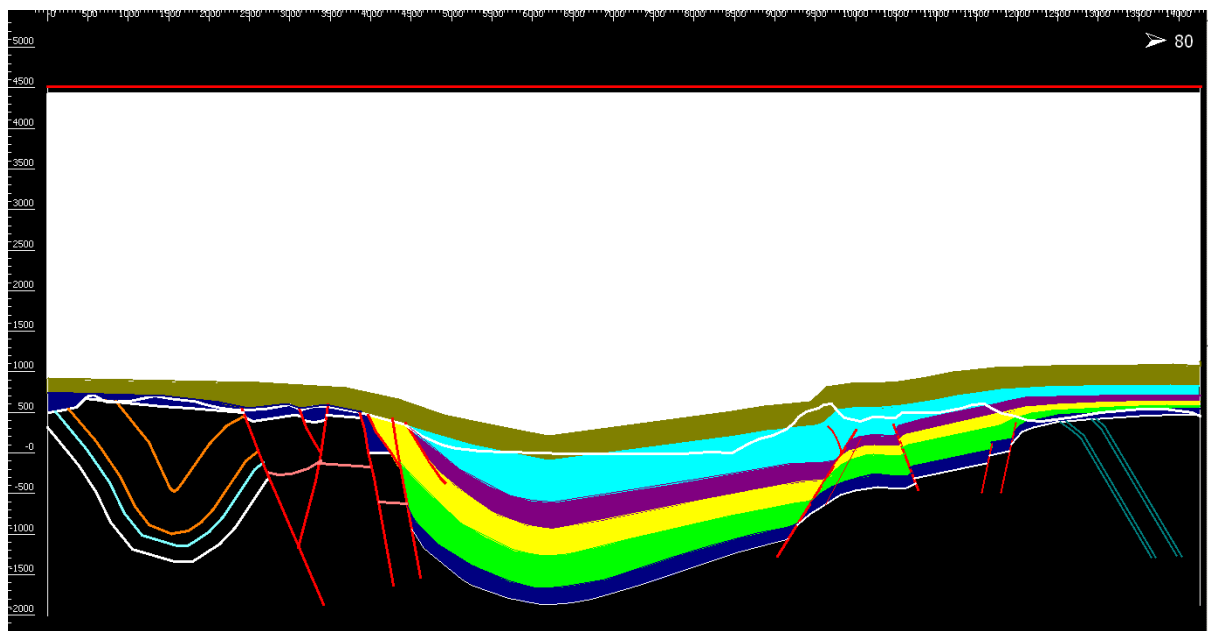
$$C_{\text{Wordiekammen Formation}} = 0.55$$

$$C_{\text{Overburden}} = 0.32$$

The decompaction process only considers the initial and final magnitude of the parameters, but not its evolution or intermediate steps.

The algorithm considers initial and final porosity, depth and thickness. The Minkinfjellet Formation, however, has undergone extensive dissolution. Dissolution process caused a thickness loss of 16% (Wheeler, based on Eliassen 2002). I estimated the thickness of the Minkinfjellet Formation to be 470 meters. Dissolution would hence imply a loss of 75 meters, which are not taken in account in the decompaction algorithm.

Karstification is therefore an intermediate event that increases porosity during burial. It is a geological observation that otherwise would have been dismissed by the model. The section previous to being decompacted is shown in Figure 3.20.

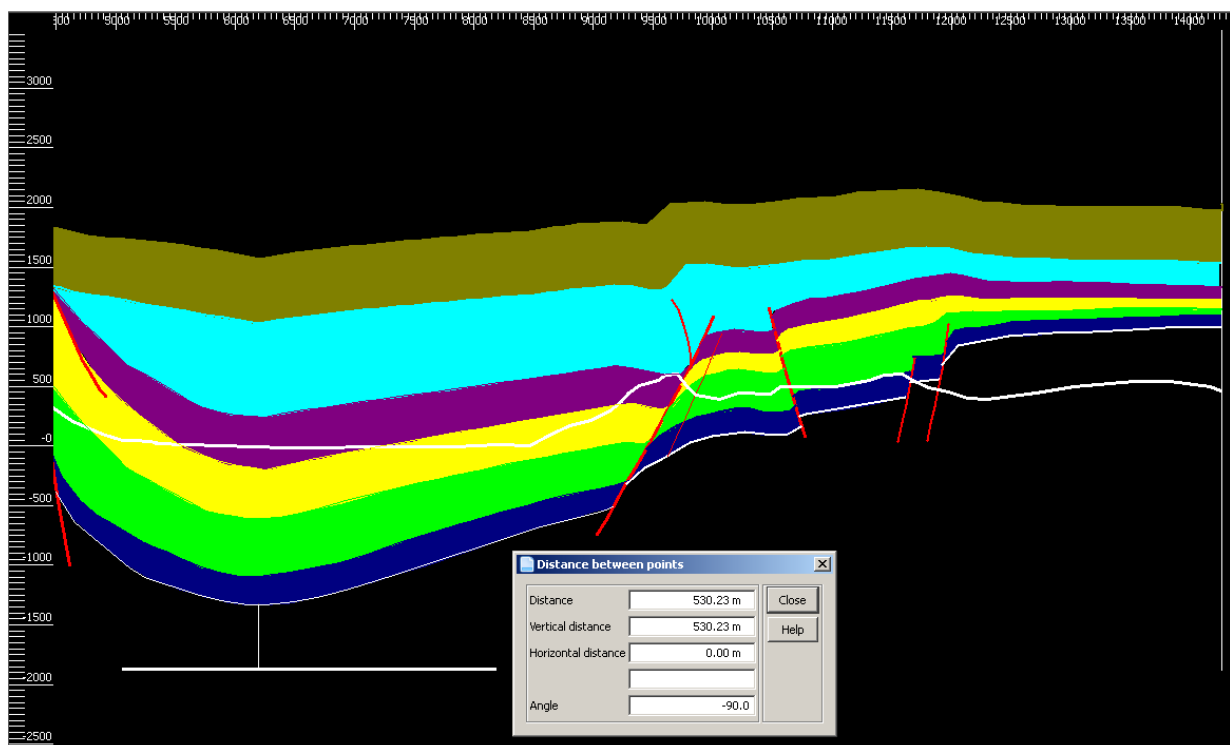


**Figure 3.20** North Billefjorden Trough cross-section previous to being decompacted. The white layer represents the eroded sequence made up of the Upper Carboniferous, Mesozoic and Tertiary strata (overburden discussed in text).

The section is compensated by considering the isostatic rebound during decompaction. The subsidence mechanisms built in 2D Move are isostatic subsidence and flexural subsidence. The flexural subsidence is based on elastic bending of the lithosphere while the isostatic subsidence is caused by physical changes in the thickness of the lithosphere.

I use the principles of flexural subsidence, based on elastic bending of lithosphere. The lithospheric plates are viewed as elastic plates that are bent by vertical loads (Stuwe 2007). The flexural subsidence is the most convenient algorithm to be used since we work at a local scale. The lithosphere is locally flexed down by the weight of the overburden.

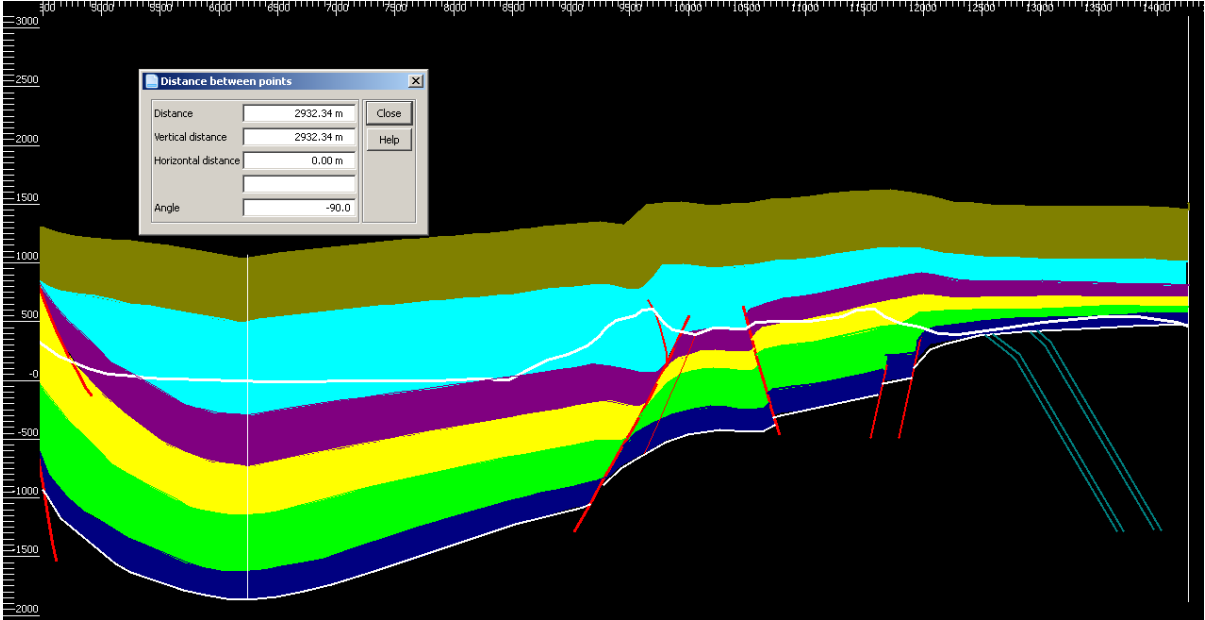
Figure 3.21 shows the amount of subsidence undergone by the basin. The Billefjorden Group, Hultberget Formation, Tricolorfjellet Member, Ebbaelva Member, Minkinfjellet and Wordiekammen Formations are lifted up 530 meters after isostatic rebound. No major deformation is observed to be associated to isostatic compensation.



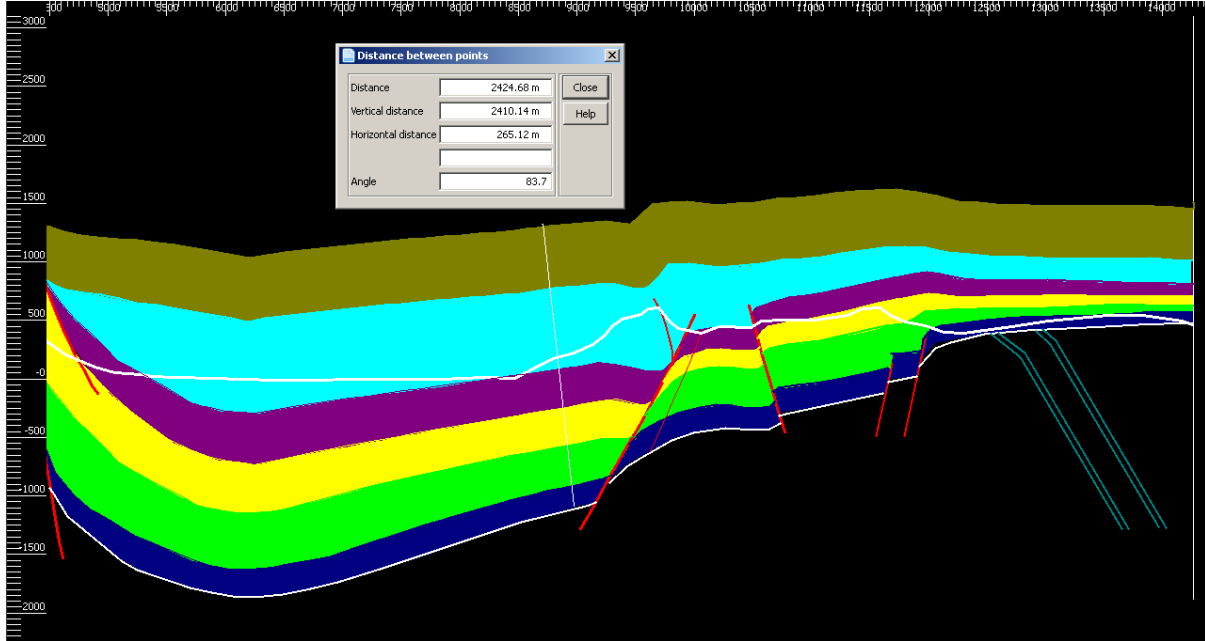
**Figure 3.21** *Decompaction and flexural isostatic compensation of the Permo-Carboniferous stratigraphic sequence deposited in the Løvehovden area. The topographic profile (white line) is unmoved and serves as reference for comparison with Figure 3.5 (b). The white basal line is a datum on which isostatic rebound is measured in 530 meters.*

The results of decompaction are shown in Figures 3.22 and 3.23. Horizons and faults have been expanded. Stratigraphic thicknesses are measured in two locations: 1) the

depoecentre and 2) the west side of the LFZ. The locations are the same as shown in Figure 3.19 where the measured stratigraphic thicknesses correspond to 2370 and 1959 meters respectively.



**Figure 3.22** Thickness at the Billefjorden Trough estimated deposcentre after decompaction. The decompacted stratigraphic thickness is 2932 meters.



**Figure 3.23** Thickness at the west side of the LFZ after decompaction. The decompacted stratigraphic thickness is 2424 meters.

### 3.6.1 Discussion

We compare stratigraphic thickness changes before and after decompaction at the Trough centre (depocentre) and west of the LFZ. After decompaction, we measure a thickness increase of 562 meters and 465 meters respectively. The percentage of thickness loss on these two locations are 19.16% and 19,18% respectively.

The model results suggest that the Permo-Carboniferous sequence has been compacted by a factor of 500 meters, equivalent to a 19,17 % of Permo-Carboniferous sediment deposition. A thickness loss of 75 meters by karstification on the Minkinfjellet Formation, must also be added, making a total of 575 meters of compaction.



## Chapter 4: DISCUSSION

### 4.1 Reinterpretation of the Løvehovden Fault Zone

The re-interpretation of the Løvehovden Fault Zone as a set of syn-depositional west-dipping Carboniferous faults is based on structural and sedimentological evidence.

#### *Sedimentological discussion:*

A correlatable sequence of gypsum-rich dolomite and shale has been identified across the Løvehovden Master Fault, in the Minkinfjellet Formation (Figure 2.19). Between shales, 26 meters of carbonate deposition was observed in the hangingwall. By contrast, the carbonates interbedded with shales are only 4 meters thick in the footwall (Figure 2.18). The common shale sequence is 7 meters thick both in the hangingwall and footwall of the Løvehovden Master Fault (LMF). The gypsum rich dolomite is 8 meters thick in the hangingwall and 5 meters thick in the footwall of the LMF (Figure 2.19).

The observed differences in carbonate thicknesses reflect sea level changes, where creation of accommodation space is controlled by transgressive cycles (Samuelsberg & Pickard 1999). Marine shale is commonly deposited in deep water conditions, whereas gypsum deposition requires of a shallow water column. The common shaly sequence reflects by itself a transgressive-regressive cycle. The amplitude of these cycles is locally controlled by the growth of the Løvehovden Master Fault.

A syn-depositional fault must not necessarily be growing keeping pace with sedimentation. There might be stages of fault slip followed by stages of sediment deposition and further slip.

The Løvehovden Master Fault slipped during Carboniferous deposition, leading to differential sedimentation across the fault. The common strata connecting the LMF walls (gypsum-rich dolomite and shale) were deposited during fault inactivity. Preferential deposition of carbonate between shales on the hangingwall can be explained in terms of normal fault slip. Fault slip created topographic gradient, causing relative sea level to rise with respect to the eastern footwall block. Higher water depth in the hangingwall favoured the deposition of the gypsum-rich carbonates. In the relatively shallow and possibly occasionally exposed area not affected by fault movement (footwall zone), the sedimentation was more limited since carbonates require of greater accommodation space and water depth in order to grow up (Coe 2005).

Footwall and hangingwall stratigraphies are significantly different below the correlatable sequence previously discussed. The hangingwall log records 5 meters thick gypsum-rich brecciated carbonate overlying an 18 meters thick sequence of evaporites (from 0-60 meters in Figure 2.17). By contrast, in the footwall log we encounter 20 meters of thick massive carbonates and dolomite breccia rich in chert clasts (from 0-10 meters in Figure 2.18).

Hangingwall strata may have their equivalent in the gaps of the footwall, or may simply be a unique deposit and do not correlate.



I interpret these litological differences related to changes in water depth. The footwall zone was topographically higher than the hangingwall, less affected by marine regimes but more influenced by continental settings. This continental influence is inferred from the presence of chert siliceous clasts on the eastern side of the LMF. The breccias observed on top of the footwall log contain clasts of sandstone, evidencing interaction between the carbonate platform and terrigenous deposition.

Chert clasts may also form *in situ* in marine settings. Marine organisms such as radiolarian agglutinate silica on their skeletons, precipitating to the sea bottom when die. As presence of silica in the hangingwall was not observed, I interpret its origin as continental-derived procedence by dissolution in continental settings.

In the Minkinfjellet Formation, white, yellow and black chert nodules are found in dolomite facies. The nodules are common but not as abundant as in pure limestones. At the upper Wordiekammen Formation, sandy limestone facies are characterized by a mixture of quartz, feldspar and sand grains. This calcarenite represents depositional setting of mixed clastic and carbonate input (Eliassen 2002).

The extended deposition of evaporites and thicker carbonate sequences observed in the down-faulted block, suggest marine-dominated deposition with no continental influence.

If the Løvehovden Master Fault was a compressional Tertiary feature, we should not expect to find such sedimentological differences between footwall and hangingwall.

*Structural discussion:*

The second criteria I discuss to demonstrate that the Løvehovden Master Fault is an extensional syn-rift fault is based on structural observations. A monocline forms on the footwall. The monocline reflects SW movement direction.

I interpret the monocline above the Løvehovden Master Fault tip as an extensional fault-propagation fold feature. As new sediments are deposited and differential subsidence occurs, the footwall strata fold. As more weight is deposited, the strata bend down over the hangingwall (Erslev 1991). The observed deformation tells us about rate of fault displacement since monoclines may form when a fault propagates at a slower rate with respect to fault slip (Guohai et al. 2005).

The monocline structure developed over the Løvehovden Fault Zone is as well an area of trishear, where deformation is distributed in a triangular zone (Guohai et al. 2005).

A triangular zone of deformation is observed to form over the LMF tip, affecting the Minkinfjellet and Wordiekammen Formations. The high degree of deformation associated to the fault-propagation fold indicates propagation after rock consolidation. If, by contrast, the monocline had formed when the sediments were being deposited, we should expect a trishear zone with a broader trishear angle, where the monocline would be broader. Extensional fault-propagation studies carried out by Finch et al. (2004) suggest that the reduction of the strength of the strata involved results in an increase of monocline width. By contrast, stronger strata would result in the formation of a sharper monocline. The observed monocline is sharp and abrupt, which supports the interpretation of its formation after rock consolidation.

This configuration is in agreement with the high degree of deformation observed at the vicinity of the Løvehovden Master Fault tip. The strain propagates from the Løvehovden Master Fault into the surrounding areas, opening newer normal faults with a more limited offset. A similar array of secondary faults was observed in field. The most outstanding is the “Secondary Fault”. It is a conjugate fault to the Løvehovden Master Fault. The Propagation and Marginal Faults are normal faults linked to the propagation of the LMF strain. Particularly, the Propagation Faults, may have been formed by compaction after extension stopped, since they occupy high stratigraphic levels within the Minkinfjellet Formation. (Figure 2.1). The Secondary Fault defines the western limit of trishear propagation fault geometry. The orientation of the Secondary Fault implies that it developed simultaneously with the Master Fault as new space was being created by extension.

The averaged strike and dip of the Løvehovden Master Fault is 310/57 SW. The Propagation Faults and Marginal Faults are normal faults, which reinforces the interpretation of the Løvehovden Fault Zone as a system of extensional syn-rift faults.

#### *Geometry and kinematics of the LFZ:*

Normal slip favours the hangingwall strata to move away from the footwall, creating an extensional gap that is structurally compensated by the development of antithetic faulting (Davis & Reynolds 1996). The Secondary Fault, defined by a lineation of intense deformation and fracturing, occupies the gap created by Carboniferous extension. The offset created by the Secondary Fault is limited and fault throw was not observed.

The monocline structure forms on the footwall of the LMF, whereas a syncline is observed on the hangingwall. This structure is the result of the breakup of the previous monocline as the Løvehovden Master Fault propagates. Such an anticline-syncline form is not the result of drag against the fault (Finch et al. 2004).

An analogue structure is encountered in the Gulf of Suez, where Miocene normal faults propagate into the overlying strata. According to the studies presented by Gawthorpe et al. (1997), the formation of a growth monocline by normal fault propagation consists of two stages: growth monocline above blind fault and surface-breaking fault. The comparison of this structural setting with the monocline structure observed in the study area indicates that the propagation of the Løvehovden Master Fault continued to the second stage discussed by Gawthorpe et al. (1997). In the Løvehovden area, the monocline is breached and the LMF has splitted it in two, creating a zone of intensive shear in between (Domain B<sub>1</sub> in Figure 2.1).

#### **4.2 Results from the structural models**

The structural models are intended to simulate the syn-rift geometry of the Løvehovden area across north Billefjord and to evaluate quantitatively sedimentary thickness variations, amount of compaction, isostatic rebound, amount of extension and fault propagation.

The cross-section construction, based on Dallmann et al. (2004), demonstrates that the syn-rift sequence is incompatible with the dip of the eastern Billefjorden faults presented by the author. In order to accommodate syn-depositional thickness increase, the Billefjorden Faults must be steeper (Figure 3.5 a).

The basin reconstruction presented in Section 3.5 provides quantitative data for the north Billefjorden Trough. The flexural slip unfolding evidences different bed lengths in the Carboniferous sequence. The longest bed lengths correspond to the deepest beds. Since the basin narrows in depth we should expect shorter bed lengths for deeper-lying strata. The deeper sediments are dragged over the fault surface along a greater distance than those lying above. In addition, the lowermost beds have been exposed to longer episodes of extension than the uppermost beds, which were deposited in later stages of rifting. A total 691 meters of basin shortening is carried by the Billefjorden Fault Zone. The contribution in shortening of the Ebbadalen reverse Fault has been estimated to be 20 meters. The total Tertiary-related shortening is 711 meters.

The trishear models on the Løvehovden area show that, in order to restore trishear-related deformation, the Løvehovden Master Fault tip must have been originally located 200 meters below the current fault tip. This fact implies that the Løvehovden Master Fault has propagated upward, controlling the formation of the monocline fault-propagation fold.

Thickness changes are recognised from W to E across the basin, controlled by the formation of syn-depositional normal faults (Figure 3.19). The maximum thickness is achieved at the vicinity of the Billefjorden Fault Zone (Figure 3.5 b).

The stratigraphic sequence deposited on the Løvehovden area was compacted by 513 meters. Dissolution processes on the Minkinfjellet Formation caused a thickness loss of 16% (Wheeler based on Eliassen 2002). The Minkinfjellet Formation (470 meters thick) underwent important karstification, and the cave collapse. The 75 meters of chemical compaction (16%

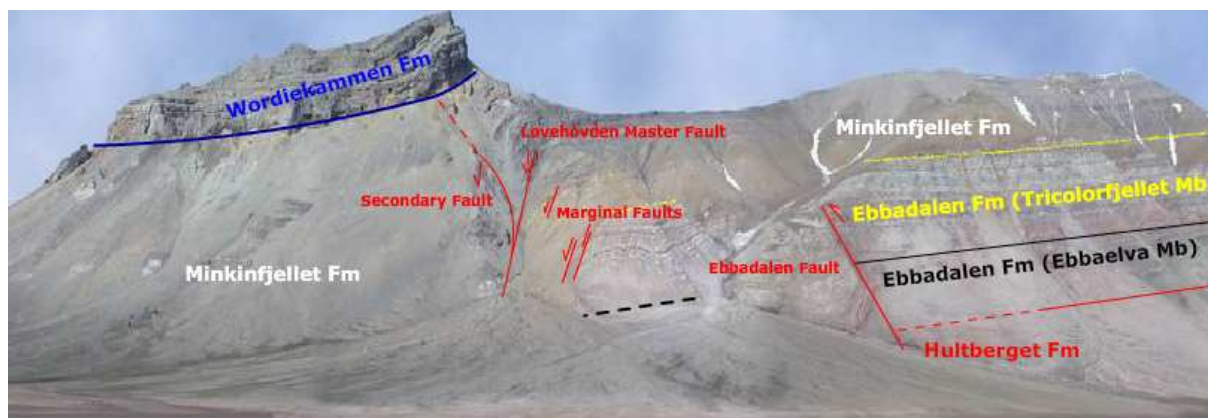
of 470 meters) is ruled out by the decompaction algorithm. Consequently, the Permian-Carboniferous sequence deposited in the study area has been compacted by 588 meters.

Discussed in Appendix II, the strata deposited in Ebbadalen constitute a petroleum system, sourced by the Billefjorden Group and stratigraphically sealed by the Tricolorfjellet Member. The Hultberget Formation and Ebbaelva Member were the primary reservoir rocks after hydrocarbon generation in Upper Permian. I calculate 89 meters of total thickness loss in the primary reservoir by compaction. Compaction can generate overpressure and preferential leakage through the Løvehovden Fault Zone to higher stratigraphic levels.

Flexural isostatic compensation shows a decompactional rebound of 530 meters which, assuming a geothermal gradient of 30C/ km, contributes with 16 degrees celsius to  $T_{\max}$ . The deformation associated to the isostatic rebound is limited (Figure 3.21).

#### **4.3 Structural and sedimentological interpretation of the outcrop**

The interpretation of the sedimentological units and structures is the result of the study of the published literature of the area and fieldwork observations and interpretations. Figure 5.1 shows the geometry, distribution and movement direction of the major sets of faults and strata boundaries.



**Figure 4.1** Panoramic view of the Løvehovden area from Ebbadalen. Faults and geological units are interpreted on the picture. The boundaries between the major depositional units are here shown in different colours: red and purple sandstones from the Hultberget Formation (in red); grey-yellow sandstones interbedded with grey shales and occasional carbonates and evaporites from the Ebbaelva Member of the Ebbadalen Formation (in black); characteristic white gypsum and anhydrite levels interbedded with carbonates from the Tricolorfjellet Member of the Ebbadalen Formation (in yellow); carbonates, sandstones, collapse breccias, evaporites and shales from the Minkinfjellet Formation (in white) and limestones from the Wordiekammen Formation (in blue). Solid line = continuity; dashed line = interpreted boundary; pointed yellow line = angular unconformity (Modified from Norsk Polarinstitut; [www.npi.no](http://www.npi.no))

#### 4.4 Analogy to the Barents Shelf

At seismic scale, the geology of the study area is analogous to the Barents Shelf geology, where the Carboniferous stratigraphic record is equivalent (Dallmann et al. 1999). In the Løvehovden area, the hydrocarbons migrated through the syn-rift Løvehovden Fault Zone. The overlying Mesozoic and Tertiary strata are removed by erosion. On the Barents Shelf, migration would have been stopped by the Upper Permian post-rift Kapp Starostin Formation. The lithology of the Kapp Starostin Formation is characterized by a thick tight sequence of biogenic chert, which would act as regional seal rock.

Further Paleozoic plays on the Barents Shelf should focus on the identification of syn-rift Carboniferous faults and associated monocline structures. These monocline structures can potentially constitute a structural trap for hydrocarbons migrated through Carboniferous faults

to overlying strata as long as they are stratigraphically sealed by the Kapp Starostin Formation.

#### **4.5 Error factor and uncertainties**

The data here presented is subjected to error factor and uncertainties. The log records on the Minkinfjellet Formation contain gaps, which are source of uncertainty in fault wall correlation.

The interpretation of the underground geology from fieldwork observations in the structural models is as well constrained to uncertainty. In the models, I work assuming homogeneous syn-rift thickening towards the centre of the north Billefjorden Trough. Faults are projected in the subsurface according to field interpretations and published literature. The vertical extent of the Billefjorden Fault Zone is poorly constrained.

The structural modelling is based on the choice of determined algorithms in order to simulate the basin structure and to quantify parameters. Each of these choices conditions the final results. The flexural slip algorithm is elected instead of line-length to unfold Tertiary-related folding. Flexural subsidence is chosen to evaluate local flexural unload instead of isostatic subsidence (See text for discussion).

Stratigraphic thickness is the most vulnerable parameter since the true thicknesses of the buried and eroded stratigraphic units deposited in the study area are extrapolated from field observations, measurements on lidar data, log correlation and extrapolation from thicknesses and stratotype thicknesses given by Dallmann et al (1999 & 2004). Although they



are quite accurately inferred, thickness-related uncertainty may influence the results of sediment compaction and isostatic rebound.

The accuracy of the geothermal gradient of the study area from Carboniferous to Cretaceous presented by Michelsen & Khorasani (1991) constrains  $T_{\max}$  and prospect evaluation discussion (Appendix II).



## 5. Conclusions

The North Billefjorden Trough has been interpreted as a half-graben basin, where the Permo-Carboniferous deposition was controlled by the Billefjorden Fault Zone. My work on the eastern side of the Billefjorden Trough has revealed that the Løvehovden Faults are not East-dipping Tertiary reverse faults, but West-dipping extensional syn-rift Carboniferous Faults (Maher & Braathen *manuscript in prep.*). I calculate the Løvehovden Master Fault throw from log correlation, backed up by lidar data, as 183 meters. The Løvehovden Master Fault strike and dip is here calculated to be 310/57 SW.

I base the interpretation of the Løvehovden Faults on sedimentological and structural evidence. The footwall and hangingwall of the Minkinfjellet Formation contain different lithologies. The sedimentation on the LMF footwall evidences terrigenous-influence where chert nodules and sand clasts are found. On the footwall the sequence is purely marine. This would not be expected across reverse faults.

Differential compaction leads to the formation of an extensional fault-propagation monocline feature. Kinematic modelling indicates that the Løvehovden Master Fault has propagated 200 meters.

In order to build syn-rift geometry in the structural models, the Pyramiden Faults (western faults of the BFZ according to Dallmann et al. 2004) of the Billefjorden Fault Zone must be sub-vertical in order to create enough accommodation space for syn-rift thickness increase.

The results of the 2D Move models show 691 meters of basin shortening is carried by The Billefjorden Fault Zone. The Ebbadalen reverse Fault contribution in shortening is 20 meters. The total basin Tertiary shortening is 711 meters.

The results of testing and modelling the trishear geometry conclude that the Løvehovden trishear zone is characterized by trishear angle of 103 degrees and trishear apex of 79 degrees. In order to create the observed deformation, the apex position must lie in 200 meters down-fault, implying 200 meters of fault propagation.

The Permo-Carboniferous sediments deposited in the study area were compacted 500 meters, equivalent to a factor of 19.17% of compaction. The isostatic rebound associated to flexural unloading by erosion is measured to be 530 meters and has no major associated deformation.

The analogy of the study area to equivalent geological setting on the Barents Shelf suggests the potential of monocline structures developed over permeable Carboniferous faults as structural traps for hydrocarbons. According to the kinematic models, in order to create a structure such as the Løvehovden monocline, fault slips of 200-250 meters are required.

## References

- Allen, P.A. & Allen, J.R. (1990):** Basin Analysis Principles & Applications. Blackwell Science, 451. pp
- Bellian, J.A., Kerans, C., Jennette, D.C. (2005):** Digital outcrop models: applications of terrestrial scanning lidar technology in stratigraphic modelling. *Journal of Sedimentary Research*, vol.75, pp. 166-176
- Bergh, S., Harmon, M & Braathen, A. (1999):** Expedition to Billefjorden Trough, Svalbard. Norwegian Geological Survey
- Buggisch, W., Piepjohn, K., Thiedig, F., Werner von Gosen. (1992):** A Middle Carboniferous Conodont Fauna from Blomstrandhalvøya (NW-Spitsbergen): Implications of the age of Post-Devonian Karstification and the Svalbardian Deformation. *Polarforschung* 62 (2/3), pp. 83-90
- Cardozo, N. (2005):** Trishear modelling of fold bedding data along topographic profile. *Journal of structural geology* 27, pp. 495-502
- Cardozo, N. (2008):** Trishear in 3D: Algorithms, implementation and limitations. *Journal of Structural Geology* 30, pp. 327-340
- Coe, L.A., Bosence, D.W.J., Church, K.D., Flint, S.S., Howell, J.A., Wilson, R.C.L. (2005):** The sedimentary record of sea level change. Cambridge University Press 288.pp
- Dallmann, W.K. (1993):** Notes on the stratigraphy, extent and tectonic implications of the Minkinfjellet Basin, Middle Carboniferous of Central Spitsbergen. *Polar Research* 12.(2), pp. 153-160
- Dallmann, W.K., Dypvik, H., Gjelberg, J.G., Harland, W.B., Johanessen, E.P., Keilen, H.B., Larsen, G.B., Lønøy, A., Midbøe, P.S., Mørk, A., Nagy, J., Nilsson, I., Nøttvedt, A., Olaussen, S., Pcelina, T.P., Steel, J.R., Worsley, D. (1999):** Lithostratigraphic Lexicon of Svalbard. Review and recommendations for nomenclature use. Stratigrafisk Komité for Svalbard (SKS), pp.17-123
- Dallmann, K.W., Piepjohn, K., Blomeier, D. (2004):** Geological Map of Billefjorden, Central Spitsbergen, Svalbard with geological excursion guide. Geological Map Svalbard 1:50000
- Davis, G.H & Reynolds, S.J. (1996):** Structural Geology of Rocks and Regions, Second Edition, published by John Wiley & Sons, Inc pp. 273-356; 776. pp
- Eliassen, A. (2002):** Sedimentological and diagenetic investigations of the Minkinfjellet formation, central Spitsbergen, Svalbard: with particular emphasis on the origin and evolution of a large gypsum paleokarst system. Dr.Scient University of Bergen, 122. pp.

**Eliassen & Talbot. (2003):** Diagenesis of the Mid-Carboniferous Minkinfjellet Formation, Central Spitsbergen, Svalbard. Norwegian Journal of Geology, vol.83, pp. 319-331

**Eliassen, A & Talbot, M. (2003):** Sedimentary facies and depositional history of the Mid-Carboniferous Minkinfjellet Formation, Central Spitsbergen, Svalbard. Norwegian Journal of Geology, vol.8, pp. 299-318

**Eliassen, A & Talbot, M. (2005):** Solution-collapse breccias of the Minkinfjellet and Wordiekammen Formations, Central Spitsbergen, Svalbard: a large gypsum paleokarst system. International Association of Sedimentologists, vol.52, pp. 775-794

**Elvevold, S., Dallmann W.K., Blomeier, D. (2007):** Geology of Svalbard. Tromsø: Norwegian Polar Institute, pp. 6-7

**Erslev, E.A. (1991):** Trishear fault-propagation folding. Geology, vol.19, pp. 617-620

**Finch, E., Hardy, S., Gawthorpe, R. (2004):** Discrete-element modelling of extensional fault-propagation folding above rigid basement fault blocks. Basin Research 16, pp. 489-506

**Forsyth, D.W. (1992):** Finite extension and low-angle normal faulting. Geology, vol. 20, pp. 27-30

**Friend, P.F. (1996):** The development of fluvial sedimentology in some Devonian and Tertiary basins. Department of Earth Science (University of Cambridge), Cuadernos de Geologia Iberica, num. 21, pp. 55-69

**Friend, P.H., Harland, D.A., Rogers, I., Snape., R.S.W Thornley. (1997):** Late Silurian and Early Devonian stratigraphy and probable strike-slip tectonics in northwestern Spitsbergen. Geological Magazine 134 (4) pp. 459-479.

**Gawthorpe, R.L., Sharp, I., Underhill, J.R., Gupta, S. (1997):** Linked sequence stratigraphic and structural evolution of propagating normal faults. Geology, vol. 25, pp. 795-798

**Grogan, P., Nyber, K., Fortland, B., Myklebust, R., Dahlgren, S., Riis, F. (1998):** Cretaceous Magmatism South and East of Svalbard: Evidence from Seismic Reflection and Magnetic Data. Polarforschung 68, pp. 25-34

**Guohai, J., Richard, H., Groshong, Jr. (2005):** Trishear kinematic modelling of extensional fault-propagation folding. Journal of Structural Geology 28, pp. 170-183

**Harland, W.B., Cutbill, J.R., Friend, P.F., Gobbett, D.J., Holliday, D.W., Maton, P.I., Parker, J.R & Wallis, R.H. (1974):** The Billefjorden Fault Zone, Spitsbergen –the long history of major tectonic lineament. Norsk Polarinstitutt Skrifter 16, pp.1-72

**Harland, W.B. (1997):** The Geology of Svalbard. Geological Society of London Memoir No. 17, pp. 47-75 ; 310-340

**Lavier, L.L., Buck, W.R & Poliakov, A.N.B. (1999):** Self-consistent rolling-hinge model for the evolution of large-offset low-angle normal faults. *Geology* vol.27 no.12, pp.1127-1130

**Maher, H.D., Jr. & Braathen, A. (manuscript in prep.):** Løvehovden fault and Billefjorden rift basin segmentation and development, Spitsbergen

**Michelsen, J.K & Khorasani, G.K. (1991):** A regional study on coals from Svalbard: organic facies, maturity and thermal history. *Société Géologique de France* t.162 n° 2, pp. 385-397

**Manby, G.M., Lyberis, N., Corowicz, J., Thiedig, F. (1994):** Post-Caledonian tectonics along the Billefjorden fault zone, Svalbard, and implications for the Arctic Region. *Geological Society of America Bulletin*, vol.105, pp. 201-216

**Mavko, G., Mukerji, T. and Dvorkia, J. (1996):** *Rock Physics Handbook*. Stanford Physics Laboratory, Stanford University, pp. 241-244

**McCann, A.J. & Dallmann, W.K. (1996):** Multiple tectonic event history of the Billefjorden Fault Zone in north central Spitsbergen, Svalbard. *Geological Magazine* 133 (1), pp. 63-74.

**McClay, M.G., Norton, M.G., Coney, P., Davis, G.H. (1986):** Collapse of the Caledonian Orogen and the Old Red Sandstone. *Nature* vol. 323, pp. 147-149

**Nordeide, H.C. (2008):** Spatial distribution and architecture of breccia pipes features at Wordiekammen, Billefjorden, Svalbard. Master's Thesis, Department of Earth Science, University of Bergen, pp. 75-81 ; 99-110

**Nøttvedt, A., Livbjerg, F., Midbøe, P.S. & Rasmussen, E. (1993):** Hydrocarbon potential of the Central Spitsbergen Basin. *Arctic Geology and Petroleum Potential*, Norwegian Petroleum Society, Special publication no.2, Elsevier, pp. 333-361

**Lamar, D.L., Douglass,D.N. (1995):** Geology of an area astride the Billefjorden fault zone, northern Dicksonland, Spitsbergen, Svalbard. *Norsk Polarinstitutt Skrifter* 197, pp.5

**Loucks, R.G. (1999):** Paleocave carbonate reservoirs: Origins, burial-depth modifications, spatial complexity and reservoir implications. *AAPG Bulletin* 83, pp. 1795-1834

**Ohta, Y. (1978)** Caledonian metamorphism in Svalbard, with some remarks on the Basement. *Polarforschung* 48, pp. 78-91

**Pelz, K., Rohrmoser,I., Seyfried,H. (2006):** Trishear fault propagation folding and faulting of growth strata in an extensional setting: clues to the geometry of a listric oblique-slip fault. *Geophysical Research Abstracts*, vol.8

**Rabitsch, W.K.R & Hausegger,S. (2007):** Formation of fault breccias and cataclastic shear zones within layered carbonates: example from the Eastern Alps. *Geophysical Research Abstracts*, vol.9

**Rachlewicz, G. (2002):** Polish polar studies: the operation and monitoring of geocosystems of polar areas. Institute of Paleogeography and Geocology, Adam Mickiewicz University, Poznan, Poland, pp. 209-219

**Shreiber, B.C., Helman, M.L. (2005):** Criteria for distinguishing primary evaporite features from deformation features in sulphate evaporites. *Journal of Sedimentary Research* vol. 75, pp. 525-533

**Samuelsberg, T.J & Pickard, N.A.H. (1999):** Upper Carboniferous to Lower Permian transgressive-regressive sequence of central Spitsbergen, Arctic Norway. *Geological Journal* 34, pp. 393-411

**Steel, R.J & Worsley, D. (1984):** Svalbard's post-Caledonian strata: an atlas of sedimentational patterns and palaeogeographic evolution. *Petroleum Geology of the North European Margin*, Norwegian Petroleum Society, pp. 109-135

**Stemmerik, L & Worsley, D. (2005):** 30 years on –Arctic Upper Paleozoic stratigraphy, depositional evolution and hydrocarbon prospectivity. *Norwegian Journal of Geology*, vol 8, pp. 151

**Stuart, H & McClay, K. (1999):** Kinematic modelling of extensional fault-propagation folding. *Journal of Structural Geology* 21, pp. 695-702

**Stuwe, K. (2007):** *Geodynamics of the lithosphere: an introduction*. Second Edition, 493 pp.

**Sundsbo, G. (1982):** Facies analysis of Late Carboniferous and Early Permian carbonates in the Billefjorden area, Spitsbergen. Master's Thesis, University of Bergen, pp. 91

**Sushchevskaya, N. M., Evdokimov, A.N., Maslov, V.A., Kusmin, D.V. (2004):** Genesis of basaltic magma from the quaternary volcanoes of Spitsbergen (Svalbard) Archipelago. *Informational Bulletin of the Annual Seminar of Experimental Mineralogy, Petrology and Geochemistry*, pp. 1-4

**Torsvik, T.H & Cocks, R.L.M. (2005):** Baltica from the late Precambrian to mid-Palaeozoic times : the gain and loss of a terrane's identity. *Earth-science reviews* vol. 72, pp. 39-66

**Wisshak, M., Volohonsky, E & Blomeier, D. (2004):** Acanthodian fish trace fossils from the Early Devonian of Spitsbergen. *Acta Paleontologica Polonica* 49 (4), pp. 629-634.

**Witt-Nilsson, P. (1997):** Ultramylonitic granites along the Billefjorden fault zone, Svalbard's Eastern Terrane: A result of thrusting, or related to major strike-slip movement during terrane assembly. *The Geological Society of London 28th Annual Tectonic Study Group Meeting, Abstract*

**Worsley, D. (2006):** The post-Caledonian geological development of Svalbard and the Barents Sea. *NGF Abstracts and Proceedings*, vol.3, pp. 1-20

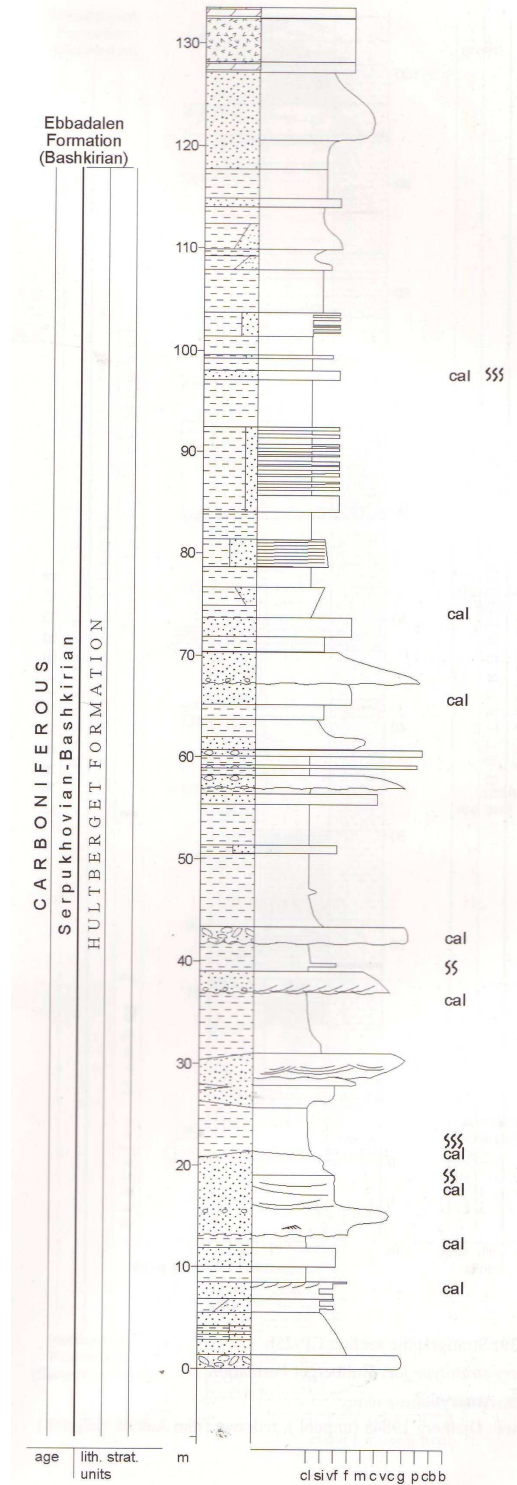
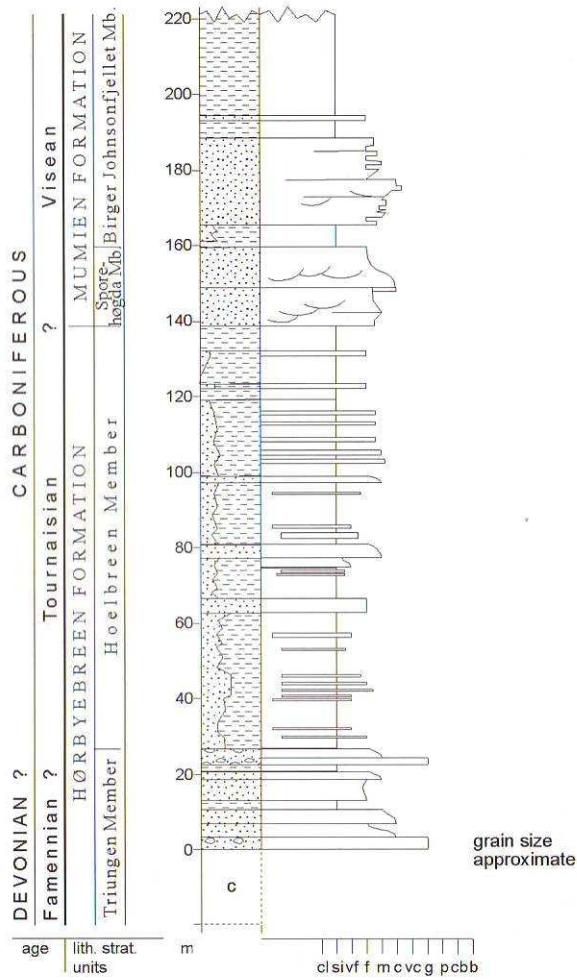


**Worsley, D. & Aga. (1986):** The Geological History of Svalbard: Evolution of an Arctic archipelago. Statoil, 120 pp.

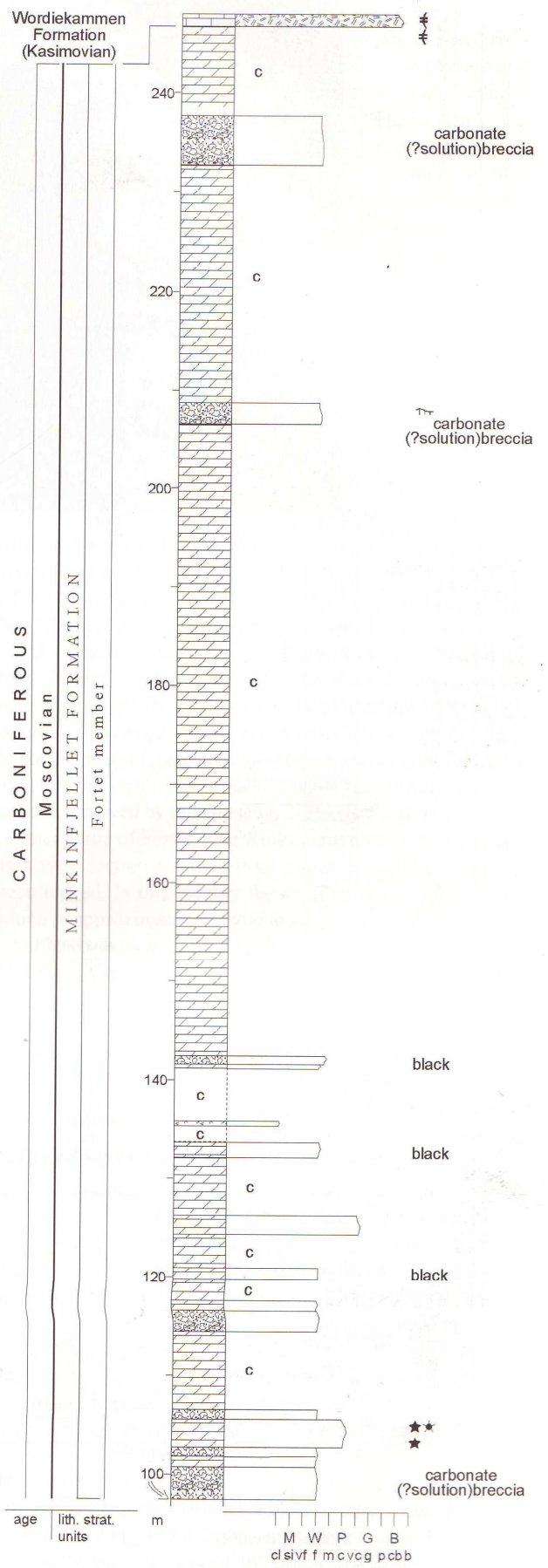
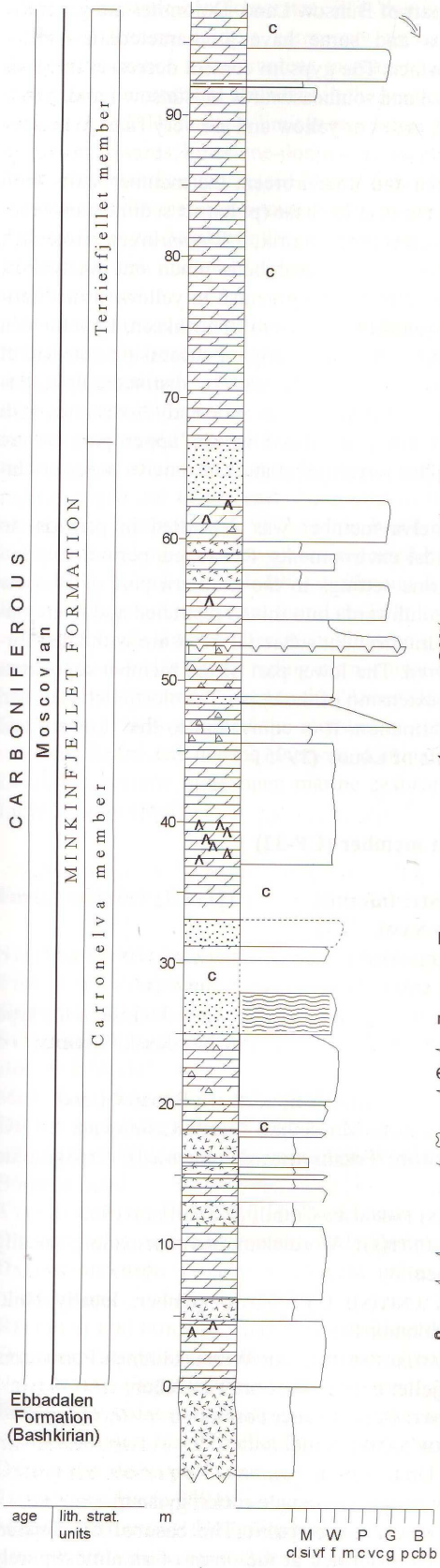


## Appendix I Stratigraphic columns in Section 1.3.2.1.2

Stratigraphic columns for the Paleozoic strata preserved at the Løvehovden area and corresponding legend from Dallmann et al. (1999).

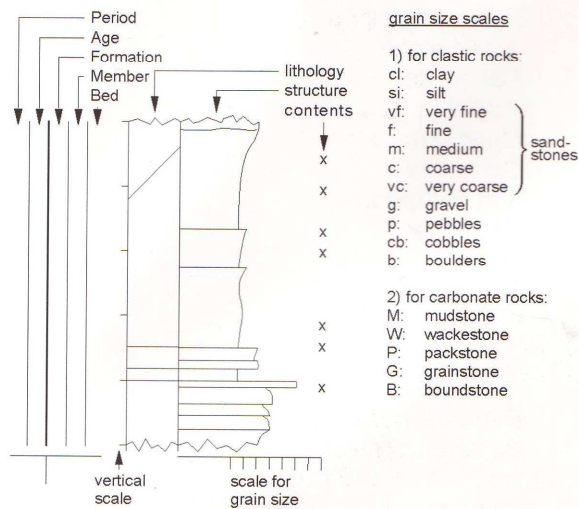






**Fig. 2-49: Stratigraphic section CP-30/31a**  
 Stratotype for: Minkinfjellet Formation, Carronelva member  
 Locality: Urmstonfjellet W  
 Reference: Lønøy, A. (unpubl.)

# LEGEND FOR STRATIGRAPHIC TYPE SECTIONS



## LITHOLOGY:

### 1. Siliciclastic rocks

- Breccia
- Conglomerate
- Gravelstone/gritstone
- Pebbly sandstone
- Sandstone
- Silty sandstone
- Siltstone
- Sandy shale
- Shale, mudstone, claystone
- Sandy chert
- Chert
- Paper shale

### 2. Mixed carbonate-siliciclastic rocks

- Calcite-cemented sandstone
- Dolomite-cemented sandstone
- Calcareous shale
- Dolomitic shale
- Sandy limestone
- Silty limestone
- Clayey limestone
- Cherty limestone
- Sandy, dolomitic limestone
- Sandy, calcitic dolomite
- Sandy dolomite
- Siderite-cemented sandstone

### 3. Carbonate rocks

- Limestone, calcareous ...
- Dolomite, dolomitic ...
- Dolomitic limestone
- Calcitic dolomite
- Siderite

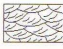




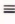
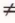

















### 4. Other layered lithologies

- Gypsum & anhydrite
- Coal
- Dolerite sill / dyke
- Basalt lava

### 5. Secondary lithological content



- Cherty nodules
- Calcareous nodules
- Dolomitic nodules
- Sideritic nodules
- Gypsiferous/anhydritic nodules
- Pyritic nodules
- Septarian nodules
- Phosphate nodules
- Sandstone lens
- Clay-ironstone or siltstone nodules
- Conglomerate beds
- Polymict conglomerate beds
- Mud flakes
- Mud clasts
- Sandy
- Silty
- Shaley
- Cherty
- Calcareous
- Dolomitic
- Sideritic
- Gypsiferous/anhydritic
- Halitic
- Coaly, coal lenses or fragments
- Bentonite
- Glauconite
- Quartzite
- Caliche

## STRUCTURE:




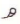













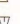





	Trough cross-bedding, undifferentiated
	Trough/planar cross-bedding, adjusted to appearance in outcrop
	Tabular/planar cross-bedding
	Herringbone cross-bedding
	Bioherm/reef
MPS	Maximum particle size (cm)
	Beds distinct
	Unbedded
	Cross bedding, ripple lamination
	Ripple structures
	Climbing ripple lamination
	Dunes
	Flaser bedding/lenticular bedding
	Wave ripples
	Wavy lamination
	Planar lamination
	Cone in cone
	Convoluted lamination and soft-sediment deformation
	Flow structures
	Karst
	Stylolites
	Mud cracks
	Hiatus/erosion surface
	Loading
	Hummocky bedding/lamination

## FOSSILS AND PARTICLES:














### 1. Vertebrate fossils

	Vertebrates
	Fish remains


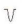


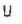










### 2. Invertebrate fossils

	Calcispheres
	Corals
	Bivalves
	Rudists
	Gastropods
	Brachiopods
	<i>Lingula</i>
	Bryozoans
	Trilobites
	Sponges
	Foraminifera, undifferentiated
	Foraminifera, benthic
	Foraminifera, encrusting
	Foraminifera, planktonic
	Fusulinids
	<i>Orbitolina</i>
	Ostracods
	Molluscs
	Cephalopods, mostly belemnites
	Ammonoids
	Echinoderms
	Crinoids
	<i>Palaeoaplysina</i>












### 3. Plant fossils

	Laminar stromatolites
	Columnar stromatolites
	Encrusting algae
	Green algae
	Red algae
	Phylloid algae
	Algae lamination
	<i>Girvanella</i>
	Stromatoporids
	<i>Stigmaria</i>
	Plant fragments
	Tree trunks
	Roots

### 4. Trace fossils

	Burrows, horizontal
	Burrows, vertical
	Burrows, undifferentiated
	Increasing bioturbation
	<i>Arenicolites</i>
	Trails
	<i>Ophiomorpha</i>
	<i>Rhizocorallium</i>
	<i>Skolithos</i>
	<i>Terebellina</i>
	<i>Thalassinoides</i>
	<i>Zoophycos</i>
	<i>Chondrites</i>
	<i>Palaeophycus, planolites</i>
	<i>Diplocraterion</i>

### 5. Others

	Fossils, undifferentiated
	<i>Microcodium</i>
	<i>Tubiphytes</i>
	Coquina beds
	Ooids
	Oncoids
	Pellets
	Peloids
	Bioclasts
	Intraclasts
	Lithoclasts

## VARIOUS:

	Break
	Fault
	Covered section

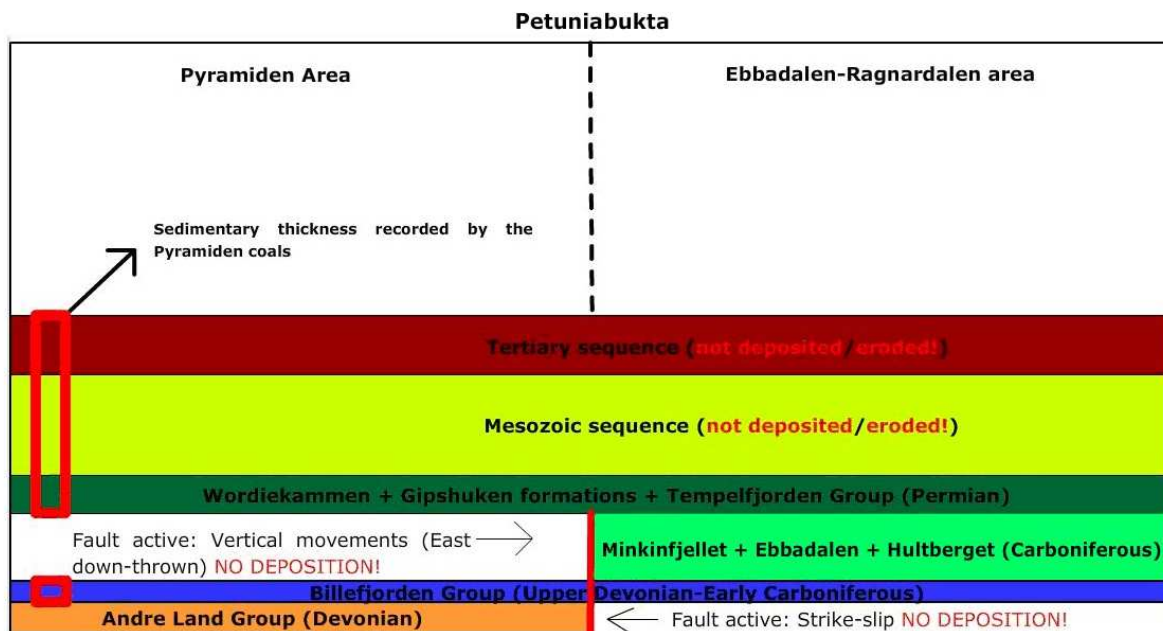




## Appendix II Petroleum Prospectivity of the Løvehovden area

### 1 Burial history & basin evolution

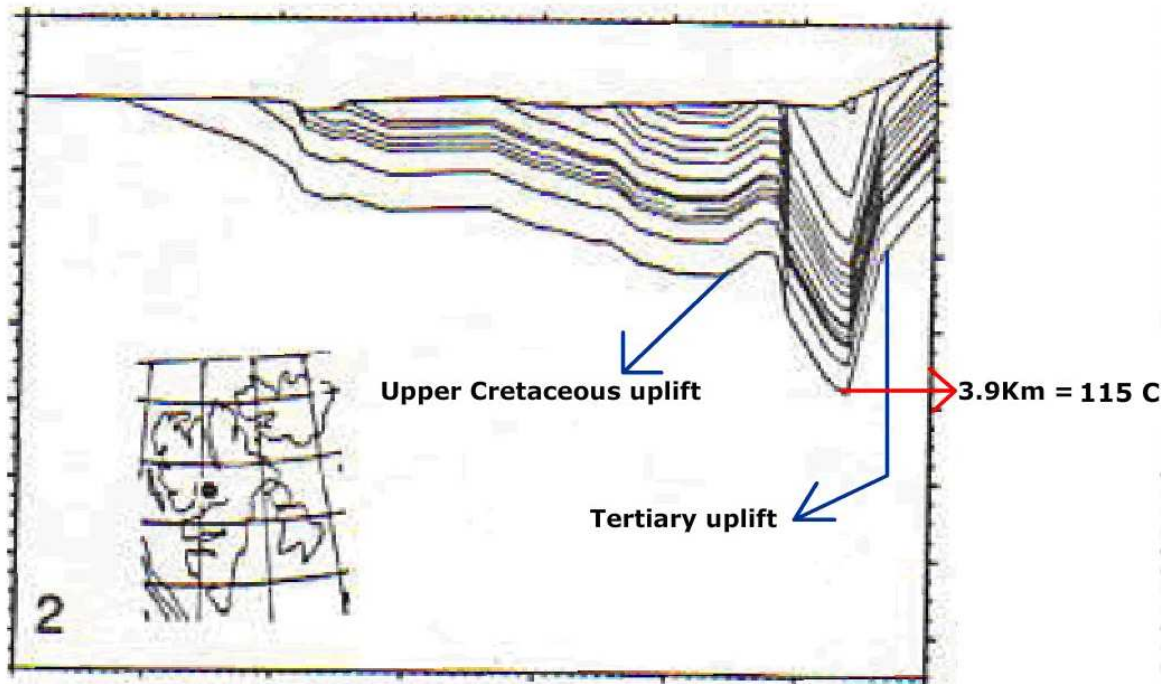
The vitrinite reflectance data from the Pyramiden coals record the maximum paleo-temperature of the basin during burial. The overburden weight was integrated by the sediments deposited from Lower Carboniferous to Tertiary times. Compared to Pyramiden, the burial history of the Ebbadalen area comprises the thickness recorded in Pyramiden + the thickness of the Permo-Carboniferous Ebbadalen deposits (Figure 1).



**Figure 1** Schematic diagram showing the stratigraphy W-E across the Pyramiden-Ebbadalen areas. The BFZ (vertical red line) was active until the deposition of the Wordiekammen Formation. The diagram shows sediment deposition, ages and hiatus on both sides of the Billefjorden Fault Zone. The red box indicates the overburden recorded by the coals from Pyramiden. In light green, the Carboniferous deposits of Ebbadalen only deposited east of the BFZ.

(Michelsen & Khorasani (1991) derived the  $T_{\max}$  for coals from the Billefjorden Group strata at Pyramiden. The Pyramiden area is approximately 3 Km SW of the study area.

The same authors developed a vitrinite reflectance analysis on coals. The conclusions were that the coals in Pyramiden were not exposed to temperatures higher than 115°C with a corresponding maturity of  $R_0 = 0.45-0.50\%$  (Michelsen & Khorasani 1991). The interpreted maximum Paleo-Temperature in the basin was reached in Tertiary times (Figure 2).



**Figure 2** Reconstructed and decompacted overburden weight of the Carboniferous to Tertiary sediments in Pyramiden. The maximum burial and therefore maximum paleo-temperature was achieved during Tertiary subsidence before uplift. (Modified from Michelsen & Khorasani 1991).

The Carboniferous to Cretaceous geothermal gradient has been estimated as 30°/Km by the authors. It is a relatively high gradient principally caused by the Carboniferous extension coupled by the tectonic activity pre-dating the Mesozoic. No Carboniferous volcanic rocks are recorded in the area. This fact makes us think that the extension consisted in a crust-thinning cold rift. However, the geothermal gradient during Tertiary times should have been lower since it was a period of basin infill with no major extension nor volcanics.

The 3.9 Km record Upper Devonian (Billefjorden Group) to Tertiary in Pyramiden. In the Ebbadalen area, the burial history has been slightly different since we must add the sediment thickness of the Lower and Upper Carboniferous sequence.

The burial history of Spitsbergen is strongly dependent on local thickness differences caused by fault dynamics. It is recorded by the stratigraphy and tectonics discussed in Sections 1.1.3 & 1.3.3. At a regional scale, the strata thicken towards west of Spitsbergen.

In the study area, the only published paleodepths are from Michelsen & Khorasani (1991), who compared the paleodepth of two localities: the Trygghama area (west of Billefjord) and Pyramiden, next to the Billefjorden Fault Zone, in north Billefjord (Pyramiden in Figure 2). They provide detailed paleodepth and paleotemperature information of the Pyramiden area. Pyramiden and Ebbadalen are located at the same latitude each at one side of Billefjord.

For comparison, during Lower Cretaceous, about 100 million years ago, the Lower Carboniferous sediments from the Trygghama area were at a depth of 4 Km. In the same time, the Lower Carboniferous sediments from the Pyramiden area (E) were only buried at 2 Km. Therefore, depending on the local tectonics, the same sediments may have been buried at very different depths.

The total thickness and maximum column of strata has to be measured indirectly since an important part has been eroded. The sedimentary records from the Ebbadalen area range almost uninterruptedly from the uppermost Devonian to the Lower Permian. Regionally there is record of Permian, Mesozoic and Tertiary strata in many areas.

Before reconstructing the burial history, two assumptions are considered:

1. The Billefjorden Fault Zone and Løvehovden Master Fault controlled the sedimentation in the Billefjorden Trough. The underexposed Nordfjorden Block, situated west of the BFZ, was giving protection to the environment (Sundsbø 1982). The Nordfjorden Block was not completely transgressed until Early Permian and is then when the sedimentation restarts west of the BFZ. These considerations imply that west of the BFZ, the Carboniferous sequence was never deposited, and the Wordiekammen and Gipshuken Formations lie directly over the Billefjorden Group (Figure 1).
2. The Upper Carboniferous-Lower Permian strata overlie the BFZ in other areas. Its activity and control on sedimentation stopped in Lower Permian. Thus, after the deposition of the Wordiekammen Formation, sediment thickness deposited *a posteriori* should be equal in both the Ebbadalen area (E of BFZ) and the Pyramiden area (W from BFZ).

The missing Permo-Carboniferous sequence on Pyramiden is listed as follows from Dallmann et al. (2004). Particularly, the thickness of the Ebbadalen Formation is measured on lidar data and the thickness of the Minkinfjellet Formation was inferred from log comparison (Section 2.3.6.3)

Hultberget Fm: 250 m

Ebbadalen Fm (Ebbaelva Mb): 150 m

Ebbadalen Fm (Trikolorfjellet Mb): 125 m

Minkinfjellet Fm: 470 m

Minkinfjellet Fm (dissolution): 75 m

TOTAL estimated thickness = 1070 m

The estimated thermal gradient during Carboniferous is 30°/km (Michelsen & Khorasani 1991). The extra 1070 meters represent a temperature increment of 32°C. These 32°C must be added to the calculated 115°C from Michelsen & Khorasani (1991), corresponding to the rest of sediment deposition (Figure 1). I estimate that the paleo-temperature in the Ebbadalen-Ragnardalen basin at the end of Tertiary deposition was 147°C.

I consider the temperature to be the minimum paleo-temperature. The thicknesses given by Dallmann et al. (2004) are stratigraphic thicknesses. The Carboniferous strata are found to be deposited in a 9-10 degrees west-dipping trough-shaped basin. Vertical thickness is higher than real stratigraphic thickness. I assume that after the Permo-Carboniferous extensional period, the sediments were deposited horizontally.

## 2. Hydrocarbon potential

This section is intended to describe the elements and processes of the Løvehovden petroleum system. The petroleum prospectivity of the Ebbadalen-Ragnardalen area will be here discussed in terms of elements and processes.

Coal is present in the sediments of the Billefjorden Group in the study area. Coal seams are exposed at Pyramide and easternmost side of Ebbadalen. Oil traces were found during drilling of a coal exploration borehole at a depth of 631 meters (Dallmann et al. 2004).

## 2.1 Elements: source, reservoir and seal rocks

In order to evaluate the Løvehovden petroleum system, the elements and processes must be discussed. The first step is to determine the presence of the source rock, reservoir rock and seal rock.

*Source rock:* Bituminous limestones were deposited during the Carboniferous period in the Minkinfjellet Formation. Their centimetric to several meter thicknesses imply that they would not have been the primary source for hydrocarbons. A potential source rock are coals and shales from the Billefjorden Group.

Source rock candidate 1: Hørbyebeen Formation (Hoelbreen Mb, Billefjorden Group): lacustrine and flood-plain shales, black/grey shales and mudstones, coals, coaly shales (Harland 1997; Dallmann et al. 1999).

Source rock candidate 2: Mumien Formation (Birger Johnsonfjellet Mb, Billefjorden Group): liptinitic coal seams, black/grey shales, coaly shales and dark grey claystones (Harland 1997; Dallmann et al. 1999).

Source (S1): The coals of the Birger Johnsonfjellet Member are algal-type deposited in lacustrine eutrophic conditions. The lowermost coal seams from the Birger Johnsonfjellet Member are humic as well and of waxy character and the youngest seams have a lower molecular-weight and therefore are less waxy (Michelsen & Khorasani 1991).

Source (S2): The lowermost coal seams from the Hoelbreen Member are of humic nature and the uppermost coal seams contain large amounts of liptinites (sporinite/alginate and bituminite). (Michelsen & Khorasani 1991)

The source rocks are basically coal measures which are typically gas prone. The humic liptinitic nature of the coals makes them oil and condensate-prone.

*Reservoir rock:* Candidates for reservoir rock in the Ebbadalen-Ragnardalen area include the clastic rocks (shale, sandstone and conglomerate) and carbonates. The carbonates are basically limestones, dolomites and carbonate breccias. The observed carbonate and sandstone porosities are generally high (estimated in 15%). Particularly, the carbonate breccias (if not cemented) constitute a good reservoir unit.

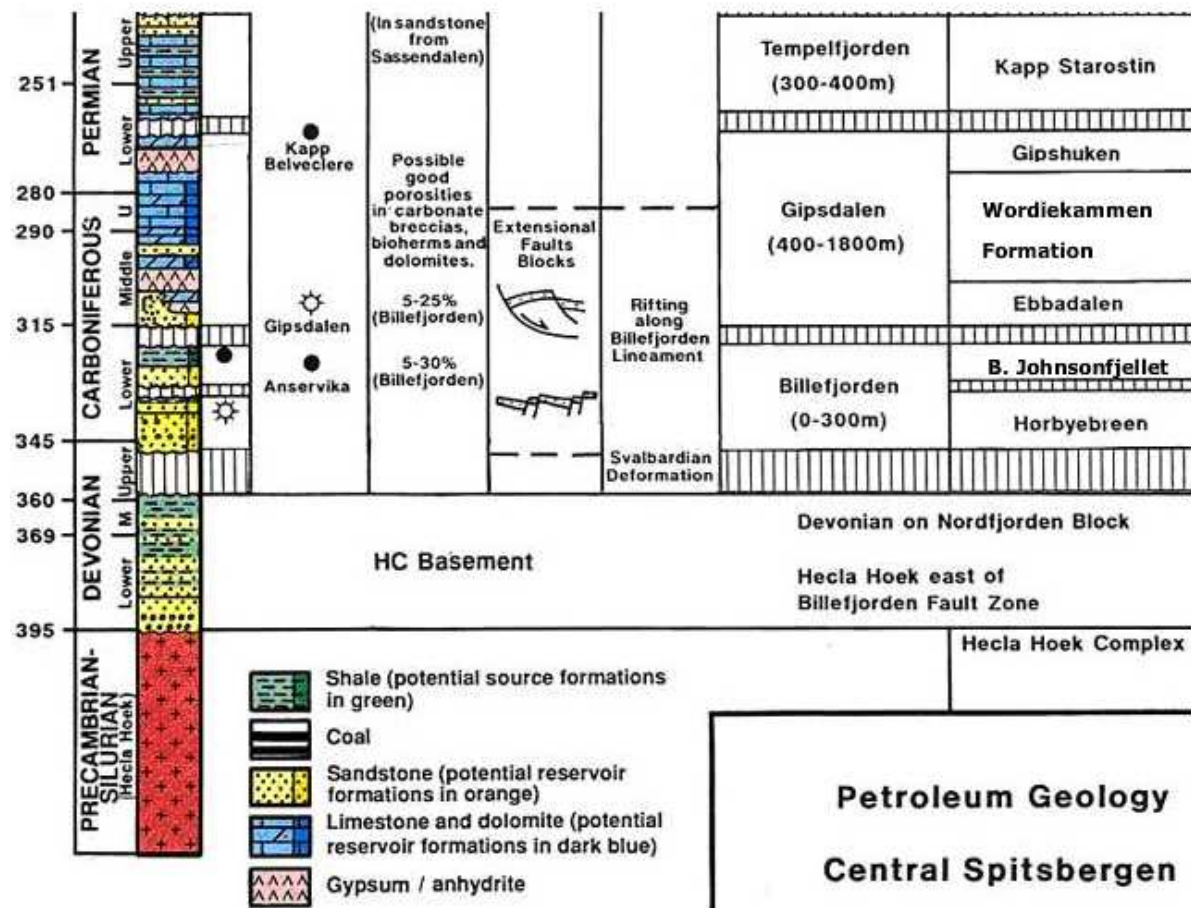
The clastic reservoir is represented by the Hultberget Formation. The carbonate reservoir is represented by the Ebbaelva Member of the Ebbadalen Formation, Minkinfjellet, Wordiekammen and Gipshuken Formations. The Gipshuken Formation has been eroded in the study area and lies on top of the Wordiekammen Formation. The effective reservoir is constituted by those facies characterized by: non cemented collapse-breccias, dolomitized intervals, brecciated carbonates, porous sandstones and breccia pipes.

*Seal rock:* Lower in the stratigraphy the Tricolorjellet Member (Ebbadalen Formation) evaporites constitute a regional seal for hydrocarbons potentially generated in the area.

The Gipshuken Formation is as well one of the plausible seal rocks since the locally massive evaporitic strata can potentially prevent hydrocarbons to escape from the petroleum system.

The Kapp Starostin Formation, consisting of cherts and silicified limestones, overlies the Gipshuken Formation and is regarded as a second and thicker potential seal rock.

The elements of the petroleum system are present, although it does not imply that the hydrocarbon generation post-dated the formation of the seal rock and trap mechanism (See Figure 3).



**Figure 3** Stratigraphy and petroleum potential of the Central Basin, Spitsbergen. (Hesthammer personal communication)



## 2.2 Processes: generation, migration and accumulation

Evidence of hydrocarbon generation is supported by oil traces found in the Hultberget Formation by the coal-exploration well. The entrance of the Billefjorden Group source rock into the oil window which may be inferred from the burial history data. Based on the thermal gradient given by Michelsen&Khorasani (1991), 2 km of deposition would emplace the lowermost sediments (Billefjorden Group) into the oil window, at 60°. The oil window was reached as the Kapp Starostin Formation (Upper Permian) was being deposited. Organic shales and coal seams from the Billefjorden Group started to generate hydrocarbons at Upper Permian times.

The following thicknesses are extracted from Dallmann et al. (1999) in the stratotype, except for the Ebbadalen and Minkinjellet Formations thickness, which are measured by own methods (See Section 1 of Appendix II). From Billefjorden Group to Kapp Starostin, the total stratigraphic thickness is about 2145 meters.

### *Billefjorden Group*

Hørbyebreen and Mumien Fm: 150 m

### *Gipsdalen Group*

Hultberget Fm: 250m (possibly thicker towards the Trough centre)

Ebbadalen Fm (Ebbaelva Mb): 150 m (possibly thicker towards the Trough centre)

Ebbadalen Fm (Tricolorfjellet Mb): 125 m

Minkinjellet Fm 470 m

Minkinjellet Fm (dissolution): 75 m

Wordiekammen Fm: 300 m

Gipshuken Fm (eroded): 245 m

## *Tempelfjorden Group*

Kapp Starostin (eroded): 380 m

TOTAL = 2145 meters

The evaporitic seal rock of the Tricolorfjellet Member (Upper Carboniferous) was already deposited and consolidated as the oil window was reached, although the Løvehovden Master Fault had already intersected the Tricolorfjellet seal rock, conducting hydrocarbons to higher stratigraphic levels.

At depositional time, when the sedimentary thickness was about 2145 meters, the Kapp Starostin Formation was an unconsolidated marine mudstone with a very low seal capacity. The hydrocarbons could therefore have leaked out to the sea through the Kapp Starostin Formation. Significant amounts of the generated hydrocarbons could have leaked during the time-lapse of Kapp Starostin consolidation.

In this early-leakage scenario, the hydrocarbons are assumed to have flowed through the permeable reservoir intervals up to the sea level as well as being flushed through the Billefjorden Fault Zone and uppermost formations.

Hydrocarbons generated after the consolidation and lithification of Kapp Starostin could have been accumulated within the underlying Gipshuken Formation reservoir rock, and eventually leaked after the Tertiary uplift and subsequent erosion of the Kapp Starostin Formation and further reservoir exposure.

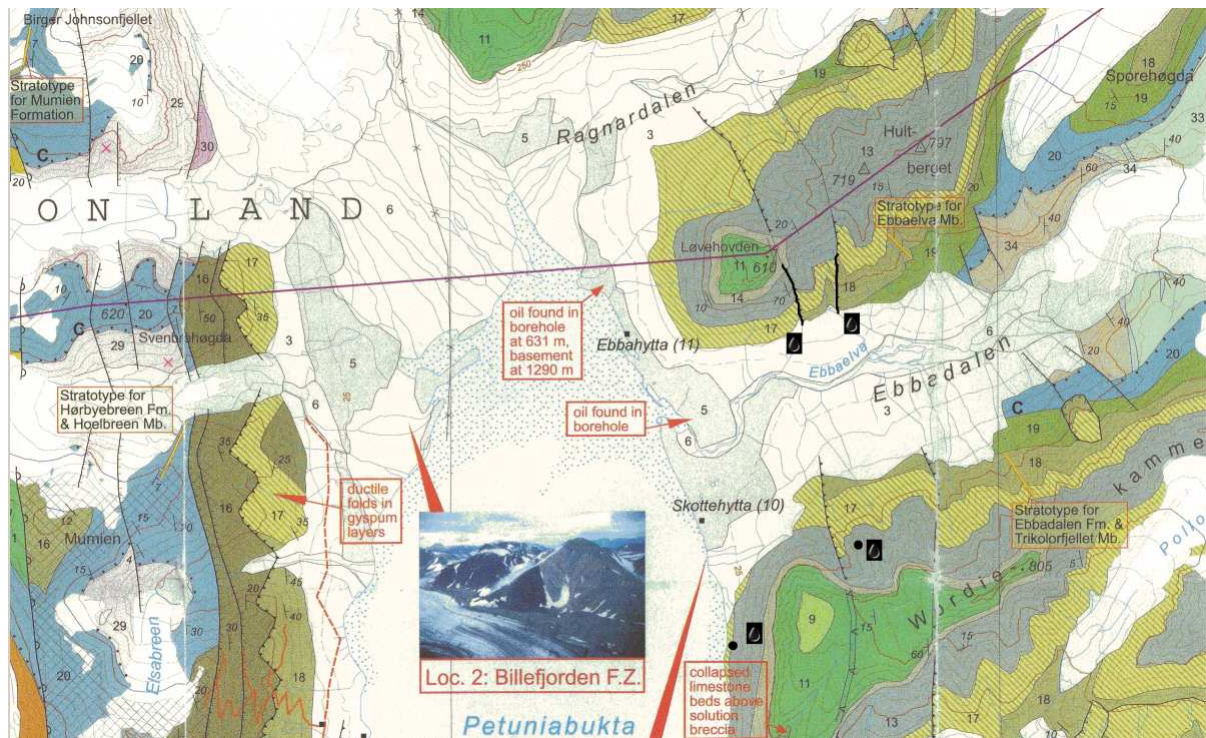
The trap mechanism may have consisted of an anticlinal-shaped structural trap formed by the accommodation of the Wordiekamme and Gipshuken formations over the Carboniferous monocline formed by the propagation of the Løvehovden Master Fault.

Oil traces left in the reservoir have not experienced further migration and oil traces remained. Further migration might have been stopped for several reasons: A) The accumulation is too insignificant to generate any fluid pressure overcoming the rock capillary entrance pressure. b) A trap mechanism prevents the hydrocarbons to migrate. C) The oil traces found in the Løvehovden Fault Zone is by-passed oil retained by capillary forces. D) The oil exposure under low temperatures increases its viscosity, holding it into the pore space.

### 2.3 Interpreted oil migration paths

The detection of oil traces is important in terms of basin evolution and for prospect evaluations. From an economic perspective, the presence of oil in the exposed fault zone is critical in order to evaluate migration routes.

I have observed four different locations where oil is found on surface, staining rocks and providing them with a characteristic odour of gasoline (Figure 4).



**Figure 4** Mapping of the observed oil seeps in the Løvehovden-Wordiekammen area. The dark oil droplets indicate where oil-stained strata have been identified. The two oil drops situated at Løvehovden (to the north on the map) symbolize fault leakage. The other two oil drops (south on the map) represent the hypothesized leakage by dissolution of the seal rock (Tricolorfjellet Member). (Modified from Dallmann et al. 2004)

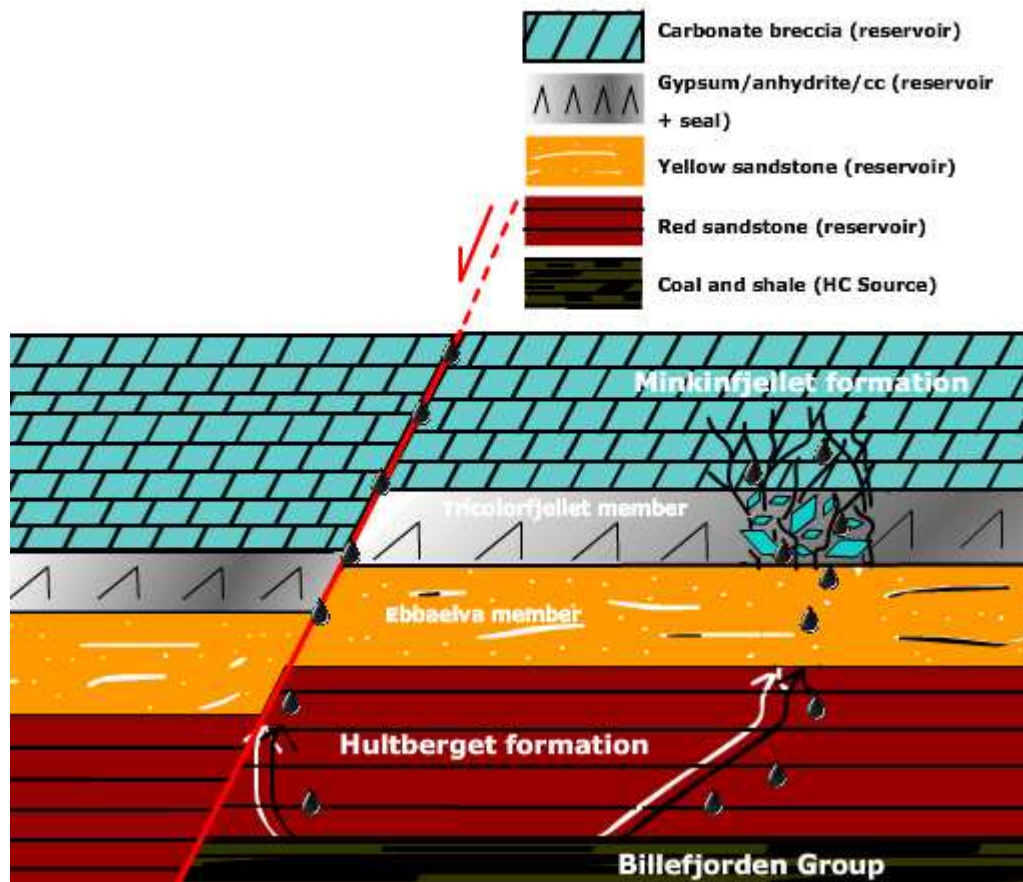
In Figure 4 I show the locations where oil has been found on the Minkinfjellet Formation. This includes two non-faulted locations and oil traces encountered in the Løvehovden Fault Zone and the Ebbadalen Fault.

The origin of the oil seeps may result from two different processes. These two processes are supported by evidence and interpretations based on the observations. The evidence refers to the faults acting as oil migration paths. The high level of fracturing of the fault zone materials provides a way out for the oil to migrate up to the surface. Both the Løvehovden Master Fault and the Ebbadalen Fault are permeable and able to conduct fluids.

The second process that may have enhanced oil migration is the formation of collapse structures and brecciation by the dissolution of the Tricolorfjellet Member evaporites. The dissolution of the gypsum levels from the Tricolorfjellet Member can trigger the collapse of the upper-laying carbonates of the Minkinfjellet Formation. The Minkinfjellet Formation has been regarded as a paleo-karstified formation. Meteoric and underground waters would have preferentially dissolved the evaporites, creating cavities and caves that posteriorly collapsed. This feature is widely observed in the Wordiekammen and Løvehovden areas (Eliassen & Talbot 2003, 2005 ; Nordeide 2008).

The collapse of the Minkinfjellet Formation strata into the Tricolorfjellet Member is one of the hypothesized processes. An observed oil seep staining the evaporites of the Ebbadalen Formation can be caused by dissolution affecting the Minkinfjellet Formation and acting further down into lower stratigraphic levels. Such dissolution would have been locally important enough thin up the Ebbadalen Formation evaporites to the extent of causing failure and collapse, opening a path for fluid flow.

This interpretation is supported by the observation of oil darkened nodular gypsums outcropping east of Petuniabukta (the southernmost locality displayed on the map in Figure 4). The two main oil migration mechanisms are ideally illustrated on Figure 5, which represents the discussed migration paths.



**Figure 5** Idealised vertical profile of the Løvehovden area. Hydrocarbon migration is interpreted to follow two main paths: a) through faults cutting the evaporitic seal rock of the Tricolorfjellet Member ; b) through the seal rock by dissolution of the seal rock evaporites. The overlying strata (Minkinfjellet Formation) undergoes further brecciation, enhancing rock permeability.

### 3. Summary of the petroleum system evolution and prospect evaluation

The main events that participated in the formation of the Løvehovden Petroleum System are summarized as follows:

1. Lower Carboniferous → Deposition of the Billefjorden Group coals and organic-rich shales of the Hoelbreen Member (Høybyebreen Formation) and Birger Johnsonfjellet Member (Mumien Formation).

2. Upper Carboniferous → Deposition of reservoir and seal rock units including the Hultberget, Ebbadalen, Minkinfjellet and Wordiekammen Formations, consisting mainly of carbonate types interbedded with evaporites with minor sandstones and shales. Formation of the syn-depositional permeable Løvehovden Fault Zone. The Løvehovden Master Fault intersects the Tricolorfjellet Member seal rock.
  
3. Upper Permian → The Billefjorden Group source rock reaches the oil window during the deposition of the Kapp Starostin Formation. The overburden approaches 2 km of sediment with a temperature close to 60° at the bottom (source rock).
  
4. Start of the oil generation in Upper Permian and deposition of the Kapp Starostin Formation. Migration and possible leakage of hydrocarbons through the Løvehovden Master Fault up to the sea bed. The Kapp Starostin Formation is unconsolidated and hydrocarbon flow can overcome the capillary entrance pressure of Kapp Starostin. The source rock keeps supplying hydrocarbons.
  
5. Deposition of the Mesozoic sediments and the Upper Cretaceous erosion.
  
6. Tertiary sedimentation. The basin bottom reaches a temperature of 147°C in the Eocene. Oil to gas cracking.
  
7. Subsequent uplift and erosion underexposing the petroleum system. Leakage of the remaining hydrocarbons potentially trapped as the Kapp Starostin Formation is eroded.

This reconstruction is based on several assumptions. It is clear that the oil generation took place and that there was hydrocarbon leakage. The critical factor is the *timing* of the hydrocarbon generation with respect to seal rock formation using a geothermal gradient of 30°/Km. The formation of the seal rock, postdated the onset of hydrocarbon generation.

Therefore, we do not expect any commercial accumulation of hydrocarbons to be found in the eastern Central Basin at the vicinity of the Ebbadalen-Ragnardalen area.